Assessment of the impact of land use land cover change on surface runoff: a case of Debre Markos town, Ethiopia

Yonathan Yimenu Ejigu

A Thesis submitted to

The Department of Geomatics Engineering

School of Civil Engineering and Architecture

Presented in Partial Fulfillment of the Requirement for the Degree of Masters of Science in Geoinformatics Engineering

Office of Graduate Studies

Adama Science and Technology University

June, 2024

Adama, Ethiopia

Assessment of the impact of land use land cover change on surface runoff: a case of Debre Markos town, Ethiopia

Yonathan Yimenu Ejigu

Advisor: Temesgen Abraham (PhD)

A Thesis submitted to

The Department of Geomatics Engineering

School of Civil Engineering and Architecture

Presented in Partial Fulfillment of the Requirement for the Degree of Masters of Science in Geoinformatics Engineering

Office of Graduate Studies

Adama Science and Technology University

June, 2024

Adama, Ethiopia

CANDIDATE'S DECLARATION

I hereby declare that the work contained in this thesis entitled "Assessment of the impact of land use land cover change on surface runoff: a case of Debre Markos town, Ethiopia" is entirely original to me and has not been previously submitted to another university for consideration. The proper citations are utilized to properly acknowledge the references used in this thesis.

Yonathan Yimenu Ejigu	___________________	_________________
Name of student	Signature	Date

ADVISOR's RECOMMENDATION

I, the advisor of this thesis, hereby certify that I have read the revised version of the thesis entitled "Assessment of the impact of land use land cover change on surface runoff: a case of Debre Markos town, Ethiopia" prepared under my guidance by Yonathan Yimenu submitted in partial fulfillment of the requirements for the degree of Masters of Science in Geo-Informatics Engineering. Therefore, I recommend the submission of the revised version of the thesis to the department following the applicable procedures.

Temesgen Abraham (PhD)	____________________	_________________
Name of Advisor	Signature	Date

APPROVAL SHEET

I, the advisor of the thesis entitled "Assessment of the impact of land use land cover change on surface runoff, a case of Debre Markos town, Ethiopia" and developed by Yonathan Yimenu; hereby certify that the recommendation and suggestions made by the board of examiners are appropriately incorporated into the final version of the thesis.

Advisor	Signature	Date

We, the undersigned, members of the Board of Examiners of the thesis by Yonathan Yimenu have read and evaluated the thesis entitled "Assessment of the impact of land use land cover change on surface runoff, a case of Debre Markos town, Ethiopia" and examined the candidate during the open defense. This is, therefore, to certify that the thesis has been accepted for partial fulfillment of the requirement of the degree of Master of Science in Geoinformatics Engineering.

Chairperson	Signature	Date
Internal Examiner	Signature	Date
External Examiner	Signature	Date

Final approval and acceptance of the thesis are contingent upon submission of its final copy to the Office of Postgraduate Studies (OPGS) through the Department Graduate Council (DGC) and School Graduate Committee (SGC).

Department Head	Signature	Date
School Dean	Signature	Date
Office of Postgraduate Studies, Dean	Signature	Date

ACKNOWLEDGEMENT

Firstly, all praises belong to the Almighty God, the son of Saint Marry and Lord of everything, for being with me throughout my life and making everything possible in my entire life.

My deepest gratitude goes to my advisor, Dr. Temesgen Abraham for his supervision, guidance, support, and constructive comments throughout the compilation of this thesis work.

I would like to express my sincere gratitude to the Ethiopian Geological Survey, Debre Markos Town municipality office, Debre Markos Town Agriculture office, and National Metrology Agency for providing me the data used in this study. Thanks should also go to the Adama Science and Technology University (ASTU) and Bule Hora University for financial support to pursue my studies and related research activities to achieve my research objectives.

I am also grateful to thank my family; I would not be where I am without your help. Your belief in me has kept my spirits and motivation high during my work.

Lastly, I would like to Mr. Eyoel Mekonnin, Mr. Kefelegn Wagamyelew, and Mr. Abdi Tena for their continuous technical and scientific guidance, encouragement, and advice as well as peer reviewing of the whole thesis. I would be remiss in not mentioning my friends, who were always supporting and encouraging me.

TABLE OF CONTENTS

Contents **Page No.**

LIST OF TABLES

LIST OF FIGURES

LIST OF ACRONYMS

ANN	Artificial Neural Network
AMC	Antecedent Moisture Condition
DEM	Digital Elevation Model
ENVI	Environment for Visualizing Images
ERDAS	Earth Resource Data Analysis System
ETM+	Enhanced Thematic Mapper plus
GIS	Geographical Information System
HSG	Hydrologic Soil Groups
LULC	Land use land cover
MCE-CA	Multi-Criteria Evaluation-Cellular Automata
MoLUSCE	Modules of Land use Change Evaluation
NRCS	Natural Resource Conservation Service
SCS–CN	Soil Conservation Service-Curve Number
SRTM	Shuttle Radar Topography Mission
SVM	Support Vector Machine
SSGI	Space Science and Geospatial Institute
TIFF	Tagged Image File Format
USDA	United States Department of Agriculture
USGS	United States Geological Survey

ABSTRACT

Urbanization is one of the most pervasive human endeavors, resulting in many physical and biochemical modifications to the hydrological system and its processes. However, the impact of urbanization driven LULC change on surface runoff remains unexplored. This study demonstrates the changes in surface runoff variables due to the changes in LULC during the period 1995-2022. The integration of remote sensing and GIS was applied to automate the estimation of surface runoff and analyzed its trends at different scales based on the SCS-CN model. Landsat TM, ETM+, and OLI/TIRS data from the USGS website was utilized to detect urban land cover changes. The area of each LULC classes in 1995, 2000, 2005, 2010, 2015 and 2022 were determined using supervised image classification approach. Accuracy assessment of image classification was processed using ENVI software and the result revealed that the overall accuracies are 97.2%, 96.6%, 96.8%, 96.4%, 90.33%, and 91.2% with the Kappa Coefficient of 0.96, 0.95, 0.96, 0.95, 0.88 and 0.89 for years 1995, 2000, 2005, 2010, 2015 and 2022 respectively. The increase in comprehensive socio-economic activities has resulted in considerable changes in the LULC of Debre Markos town. The LULC change analysis revealed that the urban area and barren land have increased annually by 17.36% and 3.3% respectively and that of vegetation, agricultural land, and meadow decreased by 1.19%, 1.32% and 0.73% respectively during the study period of 1995 to 2022. The depth and flowrate of direct runoff has increased over study period and the result showed that runoff depth and flowrate of the town increased by 3.7mm and 147.9m^3/s respectively from 1995 to 2022. High increase in runoff variables has shown at wuseta watershed than wutrin watershed. Correlation coefficient (R) and coefficient of determination (R^2) were computed to explore the associations between imperviousness and runoff variables and the result showed that +0.98 and +0.99 respectively, which revealed their strong direct relationship. Overall, urbanization lowered potential maximum storage, and thus increased runoff coefficient values. An area that experienced more urban growth had a greater potential for increasing surface runoff depth and its flowrate. Runoff responses identified in the spatiotemporal analysis emphasize the importance of monitoring and assessing the hydrological regime in Debre Markos.

Keywords: Surface runoff, SCS–CN, Land use land cover, Change analysis

Chapter One

1. Introduction

1.1. Background of the study

According to Paul & Meyer (2001) urbanization is a widespread and quick change in land use that entails transforming agricultural or natural habitats into urban settings with growing populations and economies (Wu et al., 2009). Due to various anthropogenic activities on the landscape, the vast urban expansions that have taken place over the past few decades have changed land use land cover (Moniruzzaman et al., 2020; Vojtek & Vojteková, 2019). Large agricultural regions and other non-urban land are frequently turned into impermeable land as part of the urbanization process. This causes changes in land use that immediately interrupt the natural hydrological processes (Hu et al., 2020; Yang et al., 2017). 86% of advanced nations and 64% of developing countries are predicted to be completely urbanized by 2050 (Hu et al., 2020; Mei et al., 2018).

In the context of developing countries, most of the urban growth is unplanned, leading to rapid densification, and associated construction of buildings resulting in a dramatic increase in impermeable areas due to paving and urban areas (Bajracharya et al., 2015). Numerous Ethiopian cities and/or towns have had fast horizontal growth, but effective planning interventions, inadequate institutional support, inadequate implementation capabilities, or sound city or town governance has not reined in this growth. Therefore, unchecked, fast horizontal city/town growth toward rural villages led to more social, economic, environmental, and political issues (Dadi et al., 2016; Firew Bekele, 2010). Debre Markos Town currently has issues with natural resources and the environment because of urban growth. The primary ones are the conversion of farms and forested regions into various urban land uses, including residential and commercial space. Urban land uses have not only replaced farms and vegetation, but also wetlands and grasslands (Mekuriaw & Gokcekus, 2019; Ziena, 2017).

While there are many benefits to urban growth, land surface adjustments happen as part of the urbanization process. The hydrological cycle, biodiversity, land productivity, degradation, and environmental quality are a few of the natural processes that land surface alterations may have an impact on. Regretfully, the most alarming issue is that the rate of local and global LULC change has accelerated recently (Msofe et al., 2019). It also affects groundwater recharge, runoff, and infiltration processes. Additionally, urban runoff and combined sewer overflows degrade water quality (Burns et al., 2012; Gitau et al., 2016; Passerat et al., 2011; Vietz et al., 2016). Land use land cover change also has indirect impacts on climate and the subsequent impact of the altered climate on the waters. The rapid alteration of land use land cover has caused serious disruption to natural drainage patterns and damage to the flood retention zones (Rahman et al., 2009) that account for unprecedented alteration to hydrological processes like increased surface runoff (Hu et al., 2020; A. Rahman & Netzband, 2009), reduced runoff response time and changed hydrological regimes (Hu et al., 2020).

When it comes to the distribution and occurrence of water both above and below the surface of the ground, hydrology is essential to the management and conservation of water and other environmental resources. The total amount of water that drains into a reservoir at any given period of time is known as the runoff of a catchment area. When rainwater overflows the land and the soil is, completely saturated, surface runoff takes place. The primary factors influencing runoff are the amount, duration, and dispersion of the rainfall (Cherian et al., 2017). The imperviousness of urban areas will rise as a result of changes in land use and cover, which will reduce the amount of precipitation that seeps into the ground and the ability of the area to withstand runoff. The overland flow increases in depth and velocity because of this reduction in rainfall infiltration. The SCS–CN approach is also used to evaluate the sensitivity of the local hydrologic system to alternative land use change scenarios, just by altering the CN employed in the analysis.

Because remote sensing provides information about inaccessible places and high spatiotemporal variability, it enhances the input parameters of the models (Gajbhiye, 2015) and geographic information system (GIS) by providing high storage, handling, data processing, analysis, and manipulation capabilities which are strongly required for the hydrological model (M. T. U. Rahman et al., 2017). Moreover, historical LULC dynamics can be studied thanks to archived remote sensing data. Eshanthini & Samuel (2018) estimated CN values based on the standard table for the conservation of natural resources and utilized GIS and remote sensing as a tool to compute the volume of runoff using the SCS–CN model. They came to the conclusion that for ungauged watersheds, the model SCS combined with GIS would provide a more dependable runoff.

Image classification is the process of assigning land cover classes to pixels in an image. In remote sensing, there are three primary categories of image classification methods: object-based picture analysis, supervised image classification, and unsupervised image classification. In remote sensing, supervised classification is a method that classifies pixels in an image using a set of training data. Each type of land cover that the user wishes to map is represented by samples in the training data. The training samples are chosen and categorize into the appropriate land cover classes. In unsupervised classification, pixels with similar spectral features are automatically grouped into clusters by the classification algorithm (Didore et al., 2021). The method does not require any training data from the user. One of the more dependable categorization algorithms created in recent years is the support vector machine (SVM). SVM is unique in that it processes data faster because to an efficient hyperplane searching technique that employs a limited training region. SVM is a binary classifier that accurately divides data points into two groups by identifying the optimal hyperplane.

It is becoming more and more crucial to have an accurate technique for measuring the direct runoff depth and peak flow rate from ungauged catchments in order to comprehend the effects of land use change on stormwater management, downstream water quality, and ecosystem services and functions (Lockaby et al., 2011; O'Driscoll et al., 2010; Walsh et al., 2016). Different models such as SCS-CN, Soil and Water Assessment Tool (SWAT), SWMM, The Hydrologic Engineering Center's-Hydrologic Modeling System (HEC-HMS), and MIKE System Hydrological European (Mike SHE), have been extensively used to assess the effects of land use changes on hydrologic processes (Chen et al., 2017; Liao et al., 2018). This demonstrates how hydrological models are a cost-effective way to evaluate the effects of changing land use and cover. For catchments worldwide, the rational method and/or the Soil Conservation Service-Curve Number (SCS–CN) methods are the most widely used classical techniques because they are straightforward, require less data, and have static assumptions for the estimation of direct runoff potential from rainfall (Hu et al., 2020; Moniruzzaman et al., 2020; Psomiadis et al., 2020). The SCS–CN method, now natural resource conservation service (NRCS) method, of estimating direct runoff from storm rainfall was the product of a major field investigation and the work of numerous early investigators (Andrews, 1954; Mishra & Singh, 2003). The hydrologic legacy that was established in the United States during the first part of the 20th century is directly descended upon by the method. The technique is mostly used to estimate runoff amounts in flood hydrographs. SCS-CN can be used in smaller, ungauged watersheds without measurable runoff data since it does not require the same stringent calibration as the other models (Zare et al., 2016).

The collection of statistical procedures known as regression analysis can be used to evaluate the associations between a dependent variable and one or more independent variables. It is the standard procedure for examining the connection between a quantitative result and a quantitative explanatory variable (Seltman, 2018). The most common form of regression analysis is linear regression, in which one finds the line combination that most closely fits the data according to a specific mathematical criterion.

1.2. Statement of the problem

The natural environment in an urban setting covered with impermeable surfaces, which causes surface water runoff's hydrological processes to deepen and accelerate. Building of streets, culverts, and dwellings may result in a decline in the groundwater table, a reduction in base flows during dry spells, an increase in storm flows, and a decrease in infiltration. Increased imperviousness will shorten the period of time that runoff concentrates after residential and commercial building development, resulting in larger peak discharges that happen sooner after rainfall begins in basins. In addition, urbanization significantly affects hydrology by affecting the kind of runoff and other hydrological features, supplying pollutants to rivers, and managing erosion rates (McGrane, 2016).

However, in many cases, runoff cannot be measured and must instead be calculated using various hydrologic models. It is necessary to estimate the runoff in order to ascertain and predict its impacts. Hydrologic modeling revolves around the difficulty of estimating runoff from a storm event (Jiang et al., 2015). Although it is rarely feasible for most sites to estimate direct rainfall runoff at the desired time, it is always efficient. Numerous Ethiopian cities and/or towns have had fast horizontal growth, but this growth has not been adequately managed due to inadequate planning, poor institutional capacity, and poor governance in the cities and/or towns. Therefore, unchecked, fast horizontal city/town growth toward rural villages led to more social, economic, environmental, and political issues (Terfa et al., 2019).

Although a considerable amount of previous research has explored the effects of land cover changes and associated surface modifications on hydrological regimes, most of these studies especially in Ethiopia, have investigated the impact on basin-scale that focused on characterizing the contributions of human activities to hydrological variations. Knowledge of the quantitative hydrological response to impervious surface dynamics remains limited though increased runoff usually accompanies urbanization.

Due to the town's growing economy and the high rate of people migration from rural to urban areas, the land cover surrounding the town has changed to urban land over time which led the town to face environmental and natural resource problems. This will enhance the surface's imperviousness while also reducing the amount of time that rainwater to seep into the ground and the concentration of runoff. Debre Markos is among the municipalities with the highest yearly rainfall levels that could potentially result in flooding. To link these changes, one has to a solid understanding of the many hydrological processes and their constituent parts. In the town, the relationship between urbanization and hydrological features were not well characterized. Similarly, it became harder to predict how LULC would change in the future and how runoff would behave, making it impossible to estimate the likelihood of flooding and prepare with the necessary measurements.

1.3. Objectives of the Study

1.3.1. General Objective

Generally, this study intended to analyze the impact of land use land cover change on surface runoff characteristics of Debre Markos town, Ethiopia.

1.3.2. Specific Objectives

The specific objectives of the study are to:

- analyze the changing trend of the land use land cover,
- predict the spatial extent of LULC in 2040,
- estimate the potential surface runoff characteristics in different spatial extent over the study area,
- evaluate the relationship between the LULC change and runoff characteristics.

1.4. Research Questions

The following research questions are developed in light of the above-mentioned specific objectives.

- How to assess the trends of the change in land use land cover?
- How the trends of change in the LULC and runoff for the future years are, predict?
- What impact does LULC modification have on the hydrological characteristics of watersheds?
- How the correlation between LULC change and runoff characteristics be evaluated?

1.5. Significance of the study

The hydrological cycle, the construction of hydrological infrastructure, and the topography of the drainage system are greatly influenced by rainfall-runoff process. The study that attempts to understand the dynamics of land use land cover and their impact on the environment would be beneficial to many sectors. Policymakers, urban planners, land administration, and environmental protection offices will be able to design and implement more sustainable urban planning strategies addressing current and future land use. Modeling information regarding land use land cover dynamics is essential to compare the past and present conditions, forecast future trends in the LULC change, and develop such a strategy of preserving the spread of informal settlements. Quantitative assessment of the impacts of urbanization on surface runoff is essential to-

- Understand town's watersheds yield and response; and early flood warning to reduce human casualties and harm to the environment and economy.
- Plan and evaluate water and soil conservation structures in the town.
- Provide guidance for town's storm flood management and urban planning.
- Understand urbanization effect on towns hydrological cycle.
- Provide appropriate environmental management policies and monitoring systems.

1.6. Scope of the study

The thematic scope of the study focused on assessing the trend of LULCC, predicting the future LULC, evaluating the effect of surface modification over the study period on runoff depth and flow rate, and evaluating the relationship of percent impervious area with surface runoff characteristics. The study's spatial scope is restricted to Debre Markos town, Ethiopia and its study time was limited between 1995 and 2022.

1.7. Limitation of the study

The issue was exacerbated and interpretation made more challenging by the existence of Landsat-7 picture strips and cloud cover on some downloaded satellite images. Another limitation of the present work is considering a single urban built-up LULC class. Because the study area meteorological station is ungauged, meaning there are no registered discharges data, an evaluation of the runoff model's performance was not executed. The combined effect of other natural and manmade factors like type of precipitation, deforestation, climate change etc. was not explored in this study.

1.8. Organization of the Thesis

This research study was divided into five chapters for ease of simplification: the study background, a problem statement, the objective of the study, the research questions, the study's importance, and its limits were all skillfully addressed in the first chapter. The definitions and concepts of LULC change, the use of remote sensing and GIS for LULC change detection, the introduction and use of the SCS–CN model, and an empirical review were covered in chapter two. In the third chapter, the study area, data sources, data processing and analysis techniques, and methodological flow were all given in an organized manner. Chapter Four included an examination of the results and discussion, maps and graphical presentations, LULC change data, accuracy evaluation, LULC changes analysis, and runoff characteristics and how they relate to LULC changes. Ultimately, the study's conclusions and suggestions were provided in chapter five.

1.9. Definition of Basic Terminologies

Land cover is the physical state of the land surface such as cropland, forests, and wetlands, buildings, pavements, soil type, biodiversity, surface water and groundwater (Parveen et al., 2018).

Land use is the way in which human beings exploit the land and its resources including agriculture, urban development, grazing, logging and mining (Kaiser, 2020).

Surface runoff is the unconfined flow of water over the ground surface (Rumynin, 2015).

Change detection is the technique of spotting changes in land use and land cover over time (Chughtai et al., 2021).

Curve Number is an empirical parameter used in hydrology to predict direct runoff or infiltration from rainfall excess (Soomro et al., 2019).

Potential maximum retention (S) is represents the maximum amount of rainfall that a watershed can retain before any runoff occurs (Lee et al., 2023).

Hydrologic soil group (HSG) is a classification known as the offers an indicator of how quickly water percolates through a soil (Zeng et al., 2017).

Antecedent moisture condition (AMC) he relative wetness or dryness of a watershed or sanitary sewer shed prior to a rainstorm event (N. W. Thomas et al., 2021).

Chapter Two

2. Review of Related Literature

Food and Agriculture Organization (FAO) describes the land as “a delineable area of the earth's terrestrial surface, encompassing all attributes of the biosphere immediately above or below the surface. This surface including those of the near-surface climate (the soil and terrain forms, the surface hydrology including shallow lakes, rivers, marshes, and swamps), the near-surface sedimentary layers and associated groundwater reserve, plants and animals, the human settlement pattern and physical results of human activity (terracing, water storage or drainage structures, roads, buildings etc.)” (FAO, 2022).

2.1. Land use land cover

Despite having distinct meanings, the phrases "land use" and "land cover" are sometimes used synonymously. While land cover refers to the physical features of the Earth's surface, land use is the term used to describe how humans utilize the land, primarily in relation to its functional role for economic activity (Mariye et al., 2020). "The arrangements, activities, and inputs people undertake in a certain land cover type to produce, change, or maintain it" is how the FAO defines land use in formal terms (Kutter & Neely, 1999). According to Turner et al., (1994), Land cover is the biophysical state of the earth’s surface and immediate subsurface. Land cover, therefore, includes the quantity and types of all features over the earth such as vegetation, water, soil, artificial surfaces, etc. Turner et al., (1994) further add that land use involves the intent or purpose for which land is utilized. Another term for this process is "biophysical manipulation," which refers to how people use the land to accomplish their goals. Although land use and land cover are related, it should be remembered that one land cover might be able to sustain more than one land use, and vice versa. For example, a grassland land cover can support multiple land uses, including grazing and recreation, while a single land use can occur on multiple land covers.

Land use and land cover transition, according to Lambin et al., (2003), is a dynamic phenomenon that can be caused by reciprocal relationships between environmental and societal variables at different spatial and temporal scales. Land use land cover transition can be classified as either direct (proximate) or indirect sources (Verburg et al., 2002). While land use and land use change will require additional socioeconomic data and methods to ascertain the activities occurring on the landscape, land cover can be estimated by examining remotely sensed pictures such as satellite images or aerial photos (Ellis &

Pontius, 2007). Since LULC has a significant impact on infiltration processes and direct runoff estimation, it is regarded as the primary input for the NRCS-CN technique (Dunjó et al., 2003; Garg et al., 2013; P. Kumar et al., 1991)

2.2. Urbanization and urban growth

Urbanization is the term used to describe the expansion of towns and cities, frequently at the expense of rural areas, as people migrate to these areas in pursuit of employment and the hope of a better life, hence fostering the growth of towns and cities. Another way to describe it is as the steady rise in the population of towns and cities. The idea that urban areas have made more progress in terms of economy, politics, and society than rural ones has a big impact on it (Bhatta et al., 2010). urban expansion is a demographic and spatial phenomenon that describes how important towns and cities have become as hubs for a certain economy and society (Bhatta et al., 2010). there are three distinct and well researched ideas of urban growth that are connected to population change, economic performance, and the geographical extension of urban regions in the literature on urban and regional planning (Reis et al., 2016). Migration and demographic trends are the main topics of the socio-demographic aspect of urban expansion. The first takes into account the rate of natural population increase, which is mostly determined by fertility and death rates, while the second is based on a city's ability to draw people from nearby cities or rural areas (Rieniets, 2009; Turok & Mykhnenko, 2007).

2.2.1. Trends of urban growth in the world

The world is becoming more urbanized at a rapid rate, and cities are being affected by the dynamic processes of globalization and urbanization (Haase et al., 2018a). According to (Haase et al., 2018b), Prior to 1950, the Organization for Economic Cooperation and Development (OECD) countries' changes were used to assess trends in global urbanization. Urbanization as a percentage of the world's population has been increasing quickly, and as of right now, a higher percentage of people live in cities (United Nations, 2007). Urbanization is not just a contemporary phenomenon; rather, it is a historic and swift change of human social roots on a worldwide scale, with urban culture quickly displacing rural culture (Pawan, 2016).

Globally, the number of people living in cities increased dramatically from 751 million in 1950 to 4.2 billion in 2018. Currently, 55% of people on Earth reside in urban areas; by 2050, this percentage is predicted to rise to 68%. According to new estimates, urbanization-the gradual movement of people from rural to urban areas-combined with global population growth may result in the addition of 2.5 billion more people living in urban areas by 2050, with nearly 90% of this growth taking place in Asia and Africa (United Nations, 2018). Industrialization and financial progress have led to urbanization in the developed world of North America and Europe. In contrast, it has happened as a result of the demographic phenomena in developing countries in Latin America, Africa, and Asia (Achamyeleh, 2014).

2.2.2. Trends of urban growth in Africa

According to Jelili, (2012), Africa used to be, and perhaps is still, the least urbanized continent, with growth rates of cities close to, if not the fastest in the world. But, today, in virtually every part of the continent, new cities have emerged, while the old ones have drastically expanded, some of which have become mega-cities. By 2030, for the first time in history, more of the continent's people will be living in urban areas than in rural regions and by 2050 an estimated 1.23 billion people, or 60% of all Africans will be city dwellers. Currently, even if the level of urbanization in Africa is low, the rate of urbanization is high due to population growth, which is one of the most important driving forces of change in any urban system. If the urban population swells, the city must expand upward or outward. Along with economic development and technological revolution, rapid urban growth can be characterized by the development of suburban expansion and redevelopment in city centers (Rui & Ban, 2016).

2.2.3. Trends of urban growth in Ethiopia

Ethiopia is the second most populous country in Africa next to Nigeria with a population estimated at 99.39 million in 2015 of which 19.4% live in urban and peri-urban areas (Central Statistical Agency, 2013). In 2015, nineteen million people were added to the population of 2007. The number of population is growing by the rate of 2.9% per year and is expected to nearly double in less than 33 years to around 185 million in 2050 (Efrem & Tesfaunegn, 2017). The country has the lowest number of urban dwellers residences compared to Sub-Saharan standards of a percentage of the total population residing in cities and urban settings, despite indications displaying a rapid rate of urbanization in the pace at which people are relocating to urban centers. The projection made by the ministry of urban development and housing indicates that the number of urban populations by 2025 is expected to reach between 30-35 million (27 to 30% of the total population). By 2037, the urban population will be 42.2 million (40% of the total population). This means that the urban population of Ethiopia will increase between 2015 and 2037 by as much as 39 million and that the urban population expansion accounts for around 75% of the total population increase of over 50 million during this period. Date back to the country level of urbanization, it was about 5% in the 1950s, and 10% in the 1970s, and about 13% in 1984, and reached 19% in 2014 has grown by 6% between 1984 and 2013 and this reflects an average increase of 2% per decade (Pieper & Hakalin, 2018).

The rate of urbanization in Ethiopia is one of the quickest in Africa. The normal yearly rate of development from 1960-1991 was 4.8 percent and this figure developed to 5.8 percent per annum from 1991-2000. Likewise, the yearly development rate from 2000-2010 was 5.5 percent, and abatements to 4.73 in 2017 (Mekuriaw & Gokcekus, 2019). This rate of development puts Ethiopia among the 23 quickly urbanizing nations of the world. According to (B. Cohen, 2006; Redman & Jones, 2005), the principal reasons for raising the level of urbanization and city growth are population growth, rural-urban migration, and geographical expansion of urban areas through annexation and transformation and re-classification of the rural village into small urban settlements. Associated with the rapid expansion of urbanization, a lot of land has been converted from rural to urban. Rapid pass of urbanization is passing major challenge in front of cities in developing countries. One of the significant difficulties in urban extension is an inescapable result of the urbanization process (Dadi et al., 2016; Firew Bekele, 2010).

2.2.4. Trends and Growth of Debre Markos Town

According to the state of Ethiopian cities report provided by the Ministry of Urban Development and Housing MOUDH, (2015), based on the 2007 census, the CSA officially recognized 973 urban centers in Ethiopia. From these urban centers, Debre Markos is one of the oldest and fastest-expanding town in the country.

The conversion of farmland and forest areas into different urban land uses, such as residential, commercial land, and other activities are the main ones. Concerning the settlement pattern of the town, it has more of a linear settlement form (Tigezaw, 2014; Ziena, 2017). Because of the present physical expansion of the town, various types of vegetation, agricultural lands, wetlands, and grasslands are converted into urban land uses (Tigezaw, 2014; Ziena, 2017). Deforestation has also been taking place at an alarming rate due to residential and other alternative investment uses. From 1998 up to 2017 above, 4850 hectares of agricultural land were converted to urban uses (Tigezaw, 2014; Ziena, 2017).

2.3. Land use land cover change and its drivers

LULC change involves a conversion from one LULC to another or intensification of the present or current LULC (Turner et al., 1994). Analyzing LULC change is extremely important for a better understanding of landscape dynamics over a known time period (Rawat & Kumar, 2015). It is one of the most precise techniques to understand the land condition in the past, the types of changes to be expected in the future, as well as the driving forces behind the changes (Dinka, 2012). Information on LULC change offers a full understanding of the interactions that are important for sustainable land resource management (Mmbaga et al., 2017).

Different researchers consider LULC change as the result of different main deriving factors (Lambin et al., 2003; Mather & Needle, 2000). The changes in LULC are determined by how individual landowners, communities, businesses, and governments control land use and make decisions on how to use land. Such decisions are influenced by the interactions between socioeconomic factors such as population and environmental factors that vary at different scales (Lambin and Geist, 2007). (Briassoulis, 2019) further clarifies that environmental drivers do not have a direct impact on land use change but influence land cover change that in turn influences land managers' decisions. As a result, LULC adjustment can be modeled as a function of "moving forces" (socioeconomic and environmental variables). According to (Mather & Needle, 2000), population growth is the single most influential factor for LULC change and the resulting land degradation. The study made by (Wang et al., 2008) indicated socioeconomic development as the main driving force of LULC change in the Tibetan Plateau, China. Other scholars (Garedew et al., 2009; Geist & Lambin, 2002; Tole, 2004) suggested that LULC change is due to the combined effects of anthropogenic activities such as the expansion of farmland and extraction of woods and fundamental social processes such as population growth, policy/institution and cultural factors. Lambin et al., (2003) concluded that neither population nor poverty alone constitutes the major underlying causes of LULC change worldwide. They concluded that the main driver of LULC change is peoples' responses to economic opportunities facilitated by institutional factors.

The reasons that drive LULC transition can both be classified as proximate or underlying, with the former referring to direct adjustments made by individuals on a small scale, such as individual farms, and the latter referring to subtle changes that arise at a larger scale (Lambin and Geist, 2007). Proximate driving factors usually caused by human activities such as infrastructure and agriculture expansion whereas underlying factors are caused by complex interactions between social, political, demographic, and environmental variables (Lambin et al., 2001). The rising of human and livestock populations, traditional agricultural practices, unregulated urbanization, ongoing drought, ineffective land use policies or their complete absence, inadequate implementation of the existing policies and strategies, and ineffective land use planning has been identified as the main drivers of LULC change in Ethiopia (Bewket & Abebe, 2013; Kindu et al., 2015). LULC change is the main source of land degradation, which results in various hydrologic consequences (flooding, erosion, and drought). In highland areas, land degradation usually results in increased surface runoff and soil erosion.

2.3.1. Land use land cover change detection

Change detection is the method of detecting changes in the status of an object or phenomenon by analyzing them at various times using remote sensing technique (Singh, 1989). Change detection involves applying multi-temporal remote sensing information to analyze the historical effects of an occurrence quantitatively and thus helps in determining the changes associated with land cover/land use properties regarding the multi-temporal datasets (Seif & Mokarram, 2012; Zoran & Anderson, 2006).

Change detection has a wide range of applications in different disciplines such as change analysis, forest management, vegetation phonology, risk assessment, urban expansion, seasonal changes in pasture production, and other environmental changes (Singh, 1989). Change analysis of features of Earth’s surface is essential for a better understanding of interactions and relationships between human activities and natural phenomena. This understanding is necessary for improved resource management and improved decision-making (Lu et al., 2004; Seif & Mokarram, 2012). To be useful, a change detection study should include the following elements: area change and rate of change, the spatial distribution of modified forms, land cover change trajectories, and precision evaluation of change detection effects.

2.3.2. Application of remote sensing and GIS on change detection

Remote sensing (RS) is defined as the science of obtaining information about an object, area, or phenomenon through the analysis of data acquired by a device that is not in contact with the object, area, or phenomenon under investigation (Bawahidi, 2005). It provides a large amount of data about the earth's surface for detailed analysis and change detection with the help of sensors. Most of the data that used as input to the hydrological model are extracted directly or indirectly from remotely sensed data. Some of the important data used in hydrological modeling that obtained from remote sensing include Landsat images, digital elevation model (DEM), and land cover maps. Some of the applications of remote sensing technology in mapping and studying the LULC changes are - mapping and classifying the LULC, assessing the spatial arrangement of LULC, allowing analysis of time-series images that used to analyze landscape history, report and analyze the result of inventories. It also provides data that used as inputs to GIS and is a basis for model building. All the input parameters of NRCS-CN method can be easily derived from RS data and can efficiently manage in GIS environment.

Land use land cover is changing rapidly in most parts of the world. In this situation, accurate, meaningful, and available data is highly essential for planning and decision-making. Remote sensing is particularly attractive for the land cover data among the different sources. Stefanov et al., (2001) reported that in the 1970s satellite remote sensing techniques started to be used as a modern tool to detect and monitor land cover change at various scales with useful results. Betru et al., (2019)showed that the information on LULC change that extracted from remotely sensed data is vital for updating land cover maps and the management of natural resources and monitoring phenomena on the surface. The importance of land cover mapping is to show the land cover changes in the watershed area and to divide the LULC into different classes. For this purpose, remotely sensed imagery plays a great role in obtaining information on both temporal trends and spatial distribution to project land cover changes and to support changes impact assessment (Atasoy et al., 2006). To monitor the rapid changes in land cover, classify the types of land cover, and obtain timely land cover information, multi-temporal remotely sensed images are considered as effective data sources. Geographic information system also supports the change detection process by storing, managing, analyzing, editing, output, and visualizes geographic data (Chang, 2016; DeMers, 2009).

2.4. Image Classification

In remote sensing, classification entails grouping/clustering the pixels of an image into a limited number of classes, with pixels in the same class possessing identical properties. The bulk of image classification relies on the identification of land cover class spectral response patterns (Brito & Quintanilha, 2012). Supervised and unsupervised classifications are the two primary methods to differentiate these approaches. Parallelepiped, maximum probability, minimal lengths, and Fisher classifier methods are some of the sub-classification methods in supervised classification.

To classify pixels in an image, supervised classification is a technique in remote sensing which used a set of training data that consists of samples of each land cover type that the user wants to map. The training samples from the image were manually selected by the user based on the recommendation of Sertel & Akay (2015) and assign them to their respective land cover classes. To classify the remaining pixels in the image the classifier then uses these training data. Since the user has control over the classification process, supervised classification is a more accurate approach than unsupervised classification. However, supervised classification requires more effort and expertise to select the training samples and assign them to the correct classes. The main advantage of supervised classification is that it allows for accurate and efficient classification of large areas. In addition, this flexible technique can be used in a variety of applications.

Unsupervised classification is a technique in remote sensing where the classification algorithm automatically groups pixels with similar spectral properties into clusters. The user does not need to provide any training data to the algorithm. Instead, the algorithm analyzes the spectral properties of the image and identifies clusters of pixels with similar spectral properties. Due to the user does not need to provide any training data, unsupervised classification is a faster and easier approach than supervised classification. However, it is less accurate than supervised classification because the algorithm does not have any information about the land cover types.

Support vector machine (SVM) is a non-parametric classifier and is one of the more reliable classification techniques that have been developed in recent years. Non-parametric classifiers do not base classification on a normality assumption or statistical parameters whereas parametric classifiers such as maximum likelihood assumes that the data is normally distributed (Phiri & Morgenroth, 2017). The technique can develop effective decision boundaries and hence reduce misclassification though being non-parametric (Bahari et al., 2014). The classifier can be expanded from binary to multiclass using a variety of strategies, including one versus all and one against one (Kohram & Sap, 2008). SVM can categorize data in both linear and nonlinear ways. For nonlinear data, the kernel function is utilized (Kohram & Sap, 2008; Mountrakis et al., 2011). SVM can easily handle multiple continuous and categorical variables. The method avoids the problem of overfitting and makes no assumptions about the data type. The core idea of SVM is to find a maximum marginal hyperplane (MMH) that best divides the dataset into classes and used to minimize an error. It uses a small training area and hence takes less time to process. When SVM compared with many classification approaches such as discriminant analysis, decision trees, and feed forward neural networks, it produced the best results (Foody & Mathur, 2004).

Table 2.1: Description of identified LULC classes

LULC class	Description
Urban Area	A land dominated by houses, roads, and sheds in rural villages (also including commercial areas, urban and rural settlements, and industrial areas).
Vegetation	Area covered by plantation and natural trees. Areas covered by forest, scattered small trees, shrubs, and bushes and mixed with grass vegetation. Green spaces in urban areas are also included in this class.
Agricultural Land	Areas of land prepared for growing crops. This category includes areas currently under crop and land under preparation.
Barren Land	Open space, exposed soils, abandoned land, non-vegetated areas dominated by rock outcrops, and eroded and degraded lands.
Meadow	Permanent and seasonal wetlands, low-lying areas, marshy land, rills, gully, and swamps with small green plants or grasses.

2.5. Land use land cover change prediction

Dynamic urban land use land cover change processes caused due to human activities have a wide range of effects on global climate change and land cover change either directly or indirectly (Lambin et al., 2001). It also affects human and natural systems and contributes to changes in direct surface runoff. Land use modeling is a very essential step for further improvement of urban planning and land use management. Diverse land use models that used in the land use land cover analysis have developed by the research community (Verburg et al., 2002). Modeling land use land cover changes for future time is important to know the possible scenarios. The model is run for change prediction to a specified future date for the allocation of land cover changes (Sankarrao et al., 2021). Population growth, economic activity, biophysical conditions and geographic scale are some driving variables that led to future LULC change (Meyfroidt et al., 2013).

Therefore, understanding the earlier and current LULC changes and simulating for the future is vital for the management of land and water resources (Sohl et al., 2012). The analysis of LULC change and prediction of future land use also have vital role to understand the dynamics of human environment interactions and environmental management interventions (Leta et al., 2021). Because of the significance impacts of land use land cover changes, the use of land use change models become important to understand these changes and driving factors (Verburg et al., 2004).

The rising awareness and importance of land use models in the LULC research community has led to the development of a wide range of land use change models (Verburg et al., 2002). In recent years, numerous models such as the Markov Chain (MC) model, Cellular Automata (CA) model, Land Change Modeler (LCM) and the Conversion of Land use and its Effects (CLUE) model, has developed to predict the LULC and their change detections (Alam et al., 2021). Spatial allocation models have been developed to identify neighborhood conditions that have connections with land conversion specifically for residential and commercial development. Agent-based models characterize systems in terms of independent but interconnected agents that have the ability to make decisions based on changing conditions. For most of the agent-based models that used for land use modeling, higher temporal complexity could be taken as an accurate criterion to be chosen (Parker, 2005).

2.6.1. Cellular Automata (CA) Model

Cellular Automata (CA) was a discrete dynamic system in which space divided into regular spatial cells and time progresses in discrete steps. Based on transition rules, which determine how a cell will evolve under certain conditions for simulation processes, CA models can generate complex global patterns. These models have been widely used for simulating urban sprawl and land use dynamics (Cao et al., 2013). Among the several spatiotemporal dynamic modeling approaches, CA model has been frequently used for land use change analysis. To estimate potential LULC changes number of researchers used Modules of Land use Change Evaluation (MOLUSCE); a new QGIS plugin that built with CA model and include a transition probability matrix (M. T. U. Rahman et al., 2017). In this plugin, Artificial Neural Networks (ANN), Logistic Regression (LR), Multi-criteria Evaluation (MCE), and Weights of Evidence (WoE) are well-known algorithm. A CA-ANN model in MOLUSCE is a reliable tool for predicting future LULC that may be utilize in land use planning and management. This approach also used to predict the spatial LULC shift because it estimates the pixel's current condition based on its initial situation, adjacent neighborhoods eventuality, and changeover laws. Moreover, this accurately depicts nonlinear spatial stochastic LULC change processes and produces complex patterns (Saputra & Lee, 2019). The spatiotemporal complexity of urban areas and deforestation caused by natural disasters or human actions can be replicate by CA model (Saputra & Lee, 2019). The main intentions of MOLUSCE was to study temporal LULC shifts and project future land use, anticipate prospective shifts in land cover, and detecting deforestation (Aneesha Satya et al., 2020).

2.6.2. Markov Chain (MC) model

Markov chain models are relatively simple and more powerful to model complex processes and changes in land use for planning purposes. They provide better information for analyzing time series of system evolution (Levinson & Chen, 2005). A Markovian process is one in which the state of a system at time t_2 can be predicted by the state of the system at time t_1 given a matrix of transition probabilities from each cover class to every other cover class. Since it integrates a transition probability matrix, a stationary property is one of the importance of these models. This property is critical to Markov chain model especially for future predictions of land use. The stationarity of the transition matrix in turn helps to inspect the validity of the model (Iacono et al., 2012). The Markov module in IDRISI can be used to create such a transition probability matrix (Subedi et al., 2013).

2.6.3. Land Change Modeler (LCM)

To examine the historical change and predict the future changes of LULC many researchers use the land change modeler (LCM) that embedded in the TerrSet model. Clark Labs developed it for assessing a variety of land change scenarios and contexts. LCM primarily uses the Multi-Layer Perceptron Neural Networks (MLPNN) for a spatial allocation of simulated land cover scores and Cellular Automata-Markov Chain (CA-MC) approach for time prediction (Eastman, 2012). The model is strong due to its dynamic projection proficiency, suitable calibration, and capability to simulate several types of land cover (Memarian et al., 2012). LCM evaluates changes of the land use of two different periods, determines and visualizes the changes, and presents the results with various maps and graphs. In LCM, according to (Eastman, 2012), tools for the assessment and prediction of land cover change and its implications are organized around major task areas: change analysis, change prediction, habitat and biodiversity impact assessment and planning interventions. In addition, there is a facility in LCM to support projects aimed at

Reducing Emissions from Deforestation and Forest Degradation (REDD). The REDD facility uses the land change scenarios produced by LCM to evaluate future emissions scenarios.

2.6. Impacts of land use land cover change on the hydrologic regime

Seasonal and annual distribution of stream flow within a watershed could be affected by urbanization, deforestation, and other land use practices. LULC changes have been responsible for altering the hydrologic response leading to impact river flow (Getachew & Melesse, 2012). As Woldeamlak, (2002) described, land under little vegetation cover more subjected to high surface runoff and low water retention. According to Legesse et al (2003), vegetation cover increases evapotranspiration and decreases annual river flow. In addition, curve numbers that result in changing rainfall-runoff response can be affected by vegetation cover change. Therefore, land cover change interferes with the land phase of the hydrologic cycle. The competing process may results in either an increase or decrease in dry season flow (Calder, 2002).

2.7. Runoff

Surface runoff refers to the portion of rainwater that is not lost to interception, infiltration, and evapotranspiration (Solomon H., 2005). Runoff or stream flow comprises the gravity movement of water in channels that may vary in size. Runoff is the part of precipitation that exits the basin as a stream flows at a concentrated point. In any hydrologic study, runoff is an important component contributing significantly to the hydrological cycle, to design hydrological structures and morphology of drainage systems, and to determine the risk of flood. Runoff is formed when excessive rainfall exceeds ground storage capacity, once the runoff becomes extreme due to high intensity of rainfall as well as poor basin and drainage system, water will overflow and flood the lower basin areas (Ulbrich et al., 2003). Flood is one of the worst natural disasters in world history besides tsunami and earthquake (Abbott, 2008). The ‘infiltration-excess runoff’ and the ‘saturation-excess runoff’ concepts are responsible for runoff generation. The infiltration-excess runoff concept assumed that the overland flow occurs only when the rainfall intensity is greater than the infiltration rate at the soil surface. The second type of runoff generation also occurs when the soil surface is saturated and any further rainfall, even at low intensities, generates runoff that contributes to stream flow. Natural influences and human activity influences are the two major environmental conditions that affect interception, infiltration, and evapotranspiration processes. Natural processes can have a variety of influences, but human activity typically results in less water entering the soil profile and thus more runoff at the ground surface.

Runoff is one of the basic and crucial hydrological data that needed in water resources planning and management e.g. flood mitigation measures, waterways, storage capacity, and erosion control. However, the runoff measurement is difficult and expensive to conduct, runoff information is critical for basin management in preventing the loss of human life and damage to the economy and environment. In-situ measurements are preferable due to high accuracy, but the methods are constrained by time and area to conduct the measurement. However, the conventional measurement is also time-consuming, expensive, and difficult. Therefore, many researchers and managers preferred to use runoff empirical modeling e.g. SCS–CN (Dhawale, 2013; Tejaswini et al., 2011) and Rational Method (Erena & Worku, 2019; Guo, 2001), where these methods produced high accuracy results beside their simplicity, reliability, less time-consuming and require fewer data to estimate runoff for the ungauged basin.

2.7.1. Factors Affecting Runoff

Many site-specific factors have a direct relation with the occurrence and depth of runoff. The major factors are listed below.

Vegetation: The amount of rain lost to interception storage on the foliage depends on the kind of vegetation, which acts as an erosion-retarding factor, and its growth stage. Forests and grasses provide better cover than cultivated crops. Dense vegetation covers intercept and absorb the force of rainfall and amount of energy. In addition, the root system as well as organic matter in the soil increases the soil porosity thus allowing more water to infiltrate into the ground (Pedroza-Parga et al., 2022). Forests are checkers of soil erosion. Protection is large because of under-store vegetation and litter, and the stabilizing effect of the root network. On steep slopes, the net stabilizing effect of trees is usually positive. Vegetation cover can prevent the occurrence of shallow landslides (Phillips et al., 2021). Afforestation does not necessarily decrease soil erosion. Splash erosion may increase substantially when litter is cleared from the forest floor (Fernández-Raga et al., 2017). The spectrum for the size of the drops that are formed by the canopy varies widely among different species, resulting in large differences in the potential of splash erosion (A. Thomas et al., 2021). Deforestation may increase erosion. The actual soil loss, however, depends largely on the use to which the land put after the trees have been cleared.

Catchment extent: In general, the volume and peak rate of runoff increase with the catchment area increase. However, for the same rainfall event, a long narrow catchment would be expected to have a lower peak rate of runoff than a more compact or circular one of the same area. In the longer catchment, it takes more time for the runoff from the most remote part of the catchment to reach the outlet (Edokpa et al., 2022). The runoff efficiency (volume of runoff per unit of area) increases with the decreasing size of the catchment i.e. the larger the size of the catchment the larger the time of concentration and the smaller the runoff efficiency.

Slope: Slope accelerates erosion as it increases the velocity of flowing water. Small differences in slope make a big difference in damage. According to the laws of hydraulics, a four-time increase in slope doubles the velocity of flowing water. This doubled velocity can increase the erosive power four times and the carrying capacity by 32 times. Investigation on experimental plots has shown that steep slope plots yield more runoff than those with gentle slopes. In addition, it was observed that the quantity of runoff decreased with slope length to some extent (X. Li et al., 2020).

Climate: climate factors include types of precipitation, rainfall intensity, rainfall duration, rainfall distribution, and direction of prevailing wind. Types of precipitation have a great effect on the runoff. For example, precipitation that occurs in the form of rainfall starts immediately as surface runoff depending upon rainfall intensity while precipitation in the form of snow does not result in surface runoff and if the rainfall intensity is greater than the infiltration rate of soil then runoff starts immediately after rainfall. While in case of low rainfall intensity, runoff starts later. Thus, high intensities of rainfall yield higher runoff. In addition, the duration of rainfall is directly related to the volume of runoff because the infiltration rate of soil decreases with the duration of rainfall. Therefore, medium-intensity rainfall even results in a considerable amount of runoff if the duration is longer. Runoff from a watershed depends on the distribution of rainfall. It is also expressed as ―the distribution coefficient mean ratio of maximum rainfall at a point to the mean rainfall of the watershed. Therefore, near the outlet of watershed runoff will be more. Also, the direction of the prevailing wind is the same as the drainage system, it results in peak flow. A storm moving in the direction of the stream slope produces a higher peak in a shorter period of time than a storm moving in the opposite direction.

2.8. Runoff characteristics estimation methods

Runoff is one of the most important hydrologic variables used in most water resource applications (Yigrem, 2008). Rainfall is the primary source of water for runoff generation over the land surface. Hydrological models are means to represent hydrological processes at the basin level and evaluate conditions for purposes of water resources management. Conceptual models are the simple manner in which they represent and simulate processes. They can also support prediction and decision-making processes. For example, they can be used to estimate projected hydropower generation under climate change conditions (Parra et al., 2018). to predict the hydrological components of ungauged watersheds (Devia et al., 2015), and evaluate the effects of wildfires (Moussoulis et al., 2015) or land use changes (Younis & Ammar, 2018).

There are two general runoff computation methods to be used to compute runoff characteristics. These are the NRCS methodology, which consists of several components, and the Rational Method (and the associated Modified Rational Method), which are generally limited to drainage areas less than 20 acres. The USDA Natural Resources Conservation Service (NRCS) methodology is perhaps the most widely used method for computing stormwater runoff depth, flowrates, volumes, and hydrographs. It uses a hypothetical design storm and an empirical nonlinear runoff equation to compute runoff volumes and a dimensionless unit hydrograph to convert the volumes into runoff hydrographs. The methodology is particularly useful for comparing pre- and post-development peak rates, volumes, and hydrographs. The key component of the NRCS runoff equation is the NRCS Curve Number (CN), which is based on soil permeability, surface cover, hydrologic condition, and antecedent moisture.

The disadvantages of the NRCS-CN method include a single parameter containing a variety of factors (such as land use, soil type, antecedent water condition, and surface conditions) rendering the method very delicate, the influence of spatial scale, intensity, and temporal distribution of rainfall and the effect of adjacent moisture condition are not considered.

2.8.1. Rational method

The rational method uses an empirical linear equation to compute the peak runoff rate from a selected period of uniform rainfall intensity. Originally developed more than 100 years ago, it continues to be useful in estimating runoff from simple, relatively small drainage areas such as parking lots. Use of the rational method should be limited to drainage areas less than twenty acres with generally uniform surface cover and topography. It is important to note that the rational method can be used only to compute peak runoff rates. The peak rate or discharge influenced primarily by the rainfall's distribution, which is how the rainfall rate or intensity varies over time. The method assumes a constant rainfall of intensity 'i' for a duration of Tc (hr); thus, the total rainfall depth is rainfall intensity multiplied by its duration. Since it is not based on a total storm duration, but rather a period of rain, that produces the peak runoff rate, the method cannot compute runoff volumes unless the user assumes a total storm duration.

The modified rational method is a somewhat recent adaptation of the rational method that can be used not only to compute peak runoff rates, but also to estimate runoff depth, volumes, and hydrographs. The product of the drainage area and the total rainfall depth is the volume of rainfall in inches that is available for runoff. The runoff coefficient (C) determines the proportion of the rainfall volume that appears as runoff. This method uses the same input data and coefficients as the rational method along with the further assumption that, for the selected storm frequency, the duration of peak-producing rainfall is also the entire storm duration.

2.8.2. SCS–CN method

Several runoff computation methods use the overall NRCS methodology. The most commonly used methods are the June 1986 Technical Release 55 (TR-55) – urban hydrology for small watersheds, the April 2002 WinTR-55 – small watershed hydrology computer program, and Technical Release 20 – computer program for project formulation

As there is a scare in the availability of runoff data in many sites, hydrologists have developed indirect methods to determine the runoff to accelerate the program of watershed management for conserving and developing water resources management. Many methods are used to estimate the runoff; the Soil Conservation Service Curve Number (SCS–CN) method is widely used and gives a reliable result compared with other methods. SCS model was developed by the U.S. Soil Conservation Service in 1972 and is known as the Hydrologic Soil Cover Complex Model or Natural Resources Conservation Service Curve Number method (NRCS–CN). The Natural Resource Conservation Service-Curve Number (NRCS-CN) is a very popular and widely used method of estimating rainfall excess from rainfall and relies on only one parameter, i.e., curve number (CN). SCS–CN method is an acceptable tool in hydrology and its responsiveness to four important catchment properties, i.e. land use, soil type, antecedent moisture condition, and surface condition. The method combines the watershed parameters and climatic factors in one entity called the curve number. SCS–CN is the most used method for runoff modeling and estimating runoff at various spatial scales (Wang et al., 2012).

Several studies have demonstrated that the SCS–CN model is effective in determining surface runoff in highly urbanized areas where the runoff potential is very high even in very small watersheds (Cho & Engel, 2018). Moreover, it is applicable for areas with ungauged catchments where it is difficult to obtain the actual hydrological data (Ozdemir & Elbaşi, 2015). Hence, this model estimates the potential surface runoff by integrating LULC classes, HSG layers, and rainfall data (Ara & Zakwan, 2018; A. Kumar et al., 2021). SCS–CN provides an empirical relationship for estimating initial abstraction and runoff as a function of soil type and land use. Rainfall-runoff relationship can be visualized by factors such as initial abstraction (Ia), direct runoff (Q), and actual retention (F). Due to its versatility, SCS-CN 1972 model has been widely used globally for water resources management, urban stormwater modeling, and runoff estimation that occurs during 24 hours, giving information on the amount of rainfall and site conditions (A. Kumar et al., 2021; Xiao et al., 2011).

2.8.2.1. The Curve Number (CN)

The Curve Number (CN) is an index developed by the Natural Resource Conservation Service (NRCS), to represent the potential for stormwater runoff within a drainage area with fewer calculation parameters and observation data (Ponce & Hawkins, 1996). Due to its low input data requirements, the SCS-CN method can also be applied to hydrological forecasts of ungagged watersheds (Shrestha, 2018). The curve number is an empirical dimensionless parameter indicating the runoff response characteristic of a watershed. In the SCS–CN Method, this parameter is related to land use, land treatment, hydrological condition, hydrological soil group, and antecedent soil moisture condition in the watershed. Information on soil types and land use are combined to provide an overall rating for the site (the curve number, CN), which is then used to predict the runoff depth ‘Q’ from a given rain depth ‘P’. Theoretically, the curve number ‘CN’ can range from 0 to 100; the potential maximum retention ‘S’ can vary between zero and infinity. For paved areas, for example, ‘S’ will be zero and CN will be 100; all rainfall will become runoff. For highly permeable, flat-lying soils, ‘S’ will go to infinity and CN will be zero; all rainfall will infiltrate and there will be no runoff.

The CN values for an ungauged catchment are derived from lookup tables based on the soil hydrologic group (a function of soil type and land cover/ land use), and antecedent moisture condition (AMC) (Cronshey, 1986). The relationship between the CN value and the various Hydrological Soil-Cover Complexes is usually given for average conditions, i.e. Antecedent Soil Moisture Condition Class II. Secondly, when the antecedent moisture condition classified as either Class I or Class III, there is a conversion table for the CN value based on 5-day antecedent rainfall data. The looking tables suggested by Cronshey, (1986) to determine curve numbers have in common that slope is not one of the parameters. The reason is that in the United States, cultivated land in general has slopes of less than 5%, and this range does not influence the curve number largely. However, under East African conditions, for example, the slopes vary much more. Five classes to qualify the slope were therefore introduced (Záruba & Mencl, 1982) : < 1% Flat; 1- 5% Slightly sloping 5 - 10% Highly sloping 10 - 20% Steep, and > 20% Very steep.

The category land use or cover was adjusted to East African conditions and combined with the hydrological condition. With the aid of looking tables, one can estimate the curve number for a particular watershed. The procedure is as follows: - Assign a hydrological soil group to each of the soil units found in the watershed - Make a classification of land use, treatment, and hydrological conditions in the - Delineate the main soil-cover complexes by superimposing the land use and the - Calculate the weighted average CN value according to the areas they represent.

2.9. Hydrological Soil-Cover Complex

To determine the appropriate CN value, various tables can be used. Firstly, there are tables relating the value of CN to land use or cover, treatment or practice, hydrological conditions, and hydrological soil groups. Together, these four categories are called the Hydrological Soil-Cover Complex.

2.9.1. Hydrologic Soil Groups (HSG)

Soil properties greatly influence the amount of runoff. In the SCS method, these properties are represented by a hydrological parameter: the minimum rate of infiltration obtained for bare soil after prolonged wetting. The influence of both the soil’s surface condition (infiltration rate) and its horizon (transmission rate) are thereby included. This parameter, which indicates a soil’s runoff potential, is the qualitative basis of the classification of all soils into four groups. The HSGs, as defined by the SCS soil scientists are A, B, C, and D.

The HSG serves as a key input for the SCS–CN model, and according to the United States Department of Agriculture (2009); the HSG layer was formulated by reclassifying soils based on their characteristics and potential for surface runoff. Based on the types of LULC and varying HSG a set of CN values recommended by Cronshey (Cronshey, 1986).

Concerning the Hydrological Soil Group (HSG) of Ethiopia, most of the hydrological studies in the country used the FAO soil database. Based on FAO classification, Ethiopia has HSG–A which dominates with 48.2% areal coverage followed by HSG–B (30%) and HSG–D with areal coverage of 21.6%, and the remaining area is covered by HSG–C which is very small (Belete B. et al., 2012).

Table 2.2: Characteristics of HSG

HSG	Characteristics
A	Soils have low runoff potential and high infiltration rates even under wet conditions and a high rate of water transmission. Consists primarily of 90% sand and 10% clay. They consist chiefly of deep, well to excessively drained sands or gravels and have a high rate of water transmission (greater than 0.30 in/hr).
B	Soils have moderately low runoff potential, moderate infiltration rates and a moderate rate of water transmission (0.15-0.30 in/hr). They consist mainly of 50–90% sand and 10–20% clay. Examples are moderately deep-to-deep (loamy-sand), and moderately well to well-drained soils (sandy-loam) with moderately fine to moderately coarse (loam types) textures.
C	Soils have moderately high runoff potential and slower infiltration rates. Consists of, 50% sand and 20–40% clay. Soils have low infiltration rates when thoroughly wetted and a low rate of water transmission (0.05- 0.15 in/hr). Examples are soils with a layer that impedes the downward movement of water or soils of moderately fine-to-fine (clay-loam) texture.
D	Soils have high runoff potential and low infiltration rates when thoroughly wetted and a very low rate of water transmission. Consists of, 50% sand and 40% clay. Examples are clay soils (clay loam, silty clay loam, sandy clay, silty clay) with a high swelling potential, soils with a permanently high-water table, soils with a clay pan or clay layer at or near the surface, or shallow soils over nearly impervious material.

Source: Cronshey (1986); Subramanya (2013); Ross et al. (2018)

2.9.2. Antecedent Moisture Condition (AMC)

The soil moisture condition in the watershed before runoff occurs is another important factor influencing the final CN value. AMC is the moisture content of soil at the start of a rainfall-runoff event and is widely recognized for governing early abstraction and infiltration. The AMC of a particular watershed was taken under consideration, so that the already present moisture content in the soil, which plays a significant role in generating runoff estimation. Based on the 5-day antecedent rainfall (i.e. the accumulated total rainfall preceding the runoff under consideration), AMC are classified in to AMC I (The soils in the watershed are practically dry i.e. the soil moisture content is at the wilting point), AMC II (average condition), and AMC III (The soils in the watershed are practically saturated from antecedent rainfalls), in terms of soil moisture content (Silveira et al., 2000). In the original SCS method, a distinction was made between the dormant and the growing season to allow for differences in evapotranspiration.

Table 2.3: Classification of antecedent moisture condition

AMC	Description	Sum of antecedent 5-days precipitation (P5)	
		Growing season	Dormant season
AMC I	Dry soil	P5 < 35mm	P5 < 12mm
AMC II	Average condition	35mm ≤ P5 ≤ 53mm	12mm ≤ P5 ≤ 28mm
AMC III	Wet soil	P5 ≥ 53mm	P5 ≥ 28mm

Source: USDA (1984)

2.10. Empirical Review

Several studies were going on about the methods for runoff modeling and its estimation. Sarita Gajbhiye, (2015) conducted a study on runoff estimation using remote sensing and GIS. The curve number method was used as a distributed model. Vinithra & Yeshodha, (2013) used the SCS-CN approach to estimate the surface runoff for the Krishnagiri district in Tamil Nadu. The results of this study's computation of runoff for various land covers led to the conclusion that soil texture and rainfall are the two key factors influencing runoff. Runoff has been estimated using the SCS model, which provides a rapid estimate of generated runoff. Lucas-Borja et al., (2020) use surface runoff depth (Q) and the surface runoff coefficient (C) to evaluate the surface runoff changes.

The study conducted by Li et al., (2018) used enhanced SCS-CN model that integrates GIS and remote sensing technology to study trends of direct runoff at various scales and assess the impact of land use change on the volume of direct runoff of the four-ring area in Shenyang, China. This study found that trends in the direct runoff volume varied from inner urban to suburban areas over time. The primary cause of the rise in surface runoff is determined to be surface change brought about by urbanization.

Another study by (Erena & Worku, 2019) uses a rational method to assess the hydrological influence of land cover dynamics in the city of Dire Dawa. The results of the land use land cover change analysis, which was done using decadal satellite images and the ERDAS Imagine program, demonstrated that forests are disappearing because of ongoing land clearing and settlement growth. The findings indicated that as forest cover decreased and settlement and barren land continued to grow, runoff rose. The research held by Bulti & Abebe (2020) study uses the SCS-CN method to examine how urbanization affects storm runoff at various spatial scales with respect to runoff depth. The amount of impervious area increased by 22% year over the study period, resulting in increases in runoff at the city and watershed levels of 23%, 31%, and 16.6%, respectively. The regression analysis's findings showed that, at both spatial scales, runoff and spatiotemporal changes in the imperviousness ratio are directly correlated.

Most of the previous research has modeled the runoff change considering land use land cover change analysis over the decades, which has the limitation to estimating the impact of runoff between these long-time differences. To narrow this limitation this research uses a five-year interval to assess the impact of urbanization on surface runoff characteristics. Most of previously conducted studies evaluate the impact of urbanization on runoff of single spatial location, but urbanization impact on runoff variables and the rate of flow of runoff at different spatial scale not explored.

The majority of earlier studies, particularly those conducted in Ethiopia, attempted to examine how changes in land use and cover affect surface runoff at natural watersheds or catchments. There is very little data available to estimate how changes in land cover and usage due to urban expansion affect surface runoff. This study assesses the surface runoff change in terms of surface runoff flowrate in addition to characteristics like surface runoff depth. Furthermore, during the process of determining CN, the impact of slope on the alteration of runoff characteristics has been taken into consideration, which has not been done in previous studies.

Chapter Three

3. Materials and Methodologies

3.1. Study area description

3.1.1. General background of study area

Debre Markos town was found in 1853 by Dejazmach Tedla Gualu who was then the administrator of the town for nearly three decades. The name of the town was initially called Menkorer before it changed to Debre Markos due to the establishment of Saint Markos church in 1881. King Tekle Haimanot who came to power in 1879 proclaimed that the town should be named Debre Markos instead of Menkorer (Debre Markos Town Municipal Office, 2009). During its founding, the total extent of the area was 272 hectares. Until 1995, the town was the administrative town of the province of Gojjam and currently serves as the capital of the East Gojjam zone. The town has a structural plan that was prepared in 2009. Despite the old age of the town, the socio-economic statuses of the citizens as well as infrastructural developments in the area were almost paused for several decades. However, nowadays, motivated by the liberalized free market economy and other motivating instruments by the local government, the socioeconomic status of the society is showing considerable progress (Abebaw, 2017; Esubalew, 2006; Ziena, 2017).

3.1.2. Location of study area

Debre Markos town, the capital of East Gojjam Administrative Zone, is located at a distance of 300 kilometers from Addis Ababa to the northwest direction and 265 Kilometers from the capital of Amhara National Regional State- Bahir Dar. Geographically the study area is located between 10°17′00″ to 10°21′30″N latitudes and 37°42′00″ to 37°45′30″E longitudes and its elevation ranges from 2245 to 2511 meters above mean sea level.

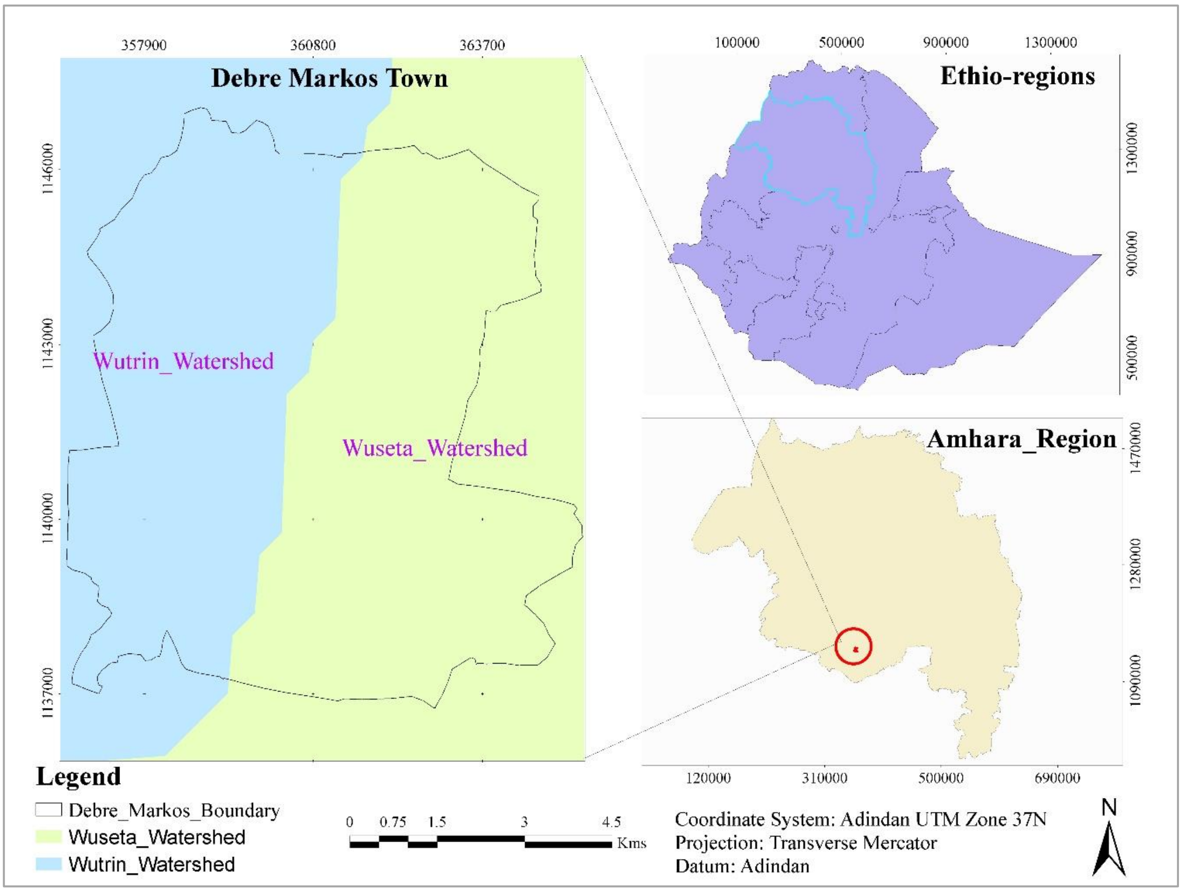

Figure 3.1: Location of the study area (source: Debre Markos town Municipality office)

3.1.3. Topography

The main natural constraints for the physical expansion of the Debre Markos town are hills, swamps, rivers, forests, and slopes ranging between 0 - 20%: while the manmade constraints are illegal settlements and urban-rural boundary conflicts. The area covered by Debre Markos town is not very suitable for urban development. This is mainly because the town is dissected by three swampy areas (mainly flood plains) and to some extent by gullies, ridges, and escarpments. In addition, the town is drained by three rivers: Wuseta, Wutrin, and Abahim, which flow to the south but in different directions. For instance, Wutrin drains the Western part of the town, while Wuseta drains the Eastern part of the town. Particularly the swampy area of Wutrin is the major source of water supply. Overall, the swampy areas along these riverbanks are the main sources of grazing land for the town and its hinterland (NUPI, 2001 cited by Ziena, (2017). According to the document obtained from the town municipality office, there are three major slope categories. Land with 0 - 2.5% slope: this area refers to the swampy areas, which cover 20% of the total urban land. Land with 2.6 - 20% slope: land with this slope class constitutes 75% of the area of the town. This is suitable for settlement and other functions. Land with >20% refers to the land characterized by gullies, ridges, and escarpments, which account for 5% of the land resources (Debre Markos town municipality, 2009).

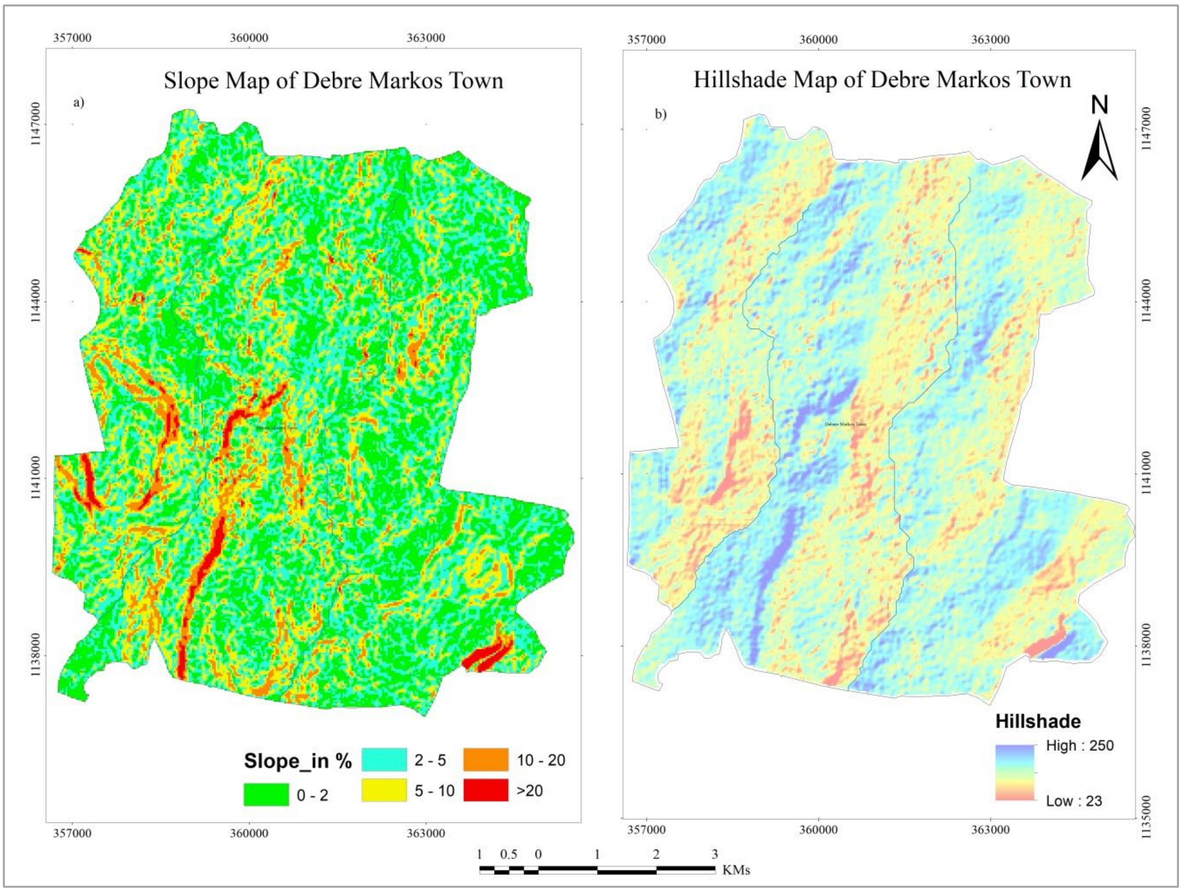

Figure 3.2: Shows the topography of the study area (source: https://search.asf.alaska.edu/)

3.1.4. Demography

According to CSA (2007), the population of the town was 62,497. Out of this 29,921 (47.88%) were males and 32,576 (52.12%) were females; 16,325 (26.14%) were within the age group of 0-15 years, 42,185 (67.49%) 16-60 years, and 3,987 (6.37%) 61 years and above. The population growth rate at the low variant was 2.4%, while household size in the town is calculated to be 3.2. The majority of the residents, 97.03% practiced Ethiopian Orthodox Tewahido Christianity, while 1.7% and 1.1% of the population were Muslim and Protestants respectively. While 97% of the inhabitants are speakers of the Amharic language, the remaining 3% of the inhabitants are speakers of Tigiregna, Agew, and Afan Oromo (Maru Abebaw and Juliet Akola, 2016). According to CSA (2022), the population projection figure of the town had been estimated at 66,204 male and 67,606 female inhabitants, which is a total population of 133,810. The area of the town is expected to be 65.82 km^2 with the population density of 2138 /square kilometer.

3.1.5. Weather Condition

The weather condition of the town is woinadega (temperate climate) which makes it suitable to live in. The town enjoys a tropical climate with a mean annual rainfall of 1380mm and a mean annual temperature of 16°C, while the maximum and minimum-recorded temperatures are 24 °C and 4°C respectively (EGFED, 2012). Its' existing wind direction is from north to south. The main rainy season is from June to October and most of the annual rainfall is precipitating in these four months. The second annual rainfall precipitates from March to May in three months. The remaining months are relatively dry (Debre Markos Town Municipal Office, 2009). The hottest month is April, when the maximum temperature is about 24°C, the second week is the warmest usually. The coldest month is July. In this month, the temperature could be even 9°C at night.

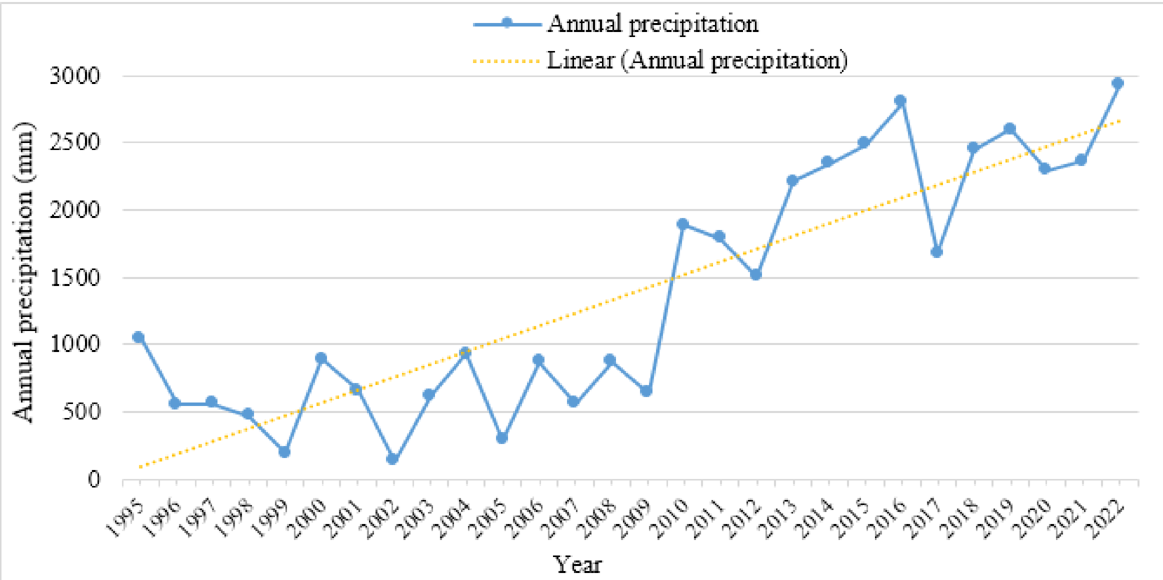

Figure 3.3: Annual precipitation trend (1995 to 2022) of the study area (source: Ethiopian National Meteorological Agency)

3.1.6. Soil type

Based on the data obtained from the Ministry of Agriculture, the study area has two soil classes namely, Eutric Vertisols and Humic Nitisols with the texture of loam and clay respectively. Humic Nitisols are the dominant type with 95.3% and Eutric Vertisols cover the remaining 4.7% of the study area. As per the United States Department of Agriculture (USDA) soil classification, loamy soils were classified into HSG B, which has moderate infiltration rates, and moderate runoff potential, and very clayey soils were classified into HSG D, which has remarkably high runoff potential and very low infiltration rates of water.

The grain size analysis test result taken from eight sample areas showed that the dominant proportion of soil particles is clay, which has clay content ranging from 50 % – 73%, silt fraction 15.88% – 40.21 %, and sand fraction 0.36% - 13.28%. From the index property test results, the majority of soil type is red clay having a specific gravity range from 2.69 to 2.84 (Ebrahim, 2014). In nature, clay soils are impervious and their CN value will be maximum i.e. they will have a CN value of 100.

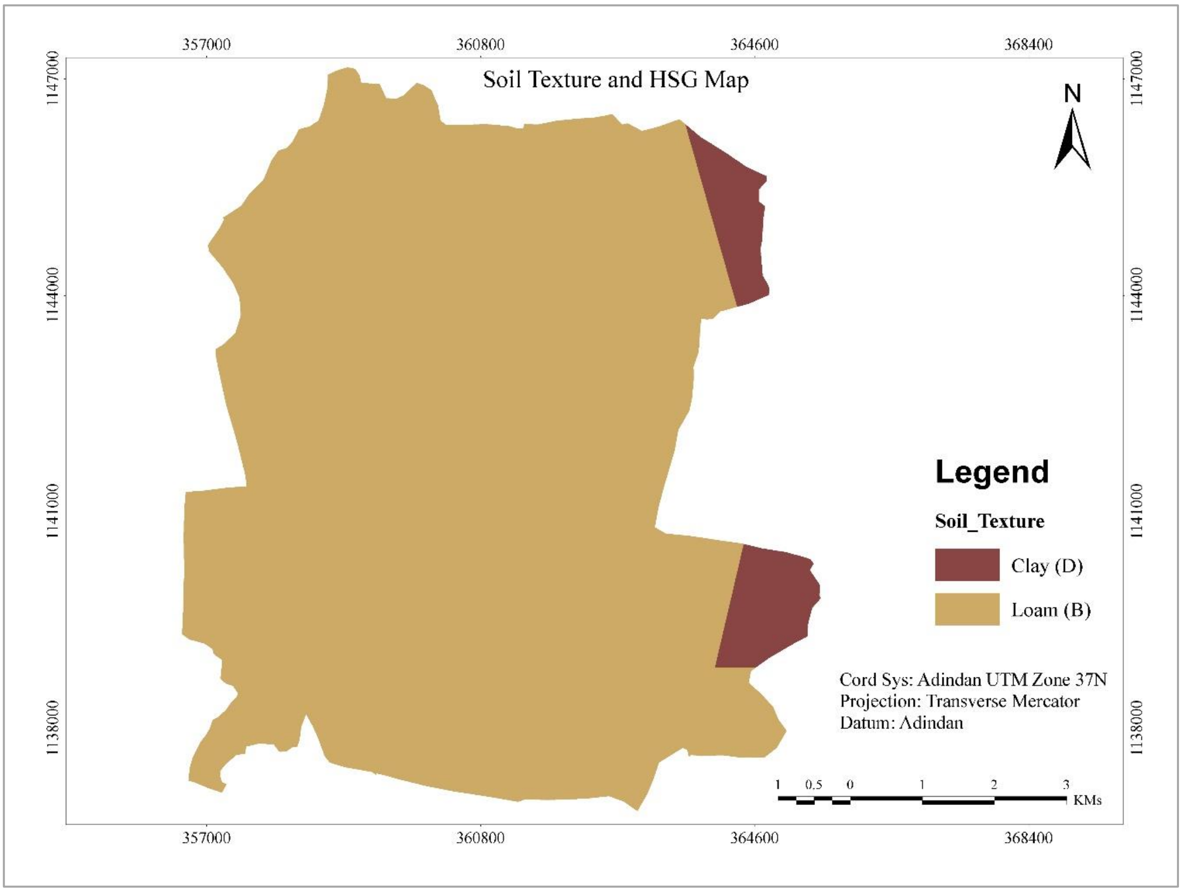

Figure 3.4: Proportional coverage of town’s soil type (source: Ministry of Agriculture)

3.2. Data sources

To complete this study, all the required data were collected from their respective governmental institutions and websites. Temporal satellite imageries for time series years 1995, 2000, 2005, 2010, 2015, and 2022 were downloaded from the USGS website. Landsat 5 TM, Landsat 7 ETM+, and Landsat 8 OLI/TIRS were used to prepare the LULC map of the study area. Although they have medium spatial resolution and mixed pixel problems, Landsat image is widely used for urban LULC mapping (Lu & Weng, 2007).

Its' free accessibility, temporal continuity, and large area coverage property make it preferable. Considering the vulnerability of seasons to fog and cloud, one image from each year with cloud coverage of less than 10% was downloaded from the United States Geological Survey (USGS) website (https://earthexplorer.usgs.gov/). To avoid a seasonal variation in land cover throughout a year, the selection of dates of the acquired image for desired years was made as much as possible in almost the same dry season. Since the sky is clear during this period, the images have the minimum cloud cover and more similarity in the reflectance values of different LULC types across the images taken at different temporal scales. To view and discriminate the surface features clearly, all the satellite image bands were composed using the RGB color composition. The information for Landsat imageries used in this study is summarized in Table 3.1 below.

Table 3.1: Detail information of Landsat imageries

Spacecraft	Sensor Identifier	Path/row	Acquisition date (D/M/Y)	Spatial Resolution (m)	Cloud cover
Landsat 4-5	TM	169/053	26/03/1995	30	< 10%
Landsat 7	ETM+	169/053	15/03/2000	30	< 10%
Landsat 7	ETM+	169/053	29/03/2005	30	< 10%
Landsat 7	ETM+	169/053	06/11/2010	30	< 10%
Landsat 8	OLI/TIRS	169/053	18/04/2015	30	< 10%
Landsat 8/9	OLI/TIRS	169/053	15/05/2022	30	< 10%

Source: https://earthexplorer.usgs.gov/

A digital elevation model (DEM) of the study area with a spatial resolution of 12.5 meters was downloaded from the ALOS PALSAR website. Digital elevation model (DEM) data is required to extract stream networks and watershed area delineation. The daily precipitation depth data of the study area were collected from the Ethiopian National Meteorology Agency. Hydrologic Soil Groups have obtained from Town Municipal Office, and it compared and verified with the data obtained from a Group of Global Hydrological Soil from (NASA): (https://daac.ornl.gov/SOILS/guides/Global_Hydrologic_Soil_Group.html). Some additional datasets were also used for demographic study, rainfall analysis, and soil map preparation for various hydrological soil groups (Table 3.2)

Table 3.2: Required data and their sources

No.	Data types	Data sources	Format	Importance
1	Landsat imageries	https://earthexplorer.usgs.gov/	TIFF	To analyze the LULC change trend of the town
2	DEM	ALOS PALSAR https://search.asf.alaska.edu/	TIFF	To extract the elevation, slope, watersheds and streams of the study area
3	Daily rainfall	National Meteorology Agency, Ethiopia	Excel (.xls)	To compute the runoff depth and its flowrate
4	Soil type	Ministry of Agriculture	Shapefile (.shp)	To prepare the soil map and determine the hydrological soil groups of the study area
5	Administrative boundary	Debre Markos town Municipality office	Shapefile (.shp)	To limit the spatial extent of the study

3.3. Software and instruments used

The choice of the software programs employed in this study was made based on their availability and capacity to solve current issues to accomplish the stated objectives. The software used in this study are listed in Table 3.3 below.

Table 3.3: Software used

No.	Name of Software	Version	Purpose
1	ENVI	5.3	To perform Landsat image preprocessing, processing, and post-processing.
2	ArcGIS	10.4.1	For data analysis and map layout preparation
3	Google Earth	pro	To support the image classification process
4	QGIS	2.18	For change analysis, multi-criteria decision support, simulation modeling, and prediction for the future LULC class of the area.
5	Microsoft Office	2016	for regression analysis, compile overall documentation and presentation

3.4. Methods of Data Processing

3.4.1. Image Preprocessing

Landsat imageries from USGS with cloud coverage of less than 10% were downloaded for the preparation of the LULC map for the years 1995, 2000, 2005, 2010, 2015, and 2022. Before the change analysis has taken place, satellite image pre-processing is very important to establish a more direct association between the acquired data and biophysical phenomena. The expression 'image pre-processing' refers to operations on photographs at the most basic level. Pre-processing aims to optimize image data by suppressing unwanted distortions or enhancing certain image features that are essential for subsequent processing and study (Sonka et al., 1993). Due to the acquisition system and platform movements, generally, remotely sensed data from aircraft or satellites are geometrically distorted. Satellite remote sensing and GIS are the most common methods for quantification, mapping, and detection of patterns of LULC change because of their accurate geo-referencing procedures, a digital format suitable for computer processing and repetitive data acquisition (A. Rahman & Netzband, 2009).

In this research, some pre-processing techniques of image transformation including atmospheric correction and radiometric calibration have been utilized to remove the impacts of the atmosphere and shades that have direct effects on the signal measured by the satellite sensor. In addition, using image analysis window tools image adjustments such as adjustment of the displayed contrast, brightness, and transparency characteristics of an image were applied to all-year Landsat images.

Layer staking- is the method of merging several images into a single image. To do this, the images must have the same degree (number of rows and columns), which necessitates resampling other bands of different spatial resolutions than the desired resolution. To put it another way, all images/bands must have the same spatial resolution to perform layer stacking. Combining images/bands, on the other hand, would increase the final stacked image scale, and therefore the processing time as you perform the research. If you know you will not need any of the images/bands in your study, stacking all of the images into a single image is not necessary; instead, choose only the images that attract you.

Image Enhancement- is the conversion of image quality to a higher and more understandable standard for feature extraction or image analysis (Iwasokun, 2014). Image enhancement is a common technique for providing a clear display for image perception

(Uk, 2017). There are several techniques for enhancing remote sensing images, including histogram equalization, contrast stretching, and adaptive filtering. Therefore, in this study, Landsat image enhancement was performed using ENVI software.

Radiometric correction- is a process used to adjust the pixel values of an image to correct for the effects of sensor, atmospheric, and illumination variations. This process can enhance the contrast, brightness, and color balance of the image, as well as reduce errors and uncertainties in measurements. It is used in remote sensing imagery processing and can work with the data numbers (DNs) of the images. Radiometric calibration, atmospheric correction, topographic correction, and sensor normalization are the main types of radiometric corrections. They are used to convert DNs into physical units such as radiance or reflectance, to remove the effects of atmospheric scattering and absorption on the image, to correct for variations in terrain elevation that can affect the illumination of the image, and to correct for differences in sensor response between different images or sensors respectively. Radiometric calibration and correction are particularly important when comparing data sets over multiple periods (Khanna et al., 2017).

Image gap fill- is a technique used to fill in missing or damaged portions of an image. This technique is used in remote sensing imagery processing and can be used to reconstruct images that have missing data due to cloud cover or other factors. There are several methods for image gap filling, including spatial-spectral random forests, deep convolutional auto-encoder, and satellite image gap filling techniques including using Landsat 7 images, and pre-processing functions such as atmospheric correction or conversion.

Sub-setting- any of the image's non-essential elements have to be omitted, and the image's emphasis has to be narrow. To minimize the size of the image file and include only the region of interest, it is necessary to remove the project field from the entire image (AOI). This is used not only to remove unnecessary data from the picture but also to speed up the process. When using multiband data, such as Landsat TM imagery, this is critical. Sub-setting is the term for this data reduction. Each Landsat scene was clipped through by the project area boundary using ENVI software. Sub-setting Landsat images have been done after layer stacking or a composite image has operated.

3.4.2. Image processing

Classification of LULC is one of the very fundamental tasks prior to any decision making regarding LULC change detection (Miller et al., 2014; Weng, 2001). Image classification is the process of categorizing an image into one of several predefined categories based on its content. Firstly, based on image interpretation elements, Landsat imageries of the years 1995, 2000, 2005, 2010, 2015 and 2022 were visually interpreted. From the two types of pixel-based classification, supervised and unsupervised classification, in this study-supervised classification was used to prepare a LULC map of the study area. Supervised classification is a method for detecting spectrally close areas on an image by locating training locations of identified targets and extrapolating those spectral signatures to unknown target areas (Mather, 2011). In training sites with ground truth data, or homogeneous regions that represent each class, supervised classification is normally the best option. The training samples were collected based on the visual inspection of the natural color composite (RGB) of satellite images and sampled at random for each class and then partitioned into training and testing datasets.

Each image was classified using the training data using an SVM-based supervised classifier that used a radial basis function (RBF) kernel with a 1-vs-1 multiclass strategy. Here, the RBF kernel was chosen for classification since this kernel accounts for better performance for remotely sensed data compared to other kernels (Cardoso-fernandes et al., 2020) To train the SVM model for classification, a regularization parameter, C, and a bandwidth parameter of the RBF kernel, g must be chosen. For each of the images over the study period, the parameter set with the highest training accuracy was chosen. Then, using the predict function of the toolbox final classified LULC maps were produced. These land use land cover maps of different periods of the study area were important input data to compute the depth of surface runoff and flowrate within specific land use types and hence the maps were prepared by processing satellite images.

3.4.3. Accuracy Assessment

Accuracy assessment is the procedure used to quantify the reliability of a classified image. The standard accuracy assessment procedure is to construct an "error matrix." that is a square matrix in which the rows and columns represent the land cover classes from the classified image. The accuracy assessment was performed by taking randomly selected reference pixels for each class. Based on the true and predicted classes of the test data a confusion matrix was formulated which provides insight for each class about how many samples are correctly classified, misclassified, and for which class the samples were incorrectly classified. LULC classification accuracy was assessed quantitatively using an error matrix, which is the commonly used method in LULC classification accuracy assessment (Weng, 2010). For the overall accuracy and Kappa coefficient evaluation of the interpreted LULC classes, an accuracy assessment was performed by using ENVI software with the support of historical google earth image (Congalton and Green, 2019).

Using the generated confusion matrix user's accuracy (UA), producer's accuracy (PA), overall accuracy (OA), and Kappa statistics were computed. Producer's and user's accuracy is used to evaluate the classification at the class level. The matrix diagonal represents the samples that are successfully identified in each class, and the OA was determined by dividing the sum of the correctly classified instances by the total number of pixels (Story & Congalton, 1986). The PA was calculated by dividing the number of right pixels in a given class by the total number of pixels in the test set for that class, and it represents the likelihood of correctly classifying a training sample (R. G. Congalton, 1991). The UA can be calculated by dividing the number of correct pixels in a given class by the total number of pixels classified in that class. It demonstrates the map's reliability by indicating the likelihood that a pixel that is categorized as belonging to a particular class truly belongs to that class on the ground (R. G. Congalton, 1991; Story & Congalton, 1986). The Kappa statistic, a measure of agreement between the output of the classifier and the reference data, greater than 0.8 that indicates a strong agreement between classified classes and ground truth (J. Cohen, 1960; Landis & Koch, 1977).

3.4.4. Land use land cover change prediction

Modeling land use land cover changes for future time is important to know the possible scenarios. Simulation modules were used to minimize the dynamics of composite urban structures and interpret them in a clear and accessible manner. The model was run for change prediction to a specified future date for the allocation of land cover changes (Eastman, 2006). After the Landsat imageries of respective study years were classified with the acceptable level of accuracy, in this study the trend of future LULC were predicted using cellular automata simulation. The procedure determines exactly how much land would be expected to transition from the later date to the prediction date based on a projection of the transition potentials into the future and creates a transition probabilities file. Studies claim that the CA-ANN method is more effective than linear regression, thus the modules for the land-use change evaluation (MOULSCE) plugin were implemented for transition potential modelling and future simulation (El-Tantawi et al., 2019; M. T. U. Rahman et al., 2017). The MOLUSCE plugin is perfectly adapted to evaluating spatiotemporal land-use changes, transition potential modelling, and predicting future scenarios (M. T. U. Rahman et al., 2017). The artificial neural network (ANN) was used in association with cellular automata (CA) to predict the land use changes. Because of its dynamic simulation capacity, high efficiency with limited data, simple calibration, and ability to reproduce different land covers and complicated patterns, CA-ANN was chosen to simulate land use change. CA-ANN combines the CA and Markov chain to model land use changes across various categories (Memarian et al., 2012).

The future LULC map prediction of 2040 has been generated depending on the historical trends of LULC changes. The MOLUSCE plugin within QGIS was executed to establish the spatiotemporal changes with a given time period and calculate the LULC transition to generate the LULC change map. A transition potential matrix was generated in the study between (2001–2011) to create the change map. The ANN-multilayer perception method was employed for the transition potential modelling. Elevation, Slope, distance from streams, and distance from the road were the spatial parameters implemented as input parameters. The transition potential model is trained based on the LULC maps of 2000 and 2010, as well as spatial parameters to produce the predicted map of 2022. Predicting the future changing trend of LULC will used to demonstrate its future effect on surface runoff.

3.4.5. Model validation

After prediction, the validation of model was run to determine the quality of the predicted land use map concerning a map of reality. In order to validate the ANN model, the simulated map of 2022 was compared with the classified LULC map of 2022. The derived predictive LULC data in 2022 from ANN model were separately compared (pixel by pixel) with the visually interpreted LULC data in 2022 by an overlay operation to calculate the overall accuracy and kappa coefficient. It was evaluated by running a three-way cross-tabulation between the later land cover map, the prediction map, and a map of reality. The overall quality of land cover maps generated from model simulations should be evaluated using the kappa statistics parameter and agreement/disagreement marks (Foody, 2002). Satisfactory results were obtained, and the model was trained with a learning rate of 0.001 and momentum of 0.001. The ANN training process ran for 100 iteration and a neighborhood value of 3 pixels with 10 hidden layers. The trained model was then simulated to obtain the predicted maps of 2040.

3.5. Methods of data analysis

3.5.1. Analysis of LULC dynamics

Analyzing the spatiotemporal dynamics of the urban area of a particular urban landscape is the primary step in understanding the impacts of urban growth (Kindu et al., 2020). The spatiotemporal analysis is required for a comprehensive understanding of the impacts of impervious surfaces on regional hydrological responses (Liu et al., 2021). In this study, percent change, urban spatial expansion index (USEI) and urban spatial expansion rate (USER) were used to estimate the spatiotemporal expansion of urban land, percentages of changes and its rate of change. Using areal data produced from categorized maps in a GIS environment, the spatiotemporal changes of LULC were recognized. To examine the nature and rate of the changes, quantitative areal data from the overall LULC changes and gains and losses in each class were compiled. In line with previous research (Butt et al., 2015; Gashu & Gebre-Egziabher, 2019), the percentages of changes were calculated using Eq. 1. The positive and negative values in this instance indicate a gain and a loss in spatial extent, respectively.

$$\%\Delta = (A_{t1}-A_{t0}) *100 \quad (1)$$

Where, $\%\Delta$ is the percentage of change and A_{t1} and A_{t0} are the area extent of urban land at final year (t_1) and initial year (t_0) respectively.

The USEI is an indicator proposed to analyze the growth of urban areas in terms of spatial increase in urban land, but it does not show the spatiotemporal variation of the rate at which this change has happened. It quantifies the magnitude of urban expansion per unit of time over the study period using a linear change model. Due to its linear development assumption, it gives constant expansion per unit of time throughout the study period. It used to assess the speed of urban growth in the same study area over different times as well as between different countries.

$$USEI = (A_{t1}-A_{t0})/\Delta t \quad (2)$$

Where, USEI is urban spatial expansion index, A_{t1} and A_{t0} are the area extent of urban land at final year (t_1) and initial year (t_0) respectively and Δt is the time difference between t_1 and t_0.

The urban spatial expansion rate (USER) method that is one of the several quantitative methods for analyzing urban expansion and the spatial pattern of urbanized areas was used to determine the growth rate of urban extent. USER assumes that urban growth is an exponential process i.e. the increments of urban growth increase over time, at a constant rate of increase. The rate of land-use change is crucial for identifying the process of conversion related to development and growth of urban area. The equation below was adopted to compute annual rate of change (eq. 3); the positive and negative values suggest the gain and loss in spatial extent, respectively.

$$USER = (((A_{t1}/A_{t0})^{\wedge(1/\Delta t)})-1) * 100 \qquad (3)$$

Where, USER is urban spatial expansion rate, A_{t1} and A_{t0} are the area extent of urban land at final year (t_1) and initial year (t_0) respectively and Δt is the time difference between t_1 and t_0. To describe the area coverage percentage of the impervious areas of the total areas, the urban land percentage (PU) was calculated (Tian et al., 2005).

$$PU = \left(\frac{UA}{AT}\right) * 100 \qquad (4)$$

Where PU is the urban land percentage, UL is the urban land area, and UT is the total area of entire landscape.

3.5.2. Estimation of surface runoff characteristics

3.5.2.1. Estimation of runoff depth

Hydrological models are an effective tool for water and basin management. There are several hydrological models available to estimate direct runoff potential from storm rainfall. However, the selected model should be simple, have minimal data requirements, have static assumptions, and be unpretentious. The Natural Resource Conservation Service-Curve Number technique is a globally used method to derive direct runoff concerning rainfall events for catchments across the globe and relies on only one parameter, i.e., curve number. The model's characteristics extend to land use, soil type, hydrological condition, and antecedent moisture condition and work efficiently for catchments of smaller dimensions.

In this study the NRCS-CN model was used to estimate the urban runoff potential using Landsat time-series data. The model presents a simplified procedure for estimating runoff potential in small watersheds, which has been presented by using the CN method, where the CN values are assigned to various LULC classes. Thus, it has become very useful for urban areas, as the runoff potential is very high even in very small watersheds. Therefore, after integrating all parameters, i.e., LULC map, CNII map, and rainfall, the runoff characteristics were computed for the entire area. The 40.5mm rainstorm of 30th-06-2022 was the rainiest rainstorm of the study period of Debre Markos station used for AMC determination. The amount of rainfall 5 days before the rainstorm was less than 53mm; so, the soil condition of the watershed was in a moderate condition that lays under AMC-II.

The change in surface runoff was simulated by directly inputting land use maps of identified years into the SCS–CN model under the rainfall event of the specified year return period. The runoff characteristics like average surface runoff depth (Q), and average surface runoff peak flowrate (q) were computed to analyze impact of land cover change on surface runoff variations. The impact analysis was carried out by comparing the changes in runoff variables between initial and final land cover conditions.

Assigning CN is the most important task in determining the characteristics of surface runoff and defining the soil hydrologic group for the study area is the first step for CN determination. According to standard tables (USDA SCS, 1972) and by considering AMC, appropriate different CN values were assigned to each land cover class (Cronshey, 1986). From the soil hydrologic map, the dominant soil type of Debre Markos is loamy clay and clay in rare cases. Thus, based on the TR-55 tables by SCS (1986), soils with loamy clay texture are grouped as the Hydrologic Soil Group B. The hydrologic soil group map was used to locate the area of the different soil types. Land use maps and soil maps are overlaid to delineate polygons with unique land use and HSG combinations to determine CN for each land cover type and then to compute the area-weighted average CN. Considering the land use land cover classes and slope of the study area, the curve number value of 95, 76, 86, 72 and 83 were selected for urban area, agricultural land, barren land, vegetation and meadow respectively.

To account for surface heterogeneity in urban scenarios, in this study, weighted CN values were used rather than a single value. Specifically, from the sum of the initial CN values for each grid the CN value of each land cover class was calculated, which is then weighted by the area percentage. The final composite CN value that can be used in the NRCS flow curve number runoff equation to calculate depth and volume was computed using the following equation:

$$CN_w = \frac{\sum_{i=1}^{n} CN_i * Ai}{\sum_{i=1}^{n} Ai} \tag{5}$$

Where, CN_w is the weighted CN of the entire study area, A_i is the area of each land cover class and CN_i is the initial curve number values for each LULC class.

The SCS runoff curve number method developed by the Natural Resources Conservation Service (NRCS) used for estimating direct runoff from storm rainfall described in the following equation,

$$Q = \frac{(P - Ia)^2}{(P - Ia) + S} \qquad (6)$$

Where,

Q = runoff (mm)
P = rainfall (mm)
S = potential maximum retention after runoff begins (mm) and
I_a = initial abstraction (mm)

Initial abstraction (Ia) is all losses before runoff begins. It includes water retained in surface depressions, water intercepted by vegetation, evaporation, and infiltration. It is highly variable but generally correlated with soil and land cover parameters. Through studies of many small agricultural watersheds, I_a was found to be approximated by the following empirical equation:

$$I_a = 0.2S \qquad (7)$$

By removing I_a as an independent parameter, this approximation allows the use of a combination of S and P to produce a unique runoff amount. Substituting equation (7) into equation (6) gives:

$$Q = \frac{(P - 0.2S)^2}{P + 0.8S} \qquad (8)$$

S is related to the soil and land cover conditions of the watershed through the CN, which has a range of 0 to 100, and S is related to CN by:

$$S = 25.4\left(\frac{1000}{CN} - 10\right) \qquad (9)$$

3.5.2.2. Estimation of runoff flowrate

The rational method was used to estimates the peak rate of runoff of the study area as a function of the drainage area (A), runoff coefficient (C), and rainfall intensity (i) for a duration equal to the time of concentration 'TC'. Time of concentration is the time required for water to flow from the most remote point of the basin to the location being analyzed.

Quite a number of formulas exist for deriving time of concentration ‘TC’, from the physical characteristics of a drainage basin. Kirpich (1940) gives one of these empirical formulas.

$$TC = 0.0195 * L^{\wedge 0.77} * S^{\wedge -0.385} \quad (10)$$

Where, Tc = time of concentration

L = length of the main channel

S = the distance weighted slope of the main channel

Usually the runoff coefficient ‘C’ obtained from a table and defined in terms of the land use and slope. Some tables provide its value based on return period and slope; the value of C increases for the less frequent events and with increasing slope. Some tables provide a range of C-values for each land use that permits the designer to select a value that reflects on-site conditions. The value of surface roughness was assigned to each land cover class in order to determine the type of land use that is more responsible for the generation of surface runoff in the area and to divide the bigger watershed area into manageable size for rational methods. By taking in to consideration the land use land cover type and slope of the study area, 0.86, 0.37, 0.47, 0.20 and 0.15 were selected as the value of runoff coefficient for urban area, agricultural land, barren land, vegetation and meadow respectively (Sarukkalige, 2011). Weighted runoff coefficient ‘C’ can be obtained by adding the multiplication of areas of each land use with corresponding roughness values of each land use type. The surface roughness of different land use lies between 0 (no runoff) and 1(the maximum runoff). “C” is obtained by tabulating the weighted value of the coefficient of each land use land cover in the study area. The weighted “C” value calculated with the following equation.

$$C = \frac{\sum_{i=1}^{n} Ci * Ai}{\sum_{i=1}^{n} Ai} \quad (11)$$

Where,

C is surface roughness of each land use

A is the area of each land use.

Once the time of concentration, the intensity of rainfall was estimated by dividing the amount of precipitation by its duration that relate with 0.133 multiplied by time of concentration. Using the defined runoff coefficient, drainage area and rainfall intensity, the peak flow rate was computed using the following empirical formula.

$$Qp = 0.28*C*I*A \quad (12)$$

Where, Qp = Peak runoff rate [m^3/sec]

C = Runoff coefficient

I = Rainfall intensity [mm/hr]

A = Drainage area [km^2]

3.5.4. Analyzing the correlation between surface runoff and land cover change

After the runoff characteristics has determined, the correlation analysis was conducted to assess the association between the change of surface runoff and land cover change. The impact of the LULC changes on the surface runoff depth and flowrate was then examined using spatial and simple linear regression analyses. To relate the change in surface runoff and land cover, the validity of the model assumptions should be determined by examining the structure of the residuals and the data pattern through graphs. The normality assumption was validated using a normal probability plot of standardized residuals which is a plot of the ordered standardized residuals against the normal scores (Bulti & Abebe, 2020). The stronger the correlation coefficient indicates the greater the influence of land cover change on the change of surface runoff.

Linear regression analysis was used to determine the relationship of LULC change, slope length, slope steepness with the surface runoff depth and flowrate. The Pearson' correlation analysis was used to determine whether there is a correlation between runoff depth and flowrate with slope steepness, and slope length. The derived correlation coefficient (R) and coefficient of determination (R^2) values of the regression analysis were also used to explain the spatiotemporal relationship between LULC change and the surface runoff depth. The stronger correlation between impervious surface area and runoff occurs for water surfaces than for land surfaces (Liu et al., 2021).

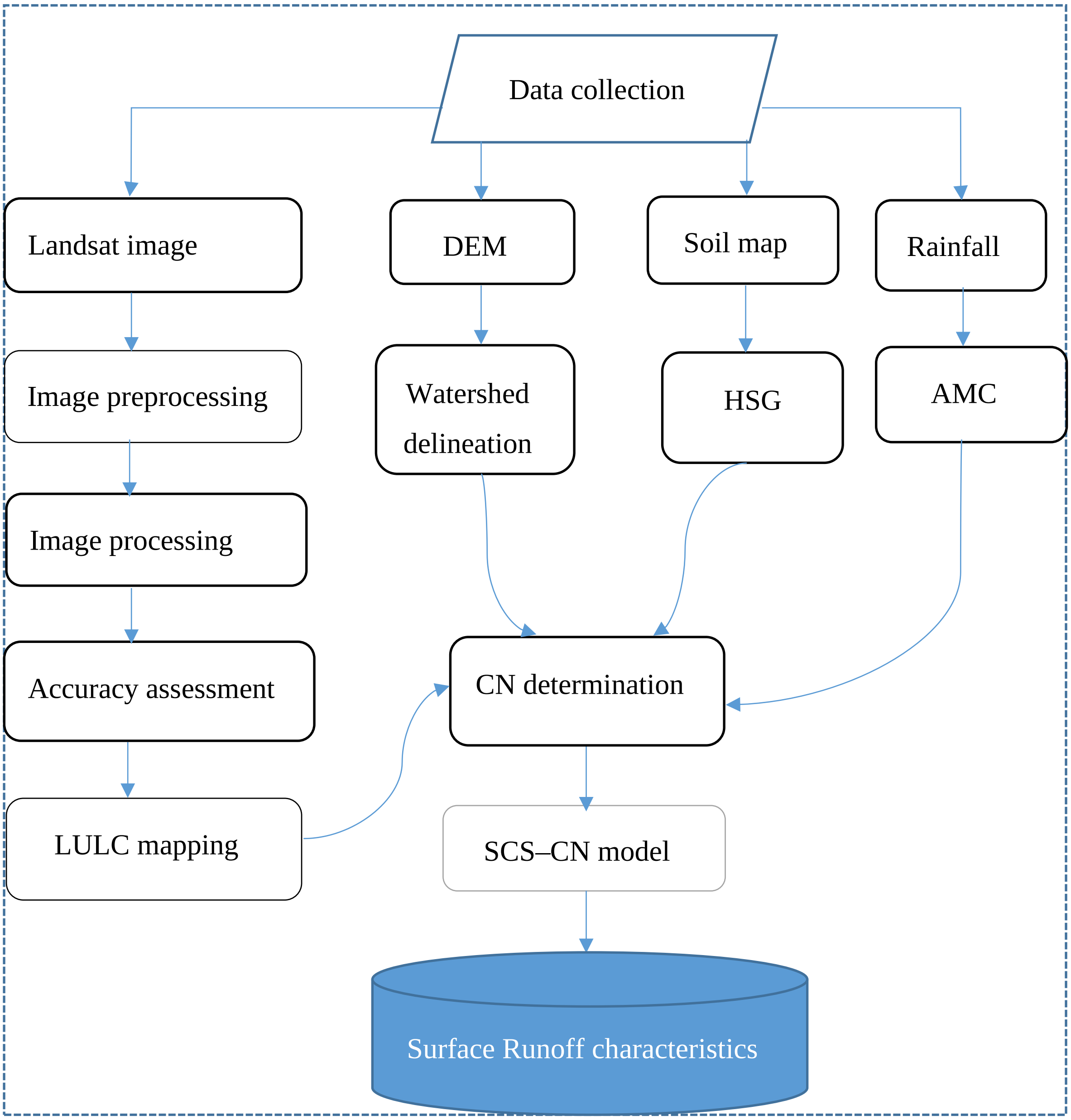

Figure 3.5: Technological scheme of the study

Chapter Four

4. Results and Discussions

4.1. Changing trend of Land use land cover

The trends of urban LULC change in study area were analyzed by observing the area coverage expansion over the last 27 years. The land cover maps were generated after running support vector machine-supervised classification using ENVI software and their areal value was computed using post-classification technique in ArcGIS environment. After the preparation of land use land cover maps, the changes that occurred over the studied periods in each land cover class were analyzed. The image classification result summarized in Table 4.1 demonstrates that the spatial extents, percentage changes over time, and the annual average percent change of each LULC class (urban area, agricultural land, barren land, vegetation and meadow) in Debre Markos town between 1995 and 2022.

Based on the data analysis performed, an overall change in LULC of all the respective years is shown in figure 4.1 below. The result shows a notable expansion in urban land and barren land and a shrinkage phenomenon in the agricultural land, vegetation and meadow during the study period (1995 to 2022). The study area has experienced spatial variations and trends (figure 4.1) on different land use land cover classes due to the corresponding horizontal expansion as well as the conversion of land cover classes during the distinct study periods. The reclassified images in figures 4.1 showed that there had been a rapid land cover conversion of each LULC category to another class. As the results showed that agricultural land was the dominant class at the beginning of the study period but declined with the continuous increase of urban area and barren land. The results indicate that between 1995 and 2022, the areas covered by urban area and barren land rose by +1391ha (+468.79 %) and +405.98ha (+90.62%) with annual average change of +17.36% and +3.36% respectively, which shows a great increasing trend. In contrast, agricultural land and vegetation were decreased by -1139.32ha (-35.53%) and -364.48ha (-32.01%) at annual average change of -1.32% and -1.19% respectively. The results also demonstrate that the areas covered by meadow continued to decrease by -293.50ha of land, decreasing at an annual average change of -0.73%. During the study timeframe, 1139.32ha of agricultural land, 364.48ha of vegetation area and 293.50ha of meadow was converted to other land uses, mainly to urban area, at an annual average change of -1.32%, -1.19% and -0.73% per year respectively.

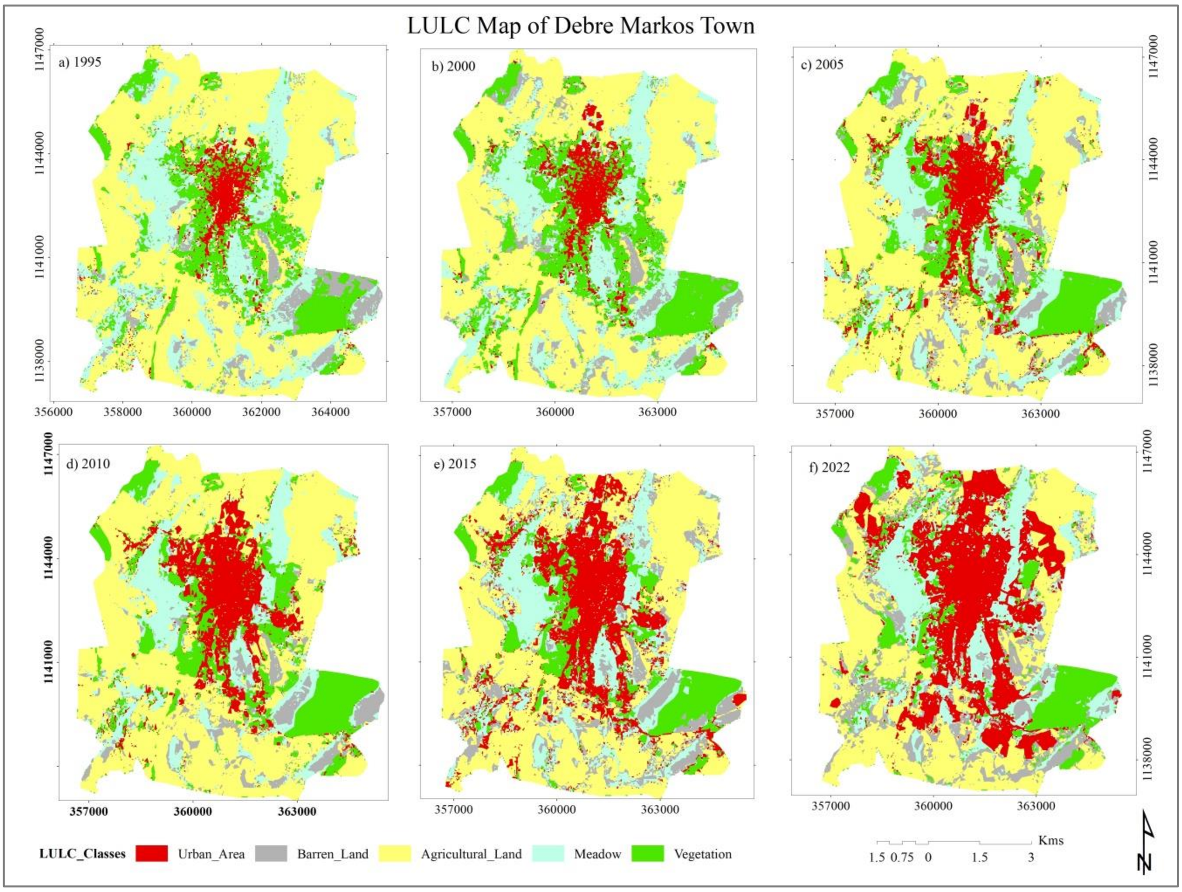

Figure 4.1: Shows land use land cover classes of the study area in 1995(a), 2000(b), 2005(c), 2010(d), 2015(e), and 2022(f)

Over the study period, the result shows a continuing shift of land use land cover due to rapid urban expansion in the town. The spatial area coverage of the urban area was 296.72ha or 4.51% of the total area in the initial study year, 1995. Its spatial extent was gradually increased throughout each study time interval and covered 1687.72 ha or 25.65% of the total study area in 2022. Between the years 2005 and 2010, the trend of growth of urban was comparatively low that shows a 25.73% increase, and a highest change was recorded between the years 2000 and 2005 (65.92%); followed by 2022, 2015, and 2000 showed the percentage change of 44.03, 39.46 and 35.74 respectively. In contrast, the area statistics of agricultural lands was 48.73% at the beginning of the study year. It slightly decreased to 44.13% in 2000 and showed some fluctuation through decreasing and increasing situations before it fell to 31.41% in the final year of the study time, 2022. When the area of agricultural land in the base year was compared with its area coverage in the last year, it showed that the area decreased by -1139.32ha or -35.53%. On the other hand, in the last study period, area of barren land increased by two fold from the initial study year, which shows an increase from 6.81% to 12.98% coverage of entire landscape. In contrast, during the study timeframe the decreasing trends of area coverage in vegetation and meadow were recorded; they decreased from 1138.7 ha to 774.23 ha (17.3% to 11.77%) and from 1490.72 ha to 1197.22 ha (22.65% to 18.2%) respectively. The area coverage difference of each land use land cover class between the base year (1995) and the final year (2022) were 1391 ha (468.79%), -1139.32 ha (-35.53%), 406.08 ha (90.64%), -364.48 ha (-32.01%) and -293.5 ha (-19.69%) for the class of urban, agricultural land, barren land, vegetation and meadow respectively. Generally, the LULC classes' area statistics are summarized in Table 4.1 below.

Table 4.1: Area coverage of the town's LULC classes from 1995 to 2022

LULC class	**Area coverage**											
	1995		**2000**		**2005**		**2010**		**2015**		**2022**	
	ha	**%**	**ha**	**%**	**ha**	**%**	**ha**	**%**	**ha**	**%**	**ha**	**%**
Urban Area	296.72	4.51	402.76	6.12	668.27	10.16	840.24	12.77	1171.79	17.81	1687.72	25.65
Agri-Land	3206.42	48.73	2904.29	44.13	3011.55	45.76	3179.63	48.32	2633.78	40.03	2067.10	31.41
Barren Land	448.02	6.81	511.82	7.78	601.24	9.14	484.67	7.36	769.05	11.69	854.10	12.98
Vegetation	1138.71	17.30	1339.97	20.36	1091.39	16.59	1071.61	16.28	844.12	12.83	774.23	11.77
Meadow	1490.72	22.65	1421.79	21.61	1208.06	18.36	1004.61	15.27	1161.35	17.65	1197.22	18.19

Table 4.2: Area change, percent change, and annual average percent change (AAPC) of town's LULC from 1995 to 2022

LULC class	**Area change (ha)**					**Percent change (%)**					**AAPC (%)**
	1995-2000	2000-2005	2005-2010	2010-2015	2015-2022	1995-2000	2000-2005	2005-2010	2010-2015	2015-2022	1995-2022
Urban Area	106.04	265.51	171.97	331.55	515.93	35.74	65.92	25.73	39.46	44.03	17.36
Agri-Land	-302.13	107.26	168.08	-545.85	-566.68	-9.42	3.69	5.58	-17.17	-21.52	-1.32
Barren Land	63.80	89.42	-116.57	284.38	84.95	14.24	17.47	-19.39	58.67	11.06	3.36
Vegetation	201.26	-248.58	-19.78	-227.49	-69.89	17.67	-18.55	-1.81	-21.23	-8.28	-1.19
Meadow	-68.93	-213.73	-203.45	156.74	35.87	-4.62	-15.03	-16.84	15.60	3.09	-0.73

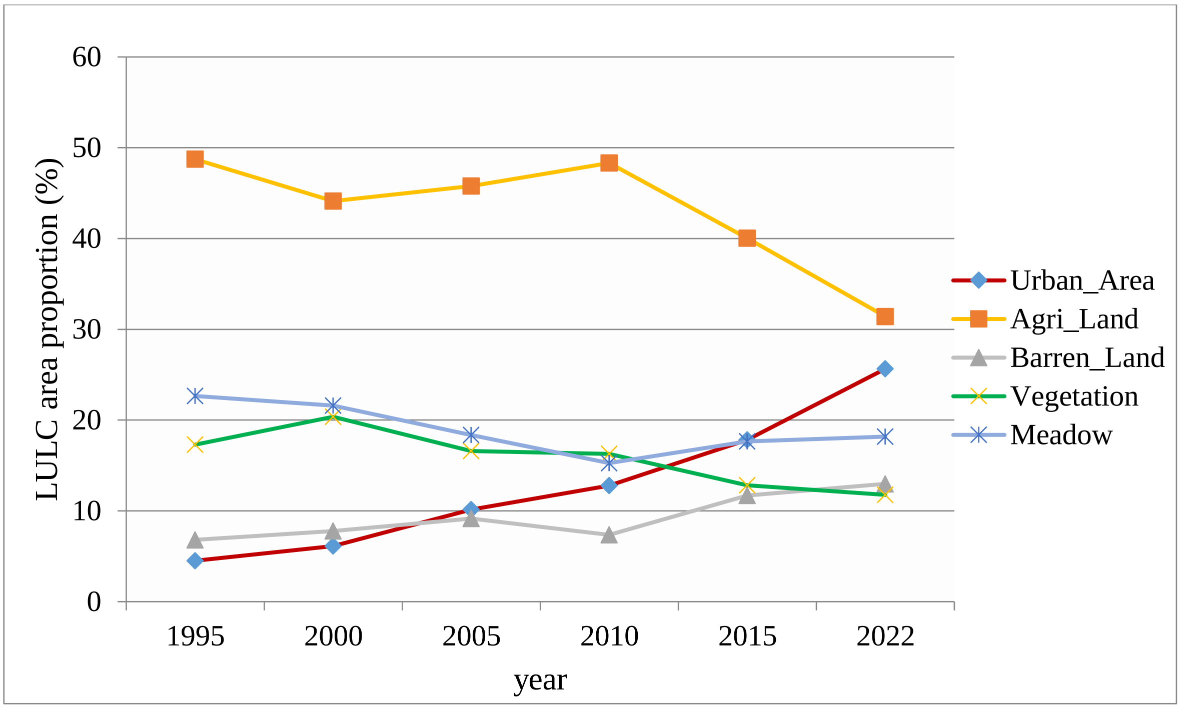

Figure 4.2: Trend of LULC from 1995 to 2022 (source: from research analysis)

Table 4.3: Spatial area extent of the LULC classes in Wutrin and Wuseta watersheds from 1995 to 2022

LULC class	Wutrin (ha)						Wuseta (ha)					
	1995	2000	2005	2010	2015	2022	1995	2000	2005	2010	2015	2022
Urban Area	125.79	185.23	319.03	389.65	538.99	695.01	170.79	217.45	349.06	450.41	632.52	992.70
Agri-Land	1679.62	1529.22	1597.23	1673.37	1330.87	1119.59	1522.70	1371.13	1410.06	1502.00	1298.59	947.51
Barren Land	114.77	201.33	211.27	115.39	243.75	399.83	332.62	309.99	389.57	368.88	524.37	454.27
Vegetation	494.41	594.41	462.19	421.55	401.18	341.78	640.07	744.66	625.11	645.85	438.90	432.45
Meadow	678.00	582.65	503.04	492.94	577.88	541.19	811.55	834.35	703.90	510.80	582.89	656.02

The area extent of wuseta urban land and its change of the respective study years were greater than that of wutrin watershed. This is condition is similar in all other land cover classes except agricultural land cover class. In contrast, of urban land and other land cover classes, the area of agricultural land of wuseta watershed was continuously decrease with the great difference from agricultural land wuseta watershed.

Table 4.4: Area change and percent change of the LULC classes in Wutrin watershed from 1995 to 2022

LULC class	1995-2000		2000-2005		2005-2010		2010-2015		2015-2022	
	ha	%	ha	%	ha	%	ha	%	ha	%
Urban Area	59.44	47.25	133.81	72.24	70.62	22.14	149.33	38.33	156.03	28.95
Agri-Land	-150.41	-8.95	68.01	4.45	76.14	4.77	-342.50	-20.47	-211.28	-15.88
Barren Land	86.56	75.42	9.93	4.93	-95.88	-45.38	128.36	111.24	156.08	64.03
Vegetation	100.0	20.23	-132.21	-22.24	-40.65	-8.79	-20.37	-4.83	-59.40	-14.81
Meadow	-95.35	-14.06	-79.61	-13.66	-10.09	-2.01	84.93	17.23	-36.68	-6.35

The area change and percent change of land cover classes of wutrin watershed was computed and the result revealed that the area change of urban land were maximum (156.03ha) between the yeas 2015 and 2022 followed by 149.33ha from 2010 to 2015 and 133.81ha from 2000 to 2005. Minimum change of urban land (59.44ha) was recorded between 1995 and 2000. Agricultural land shows an increasing trend from 2000 to 2005 and 2005 to 2010; while it shows decreasing trend between other study years. Barren land shows an increasing trend in all study periods except the sudden decreasing between 2005 and 2010 which decreased by 95.88ha. In contrast to all other land cover classes Meadow, shows decreasing trend throughout all study years. This is true for vegetation class except its increasing trend between 1995 and 2000 that shows an increasing of 100ha.

Table 4.5: Area change and percent change of the LULC classes in Wuseta watershed

LULC class	1995-2000		2000-2005		2005-2010		2010-2015		2015-2022	
	ha	%	ha	%	ha	%	ha	%	ha	%
Urban Area	46.66	27.32	131.61	60.52	101.35	29.03	182.11	40.43	360.18	56.94
Agri-Land	-151.57	-9.95	38.93	2.84	91.94	6.52	-203.41	-13.54	-351.07	-27.04
Barren Land	-22.63	-6.80	79.59	25.67	-20.70	-5.31	155.49	42.15	-70.1	-13.37
Vegetation	104.59	16.34	-119.54	-16.05	20.73	3.32	-206.94	-32.04	-6.45	-1.47
Meadow	22.80	2.81	-130.45	-15.64	-193.1	-27.43	72.09	14.11	73.13	12.55

The area of urban land was continuously increased throughout each study period though it shows minimum decreasing between the year 2005 and 2010. The maximum increasing of urban land area (360.18ha or 56.94%) was shown between 2015 and 2022 followed by study years from 2010 to 2015, 2000 to 2005 and the minimum amount of change (46.66ha or 27.32%) in urban land was recorded between 1995 and 2000. Similar to wutrin watershed agricultural land shows an increasing trend from 2000 to 2005 and 2005 to 2010; while it shows decreasing trend between other study years. Maximum decreasing and increasing amount of change in agricultural land was shown from 2015 to 2022 and 2000 to 2005 respectively. Unlike wutrin watershed that shows the decreasing of barren land only between 2005 and 2010, in wuseta watershed it shows the decreasing trend between the years 1995 to 2000 and 2015 to 2022 also. The maximum increasing and minimum decreasing of barre land was recorded from 2010 to 2015 and 2005 to 2010 respectively. In addition to the year 1995 to 2000 in wutrin watershed vegetation increasing also shown between 2005 and 2010 in this watershed. In contrast to wutrin, Meadowland cover class in wuseta watershed shows the increasing trend not only from 2010 to 2015 but also from 1995 to 2000 and 2015 to 2022.

4.2. Accuracy assessment

Accuracy assessment of image classification was processed using ENVI software and the result revealed that the overall accuracies for each year are 97.2%, 96.6%, 96.8%, 96.4%, 90.33%, and 91.2% with the Kappa Coefficient of 0.96, 0.95, 0.96, 0.95, 0.88 and 0.89 for years 1995, 2000, 2005, 2010, 2015 and 2022 respectively. The accuracy requirements for change detection analysis were determined based on the suggestion of Congalton and Green (2009). All the overall accuracies are greater than 85%, which indicates that all classifications are in an acceptable range and the kappa coefficient is greater than 0.80, which represents the existence of a strong agreement between the classified image samples and the ground truth samples. Hence, the classified land uses land cover maps met the accuracy requirements for change detection analysis. The detail of the error matrix results for each year was shown in Appendix B.

Table 4.6: Accuracy assessment of the classified images by study periods (all accuracies are in percent)

LULC class	Year											
	1995		2000		2005		2010		2015		2022	
	UA	PA	UA	PA	UA	PA	UA	PA	UA	PA	UA	PA
UA’	100	96.4	100	99.4	100	98.2	100	97.6	93.7	98.8	99.4	100
AL	98.5	100	96	99.8	95.9	100	94.3	100	91.6	100	97.9	100
BL	89.2	86.7	91.9	86.7	95.7	85.7	100	79.1	67.8	74.3	69.3	66.7
Ve	99.3	100	99.2	99.2	100	100	98.5	100	100	100	99	97.2
Me	95.1	95.5	95.7	91.5	95	92.7	95.9	94.3	93.9	80.9	85	85
OA	97.2		96.6		96.8		96.4		90.33		91.2	
KC	0.96		0.95		0.96		0.95		0.88		0.89	

Where: UA’ = urban area, AL = agricultural land, BL = barren land, Ve = Vegetation, Me = meadow, UA = user’s accuracy, PA = producer’s accuracy, OA = overall accuracy, KC = kappa coefficient.

4.3. LULC model validation and prediction

4.3.1. LULC model validation

For future simulation, the MOLUSCE plugin incorporates several popular transition potential modeling techniques, including the logistic regression, weights of evidence, ANN (multilayer perceptron), multi-criteria evaluation, and CA algorithm. The land use/cover map of 2010 and 2015 was used as input to predict the LULC for 2022 and obtained a validation kappa value of 0.903. The variables chosen for model calibration were elevation, slope, and distance from urban center, streams, main roads, and land use/cover. These variables were chosen due to their relatively strong association with LULC. In order to model and predict transition potentials, the study used the CA-ANN technique. Once the anticipated LULC was obtained, it was compared to the actual LULC for 2022 and yielded an overall accuracy of 88.8%.

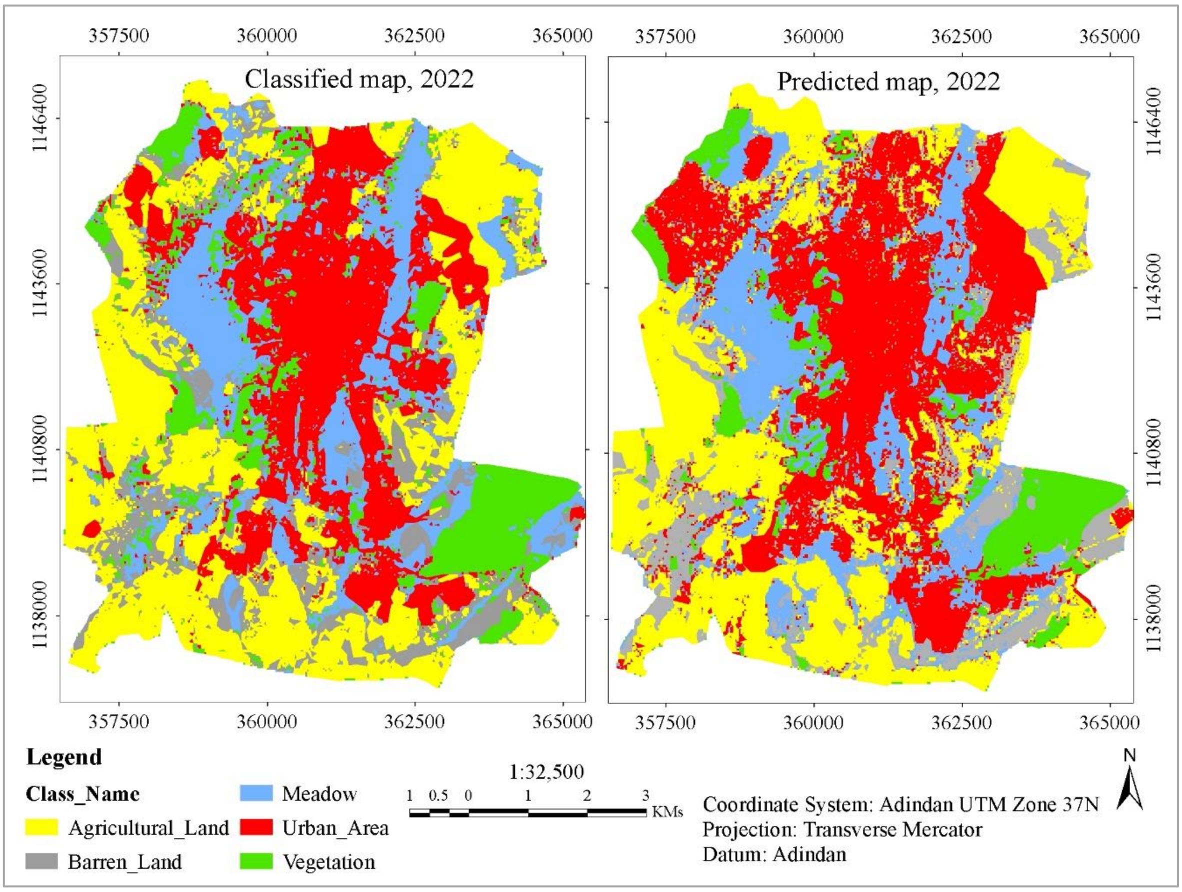

Figure 4.3: Comparison of classified and simulated map (source: from research analysis)

4.3.2. LULC prediction

The LULC change analysis explores the spatial dynamic variations in the LULC during the study period. After obtaining satisfactory results from model validation, the LULC for 2040 was predicted. By employing the spatiotemporal LULC data from 2005 and 2022, the spatial variables, and the transition probability matrix with a kappa value of 0.95, the LULC was predicted for 2040. The simulation results of the MoLUSCE's model prediction from 2022 to 2040 were demonstrated and the result shows that the urban area will increase from 1687.72ha in 2022 to 2638.63ha in 2040. On the other hand, Barren land will increase from 854ha in 2022 to 998.98ha in 2040. In contrast, area of agricultural land would be decrease to 1573.31ha in 2040 from 2067.1ha in 2022. Similar to agricultural land, the area of vegetation cover will expected to decrease from 774.23 ha in 2022 to 498.69ha in 2040. During the simulated years, the area of the meadow from 2022 to 2040 will also decrease from 1197.22ha to 871.3ha. Generally, the simulated change in areal extent, the percentage change (%), and the annual rate of change of the LULC class were presented in Tables 4.7. The results show the continuous expansion of the urban area that will increase by 950.91ha and a percentage change of 56.34% at the annual rate of change of 2.51% per year from 2022 to 2040. While agricultural land would be declined by -493.79ha and the percentage change -23.89% at an annual rate of change of -1.51% per year, the Barren land will increase by 144.98ha and a percentage change of 16.98% at an annual rate of change of 0.87% per year. Vegetation cover will decrease by -275.54ha (-35.59%) at an annual rate of change of -2.41% per year. The area of the meadow will also be decreased by -325.91ha (-27.22%) from 2022 to 2040 with the annual changing rate of -1.75%. The predicted LULC map of 2040 is depicted in Figure 4.4 below.

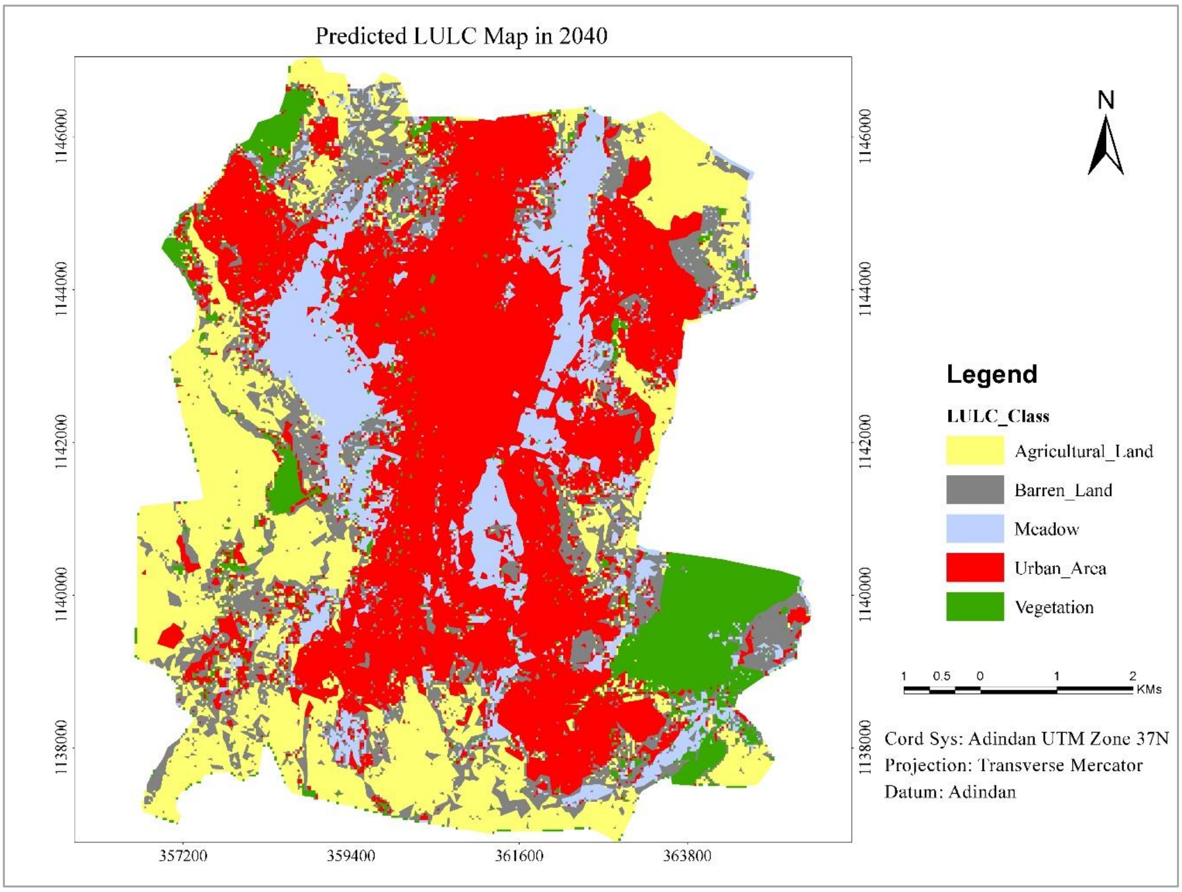

Figure 4.4: Predicted LULC maps for the year 2040 (source: from research analysis)

Table 4.7: Area extent of predicted LULC (2040) and its average annual percent change (AAPC) from 1995 to 2022

LULC Class	Area (ha)			Change (1995-2040)		Change (2022-2040)		AAPC (%)
	1995	2022	2040	ha	%	ha	%	(2022-2040)
Urban Area	296.72	1687.72	2638.63	2341.91	789.27	950.91	56.34	3.13
Agri_Land	3206.42	2067.10	1573.31	-1633.11	-50.93	-493.79	-23.89	-1.33
Barren Land	448.02	854.00	998.98	550.96	122.98	144.98	16.98	0.94
Vegetation	1138.71	774.23	498.69	-640.02	-56.21	-275.54	-35.59	-1.98
Meadow	1490.72	1197.22	871.31	-619.41	-41.55	-325.91	-27.22	-1.51

According to the LULC forecast, towns' total urban land area is projected to grow from 1687.72ha in 2022 to 2638.63ha in 2040. Stated otherwise, there will be an annual increase in urban land area of 3.13% or 56.34% over the course of the predicted year. Barren land is predicted to grow by 16.98% over eighteen-year period or by annual increase of 0.94%, despite the fact that its quantity and rate of increase diverge from those of urban land. From the base to the end of study year, vegetation cover, meadows and agricultural land will decrease by -35.59%, -27.22% and -23.89% or with annual change of -1.98%, -1.51% and -1.33% respectively.

Table 4.8: Area extent of predicted LULC (2040), wuseta watershed, and its change from 1995 and 2022

LULC Class	Area (ha)			Change (1995-2040)		Change (2022-2040)	
	1995	2022	2040	ha	%	ha	%
Urban Area	170.79	992.70	1532.73	1361.94	797.41	540.03	54.40
Agri_Land	1522.70	947.51	637.13	-885.57	-58.16	-310.39	-32.76
Barren Land	332.62	454.27	491.88	159.26	47.88	37.61	8.28
Vegetation	640.07	432.45	343.77	-296.29	-46.29	-88.67	-20.51
Meadow	811.55	656.02	472.38	-339.17	-41.79	-183.64	-27.99

From 2022 to 2040, the area coverage of urban land of wuseta watershed will expected to increase by 540.03ha or by 54.4%. Similar to urban land barren land also shown an increasing trend which increased by 8.28% within eighteen year interval. In contrast to urban area and bare land, other land cover classes like agricultural land, meadow and vegetation cover shown a decreasing trend that decreases by -32.76%, -27.99% and -20.51% respectively throughout the prediction year.

Table 4.9: Area extent of predicted LULC (2040), wutrin watershed, and its change from 1995 and 2022

LULC Class	Area (ha)			Change (1995-2040)		Change (2022-2040)	
	1995	2022	2040	ha	%	ha	%
Urban Area	125.79	695.01	1105.45	979.66	778.80	410.43	59.05
Agri_Land	1679.62	1119.59	932.78	-746.85	-44.47	-186.81	-16.69
Barren Land	114.77	399.83	506.02	391.25	340.88	106.19	26.56
Vegetation	494.41	341.78	149.96	-344.45	-69.67	-191.83	-56.13
Meadow	678.00	541.19	398.03	-279.97	-41.29	-143.16	-26.45

The Wuseta watershed's urban land coverage is estimated to grow by 410.43ha, or 59.05%, between 2022 and 2040. Barren land has also demonstrated an increasing trend, rising by 26.56% over the course of eighteen years, much like urban land. Other land cover groups, such as agricultural land, meadow, and vegetation cover, have demonstrated a decreasing tendency during the predicted year, with decreases of -20.51%, -27.99%, and -32.76%, respectively, in comparison to bare land and urban areas.

When the shifting trend of each land cover class was compared across different spatial scales with respect to study year, there was a noticeable shift with each of land cover classes. Given the comparison of the trends in urban land between the two sub-watersheds, the wutrin watershed's urban land growth is bigger than the wuseta watershed's. In addition to following the growing trend of urban land, barren land has a greater increase in wutrin watershed than wuseta. While the meadow's changing tendency in the two watersheds will be roughly comparable, the agricultural land and vegetation cover's changing trend will diverge. While the meadow's changing tendency in the two watersheds will be roughly comparable, the agricultural land and vegetation cover's changing trend will diverge. The wuseta watershed's declining percentage of agricultural land will be two times higher than the wutrin watershed's percent change. In contrast to agricultural land, the wurtin watershed's vegetation cover will vary by a factor of almost three compared to the wuseta watersheds'.

4.4. Computation of Surface runoff characteristics

4.4.1. Computation of surface runoff depth

The calculation of runoff generation in the SCS model mainly relied on CN values, which was a function of AMC, surface condition, slope, soil type and land use land cover. The town's soil map, which only includes soil group B, was used to determine the hydrologic soil group the study area. The hydrologic soil group and the land use map were intersected to form the curve number map. Using the curve number map, the hydrologic response unit (HRU) was determined. HSG-B is the obtained hydrologic soil group for each LULC class.

Overall, the results show that runoff depth for both towns and watersheds has been increasing over the course of the 27-year timeframe. This increasing trend is present in all spatial scales and of the years that were chosen for the analysis. In every case, the wuseta watershed's accumulated daily runoff depth is higher, and the opposite is true for the wutrin watershed. At the town, wutrin, and wuseta watersheds scale, the runoff depth begins in 1995 at slightly over 7.3 mm, 7.03 mm, and 7.56 mm, respectively; in the final year, this figure increases to over 11 mm, 10.55 mm, and 11.55 mm, respectively, indicating a 51%, 50%, and 53% increase over a 27-year period. Further analysis indicates that the runoff depth of the town was identified at a nearly equal amount from that of its watersheds across the entire period. During the study period, the maximum and minimum difference between the runoff depth of the town and wuseta watershed and town and wutrin watershed was -0.54mm and -0.17mm and 0.18mm and 0.47mm respectively. In response to land use changes, the trend of surface runoff showed a continuously increasing trend. The findings showed that, at all spatial scales, the maximum runoff happened in 2022 and the minimum value was in 1995.

Table 4.10: Daily runoff depth in the city and its watersheds from 1995 to 2022 (units are in millimeter)

S/N	Spatial boundary	Year						
		1995	**2000**	**2005**	**2010**	**2015**	**2022**	**ΔQ in % (1995-2022)**
1	Town boundary	7.30	7.45	8.06	8.14	9.50	11.00	50.70
2	Wuseta watershed	7.56	7.64	8.25	8.32	9.80	11.55	52.79
3	Wutrin watershed	7.03	7.24	7.85	7.96	9.17	10.53	49.87

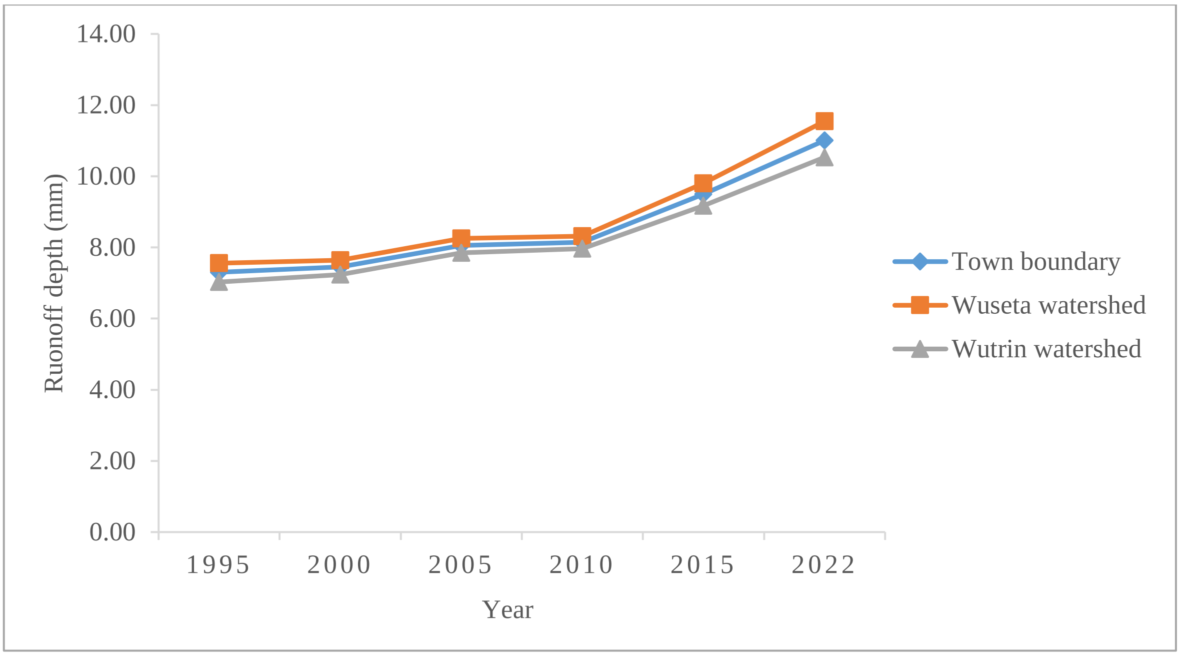

Figure 4.5: Spatiotemporal daily runoff change in the town and its watersheds (1995-2022)

4.4.2. Computation of surface runoff flowrate

The runoff coefficient of urban area, agricultural land, barren land, vegetation and meadow in wuseta watershed were assigned as 0.86, 0.37, 0.47, 0.2 and 0.15 respectively. The weighted runoff coefficient for each study period were computed and its result were 0.32, 0.32, 0.36, 0.38, 0.42 and 0.46 in the year 1995, 2000, 2005, 2010, 2015 and 2022 respectively. In this watershed the time of concentration were 2.8hr and the intensity of rainfall were 108.62mm/hr. Using these computed results, the amount of rainfall that runoff the specified outlet per unit of time were determined. The computed result shows that the amount of runoff that passes the given outlet per unit of second increases from 339.51m^3/s in 1995 to 487.42m3/s in 2022. In similar manner the time of concentration and rainfall intensity of wutrin watershed were computed and the result recorded as 2.1hr and 145.01mm/hr respectively. The watersheds weighted runoff coefficient for 1995, 2000, 2005, 2010, 2015 and 2022 were 0.32, 0.33, 0.37, 0.38, 0.4, and 0.44 respectively. The resulting runoff flow rate were increased from 399.59m^3/s to 547.88m^3/s. The trend of surface runoff generated discharge across the study period was increasing 339.51m3/s, 338.83m^3/s, 375.78m^3/s, 402.13m^3/s, 439.80m^3/s and 487.42m^3/s and 399.59m^3/s, 416.58m^3/s, 459.82m^3/s, 473.71m^3/s, 502.41m^3/s, 547.88m^3/s for wuseta and wutrin watersheds for the year 1995, 2000, 2005, 2010, 2015 and 2022 respectively. As compared with the runoff flow rate of the two watersheds, the flow rate of wutrin watershed was greater than that of wuseta watershed.

Due to its maximum area coverage, agricultural land followed by meadow was responsible to the generation of maximum amount of runoff throughout the study period at both watersheds. The amount of discharge generated from urban and barren land was relatively small over the study years in both spatial scales. Specifically, the runoff flow rate of urban area of wutrin and weseta watersheds was increased from 16.25m^3/s in 1995 to 123.12m^3/s in 2022 and from 16.67m^3/s in 1995 to 139.14 m^3/s 2022 respectively. Unlike the runoff depth, the runoff flow rate of wuseta was greater than wutrin. This increasing trend revealed that how the increasing of urban land directly affect the characteristics of runoff.

4.5. Relationship between surface imperviousness ratio and runoff characteristics

The relationship of imperviousness and runoff characteristics were evaluated using the percent change of urban land and runoff depth in the final study year in relation to the base year. The percent change of urban area between 1995 and 2000 was 35.74%, 47.25% and 27.32% at the town, wutrin watershed and wuseta watershed level respectively. These values increased to 468.79%, 452.52% and 481.23% between the base and final study year. The percentage change of runoff depth of Town boundary, wuseta and wutrin watersheds between 1995 and 2000 were 2.02%, 1.11% and 3.02% respectively. This value rose to 50.7%, 52.79% and 49.87% respectively between the base year (1995) and the final year (2022). The results are consistent with common sense that the increase in impervious land probably causes the increase in surface runoff, but the greater amount of vegetation, farmland, and meadow probably lead to decrease in surface runoff. Generally, the study result clearly showed that how the change of LULC alter the runoff characteristics.

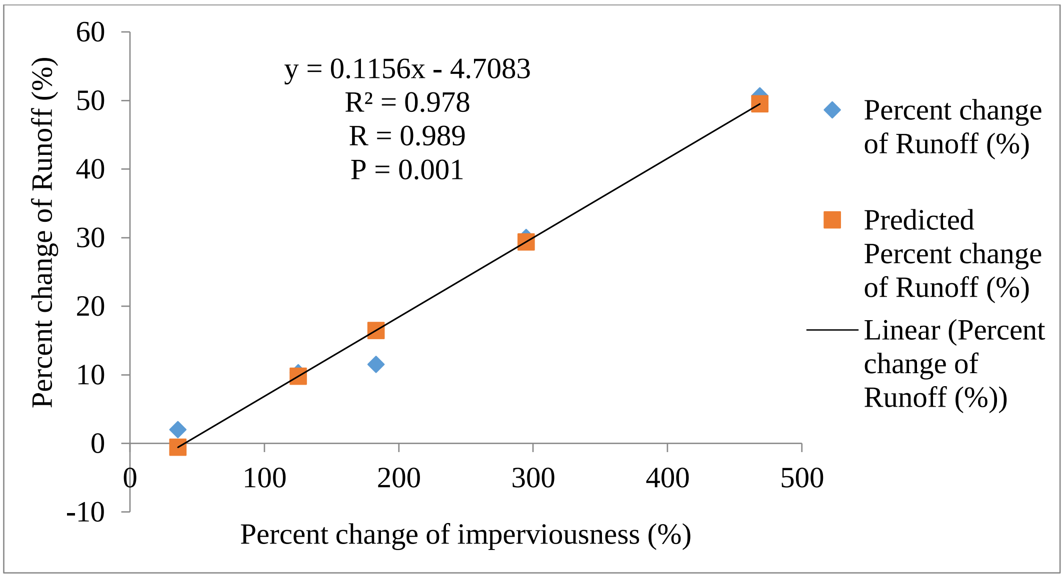

(a) Town boundary

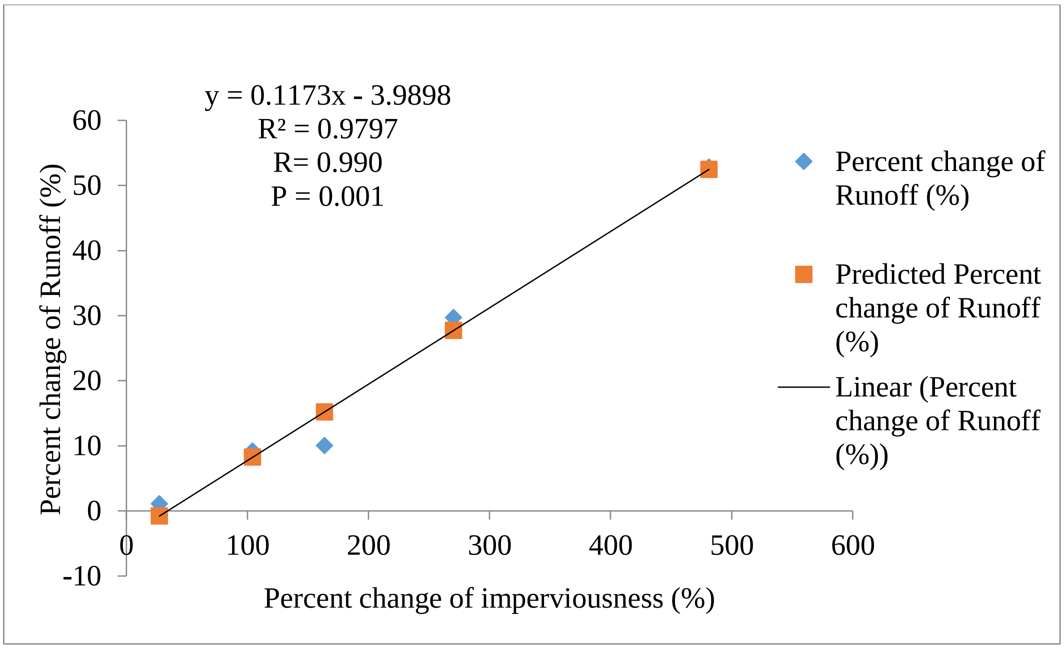

(b) Wuseta watershed

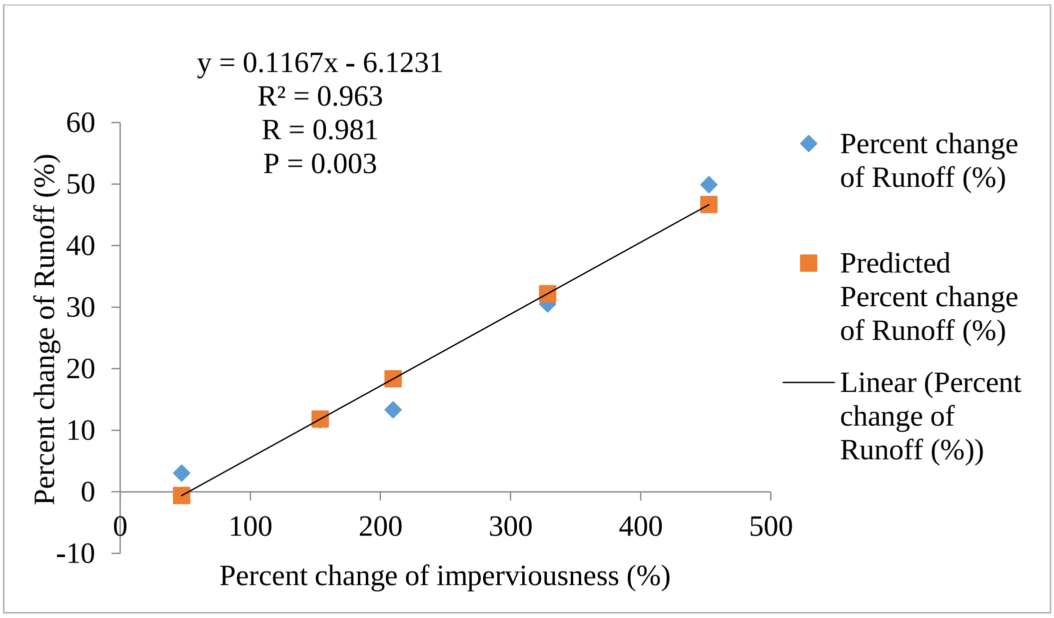

(c) Wutrin watershed

Figure 4.6 (a), (b) and (c) shows the correlation of runoff depth with imperviousness at different spatial scale

The results showed that there was a positive and significant correlation between the urban area and total surface runoff depth with R^2 of 98.9%, 98.9% and 98.1% for town, wuseta and wutrin watersheds respectively. The coefficient of determination of the town, wuseta and wutrin watersheds were 97.8%, 97.8% and 96.3% respectively, this result tells us how much the runoff can be accounted for imperviousness. In addition, regression analysis results showed that there was a linear relation between runoff depth, and slope length and slope steepness. The results depicts that the change in surface runoff positively correlated to the change in impervious land and negatively correlated to the change in vegetation and agricultural land. The percent change in runoff depth is directly related to the changes in PIA in both spatial scales. Further, the Pearson correlation coefficient appears a very strong correlation between the two variables. Further, the positive and negative values indicate direct and indirect relationships, respectively.

4.6. Discussion

By tracking the expansion of the research area's coverage during the previous 27 years, variations in urban LULC change were examined. After utilizing ENVI software to perform support vector machine-supervised classification, the land cover maps were produced, and their areal value was calculated using the post-classification technique in the ArcGIS environment. The results of the data analysis on LULC change detection for each of the corresponding years indicate a significant increase in urban and barren land over the study period, as well as a shrinkage phenomenon in agricultural land, vegetation, and meadow. Due to the corresponding horizontal growth and the conversion of land cover classes during the various study periods, the study region has seen spatial variations and trends on various land use land cover classes. As the results, demonstrated, agricultural land was the dominating class at the start of the study period but dropped as urban area and barren land continued to grow.

Due to the town's rapid urban expansion during the study period, the results demonstrate continuous shifts in each LULC category's land use and/or land cover to a different class. In 1995, the first research year, the urban area's spatial area coverage was 296.72ha, or 4.51% of the total area. Its geographic size grew over each research period, reaching 1687.72 ha, or 25.65% of the study area, in 2022. The trend of urban growth was relatively modest between 2005 and 2010, with an increase of 25.73%, while the largest change was observed between 2000 and 2005 (65.92%); 2022, 2015, and 2000 exhibited percentage changes of 44.03, 39.46, and 35.74, respectively.

The findings demonstrate a strong increasing tendency, with the areas covered by urban area and barren land expanding by +1391ha (+468.79%) and +405.98ha (+90.62%) between 1995 and 2022, respectively, with yearly average changes of +17.36% and +3.36%. In comparison, the annual average change in agricultural land and vegetation was

-1139.32ha (-35.53%) and -364.48ha (-32.01%) at annual average change of -1.32% and -1.19% respectively. The data also show that the meadow's acreage continued to decline, losing -293.50 hectares at an average yearly change of -0.73%. 1139.32 hectares of agricultural land, 364.48 hectares of vegetated area, and 293.50 hectares of meadow were changed to other land uses over the research period, primarily to urban areas, with an average annual change of -1.32%, -1.19%, and -0.73% annually, respectively.

In comparison, at the start of the study year, the area statistics of agricultural lands were 48.73%. Prior to dropping to 31.41% in the last year of the study period, 2022, it fluctuated through scenarios of both decrease and increase, falling to 44.13% in 2000. Comparing the area coverage of agricultural land in the base year with that of the previous year revealed a reduction of -1139.32ha, or -35.53%. However, compared to the first research year, the extent of barren land doubled during the most recent study period, covering 12.98% of the whole landscape as opposed to 6.81%. On the other hand, the research period saw declining trends in the area covered by meadow and vegetation; they declined from 1490.72 ha to 1197.22 ha (22.65% to 18.2%) and from 1138.7 ha to 774.23 ha (17.3% to 11.77%), respectively. For the classes of urban, agricultural land, barren land, vegetation, and meadow, the differences in area coverage between the base year (1995) and the final year (2022) were 1391 ha (468.79%), -1139.32 ha (-35.53%), 406.08 ha (90.64%), -364.48 ha (-32.01%), and -293.5 ha (-19.69%), respectively.

The area extent of wuseta urban land and its change of the respective study years were greater than that of wutrin watershed. This is condition is similar in all other land cover classes except agricultural land cover class. In contrast, of urban land and other land cover classes, the area of agricultural land of wuseta watershed was continuously decrease with the great difference from agricultural land wuseta watershed. The area change and percent change of land cover classes of wutrin and wuseta watershed was computed and the result revealed that the area change of urban land were maximum (156.03ha and 360.18ha respectively) between the yeas 2015 and 2022 followed by 149.33ha from 2010 to 2015 and 133.81ha from 2000 to 2005. Unlike wutrin watershed that shows the decreasing of barren land only between 2005 and 2010, in wuseta watershed it shows the decreasing trend between the years 1995 to 2000 and 2015 to 2022 also. In contrast to wutrin, Meadowland cover class in wuseta watershed shows the increasing trend not only from 2010 to 2015 but also from 1995 to 2000 and 2015 to 2022.

The results show that runoff depth for both towns and watersheds has been increasing over the course of the 27-year timeframe. This increasing trend is present in all spatial scales and of the years that were chosen for the analysis. In every case, the wuseta watershed's accumulated daily runoff depth is higher, and the opposite is true for the wutrin watershed. At the town, wutrin, and wuseta watersheds scale, the runoff depth begins in 1995 at slightly over 7.3 mm, 7.03 mm, and 7.56 mm, respectively; in the final year, this figure increases to over 11 mm, 10.55 mm, and 11.55 mm, respectively, indicating a 51%, 50%, and 53% increase over a 27-year period. Further analysis indicates that the runoff depth of the town was identified at a nearly equal amount from that of its watersheds across the entire period. During the study period, the maximum and minimum difference between the runoff depth of the town and wuseta watershed and town and wutrin watershed was -0.54mm and -0.17mm and 0.18mm and 0.47mm respectively. In response to land use changes, the trend of surface runoff showed a continuously increasing trend. The findings showed that, at all spatial scales, the maximum runoff happened in 2022 and the minimum value was in 1995.

The runoff coefficient of urban area, agricultural land, barren land, vegetation and meadow in wuseta watershed were assigned as 0.86, 0.37, 0.47, 0.2 and 0.15 respectively. The weighted runoff coefficient wuseta and wutrin watersheds were computed and its result were 0.32, 0.32, 0.36, 0.38, 0.42 and 0.46 and 0.32, 0.33, 0.37, 0.38, 0.4, and 0.44 in the year 1995, 2000, 2005, 2010, 2015 and 2022 respectively. The time of concentration and rainfall intensity of wuseta and wutrin watersheds were computed and the result recorded as 2.8hr and 108.62mm/hr for wuseta watershed and 2.1hr and 145.01mm/hr for wutrin watershed. Using these computed results, the amount of rainfall that runoff the specified outlet per unit of time were determined. The resulting runoff flow rate were increased from $399.59m^3/s$ to $547.88m^3/s$ in wutrin and from $339.51m^3/s$ to $487.42m^3/s$ in wuseta watershed. As compared with the runoff flow rate of the two watersheds, the flow rate of wutrin watershed was greater than that of wuseta watershed.

Pearson correlation coefficient (r) is almost equal to +1 which is a nearly perfect positive correlation, signifies that both variables move in the same direction. It also signifies that the two variables being compared have a perfect positive relationship; that means these two are strongly related. Through the study, it was also found that the infiltration and runoff are largely correlated.

5. Conclusions and Recommendations

5.1. Conclusion

The transformation of natural or agricultural ecosystems into urban settings is known as urbanization, and it represents a widespread and quick change in land use. By utilizing remote sensing techniques to analyze the phenomena at different times, these changes in their status can be found. The conversion of undeveloped land to built-up has the potential to reduce evapotranspiration, interception and time of concentration and enhance runoff depth and flowrate. Analyzing how this land cover conversion affected the characteristics of surface runoff was the main goal of this study. Soil Conservation Service Curve Number method integrated with geospatial technologies was utilized to assess the impact of urbanization driven land use land cover change on surface runoff. The quality and amount of water resources are monitored, changes over time and predicted, catchment yields and responses are understood, water availability is estimated, and changes to the hydrological cycle are all accounted for by surface runoff modeling.

Land use land cover and soil type maps have been prepared using ENVI software, which used to determine the CN map of the study area that enables to determine the runoff. GIS, an efficient tool, was used for the preparation of most of the input data required by the SCS curve number model and ENVI was used for the classification of land use land cover map. Types B and type D of soil have been classified within the region, five classes of LULC were categorized, namely; urban area, agricultural land, barren land, vegetation and meadow. This study showed an increase in urban areas and barren land. The urban area expanded from 296.72ha (4.51%) to 1687.72ha (25.65%) over 27 years. There was a corresponding reduction in agricultural land, vegetation, and meadows. In this study, it was found that the urban area having a higher curve number contributes higher runoff and the vegetation with a lower curve number contributes lesser runoff.

The CN values were determined using looking table and range from 72 to 95, and the weighted CN for the Town, wuseta watershed and wutrin watershed was range from 78 to 84. Daily rainfall data for the years 1995-2022 was used to compute the runoff characteristics during study years. SCS–CN method was applied to compute the runoff depth and flowrate for Debre Markos ungauged watershed having an area of 65.82km^2. Based on the computation result, the maximum depth of daily runoff was recorded as 11.55mm in wuseta watershed, however, the minimum runoff depth of 7.03 mm in wutrin watershed. Similarly the runoff coefficient for different LULC were determined as 0.86, 0.37, 0.47, 0.20 and 0.15 for urban area, agricultural land, barren land, vegetation and meadow respectively from looking table by considering difference in land cover and slope. The runoff flowrate in 2022 was 487.42m^3/s for wuseta and 547.88m^3/s for wutrin watershed and flowrate in the year 1995 was 339.51m^3/s for wuseta and 399.59m^3/s wutrin watershed. Over a study period of 27 years, it can be seen that runoff increased by 52.8%, 50.7% and 49.9% at wuseta watershed, town and wutrin watershed respectively. Thus, it is very evident that because of urbanization, the runoff increases at the cost of decreased infiltration. It can be concluded that the runoff mainly depends upon rainfall, soil texture, and the type of land cover.

Pearson correlation coefficient (r) is almost equal to +1 which is a nearly perfect positive correlation, signifies that both variables move in the same direction. It also signifies that the two variables being compared have a perfect positive relationship; that means these two are strongly related. Through the study, it was also found that the imperviousness and runoff are largely correlated. There was a strong relationship between the increase in impervious surface and the increase in runoff depth and flowrate. It was observed that LULC changes had influenced surface runoff leading to an increasing trend in surface runoff depth and flowrates for the study area. The estimated runoff of the area is useful for managing the urban water and drainage system.

5.2. Recommendations

Based on the population projection of Debre Markos town by the Central Statics Agency of Ethiopia 2022 report, the population of the town will increase from 49297 to 140700 from 1994 – 2022. This shows how the population of the city increases dynamically from year to year. If the population of the city continues like this the demand for housing and conversion of other land use types to urban areas also increase. As the result of this research showed, there are problems associated with a hydrological process in the town and this is due to the high rate of urbanization. Even if Such types of urban development has a great positive impression, social, economic, environmental, and political problems of uncontrolled rapid horizontal expansion of cities/towns, they may cause a major impact, on the prevailing runoff and these issues must be addressed in urban planning to promote effective solutions for maintaining the water cycle and water resources in urban areas.

The future runoff characteristics were forecasted using the future LULC change scenario only, in addition to this including the climate change scenario would be better to precisely estimate the future runoff characteristics. In addition this, the impact of spatiotemporal land use land cover change on the surface runoff characteristics was computed by taking into account the daily rainfall data, but the seasonal and annual basis hydrological impact of urbanization remains unexamined. The township contains numerous wetland areas, and there is considerable concern about both protecting wetlands and protecting recharge for local and municipal water supplies. The coming researchers should investigate the hydrologic-impact assessment on the study area from its result the township will revise the local zoning regulations.

Instead of new housing development, renewal of older buildings and infill development of high-rise buildings will be better solution to meet the demands and needs of the increasing population in the town. In addition, the construction of condominium houses is another solution. This will reduce the horizontal expansion of the town and the depth and flow rate of the surface runoff.

The use of high-resolution imageries such as IKONOS and Quick Bird are important in generating good quality land cover maps. Because urban areas have complex and heterogeneous features, high-resolution imagery provides better information by mapping these areas. Moreover, the use of the latest model and methodology for modeling and prediction helps to get better findings.

Due to the time constraint to measure the rainfall-runoff relationship at the site in this research, validating the computed amount of runoff depth and its flowrate becomes unmanageable; so the coming researchers better to validate the computed value of runoff characteristics with the most precisely measured actual values. In this regard, the researchers able to check the accuracy of the method that used in the research.

One of the limitations of the present work is considering a single urban built-up LULC class, which has resulted in very high CN value. Therefore considering different urban land use classes like residential, commercial, mixed use etc. will increase the precision of the computed result.

REFERENCE

Abebaw, A. (2017). Monitoring the urban growth of Debre Markos Town (1984-2012), Ethiopia: Using satellite images and GPS. *Journal of Geography and Regional Planning*, *10*(4), 69–76. https://doi.org/10.5897/jgrp2016.0533

Achamyeleh, G. A. (2014). Urbanization and the Struggle for Land in the Peri-Urban Areas of Ethiopia. *Bahir Dar University, Ethiopia*.

Alam, N., Saha, S., Gupta, S., & Chakraborty, S. (2021). Prediction modelling of riverine landscape dynamics in the context of sustainable management of floodplain: a Geospatial approach. *Annals of GIS*, *27*(3), 299–314.

Andrews, R. G. (1954). The use of relative infiltration indices in computing runoff. *Unpublished. Soil Conservation Service, Fort Worth, Texas*, *6*.

Aneesha Satya, B., Shashi, M., & Deva, P. (2020). Future land use land cover scenario simulation using open source GIS for the city of Warangal, Telangana, India. *Applied Geomatics*, *12*, 281–290.

Ara, Z., & Zakwan, M. (2018). *Estimating Runoff Using SCS Curve Number Method*. *8*, 195–200.

Atasoy, M., Biyik, C., Ayaz, H., Karsli, F., Demir, O., & Baskent, E. Z. (2006). Monitoring land use changes and determining the suitability of land for different uses with digital photogrammetry. *Remote Sensing and Photogrammetry, Cairo, Egypt*, *23*, 712–721.

Bahari, N. I. S., Ahmad, A., & Aboobaider, B. M. (2014). Application of support vector machine for classification of multispectral data. *IOP Conference Series: Earth and Environmental Science*, *20*(1), 12038.

Bajracharya, A. R., Rai, R. R., & Rana, S. (2015). Effects of Urbanization on Storm Water Run-off: A Case Study of Kathmandu Metropolitan City, Nepal. *Journal of the Institute of Engineering*, *11*(1).

Bawahidi, K. S. Y. (2005). Integrated land use change analysis for soil erosion study in ulu kinta catchment. *Universiti Sains Malaysia*.

Betru, T., Tolera, M., Sahle, K., & Kassa, H. (2019). Trends and drivers of land use land cover change in Western Ethiopia. *Applied Geography*, *104*, 83–93.

https://doi.org/10.1016/J.APGEOG.2019.02.007

Bewket, W., & Abebe, S. (2013). Land-use and land-cover change and its environmental implications in a tropical highland watershed, Ethiopia. *International Journal of Environmental Studies*, *70*(1), 126–139. https://doi.org/10.1080/00207233.2012.755765

Bhatta, B., Saraswati, S., & Bandyopadhyay, D. (2010). Urban sprawl measurement from remote sensing data. *Applied Geography*, *30*(4), 731–740.

Briassoulis, H. (2019). *The Web Book of Regional Science Sponsored by Analysis of Land Use Change : Theoretical and Modeling*. 248.

Brito, P. L., & Quintanilha, J. A. (2012). A literature review, 2001–2008, of classification methods and inner urban characteristics identified in multispectral remote sensing images. *Proceedings of the 4th GEOBIA*, 586–591.

Bulti, D. T., & Abebe, B. G. (2020). Analyzing the impacts of urbanization on runoff characteristics in Adama city, Ethiopia. *SN Applied Sciences*, *2*(7), 1–13. https://doi.org/10.1007/s42452-020-2961-3

Burns, M. J., Fletcher, T. D., Walsh, C. J., Ladson, A. R., & Hatt, B. E. (2012). Hydrologic shortcomings of conventional urban stormwater management and opportunities for reform. *Landscape and Urban Planning*, *105*(3), 230–240.

Butt, A., Shabbir, R., Ahmad, S. S., & Aziz, N. (2015). Land use change mapping and analysis using Remote Sensing and GIS: A case study of Simly watershed, Islamabad, Pakistan. *Egyptian Journal of Remote Sensing and Space Science*, *18*(2), 251–259. https://doi.org/10.1016/j.ejrs.2015.07.003

Calder, I. R. (2002). Forests and hydrological services: reconciling public and science perceptions. *Land Use and Water Resources Research*, *2*(1732-2016–140265).

Cao, M., Tang, G., Zhang, F., & Yang, J. (2013). A cellular automata model for simulating the evolution of positive–negative terrains in a small loess watershed. *International Journal of Geographical Information Science*, *27*(7), 1349–1363.

Cardoso-fernandes, J., Teodoro, A. C., Lima, A., Mielke, C., Roda-robles, E., & Cauzid, J. (2020). MULTI-SCALE APPROACH USING REMOTE SENSING TECHNIQUES FOR LITHIUM PEGMATITE EXPLORATION : FIRST RESULTS Department of Geosciences , Environment and Land Planning , Faculty of Sciences , University of

Porto , ICT (Institute of Earth Sciences) – Porto pole. *International Geoscience and Remote Sensing Symposium*, *1*, 5226–5229.

Central Statistical Agency. (2013). Population Projection of Ethiopia for All Regions At Wereda Level from 2014 – 2017. *Journal of Ethnobiology and Ethnomedicine*, *3*(1), 28. http://www.csa.gov.et/images/general/news/pop_pro_wer_2014-2017_final

Chang, K. (2016). Geographic information system. *International Encyclopedia of Geography: People, the Earth, Environment and Technology*, 1–10.

Chen, W., Huang, G., & Zhang, H. (2017). Urban stormwater inundation simulation based on SWMM and diffusive overland-flow model. *Water Science and Technology*, *76*(12), 3392–3403. https://doi.org/10.2166/wst.2017.504

Cherian, B., Das, D. P., John, L., Devadathan, M., & Malakeel, G. S. (2017). *A Study on Impact of Urbanisation on Surface Runoff in Muvattupuzha Municipality*. 5814–5821. https://doi.org/10.15680/IJIRSET.2017.0604195

Cho, Y., & Engel, B. A. (2018). Spatially distributed long-term hydrologic simulation using a continuous SCS CN method-based hybrid hydrologic model. *Hydrological Processes*, *32*(7), 904–922. https://doi.org/10.1002/hyp.11463

Chughtai, A. H., Abbasi, H., & Karas, I. R. (2021). A review on change detection method and accuracy assessment for land use land cover. *Remote Sensing Applications: Society and Environment*, *22*, 100482. https://doi.org/https://doi.org/10.1016/j.rsase.2021.100482

Cohen, B. (2006). Urbanization in developing countries: Current trends, future projections, and key challenges for sustainability. *Technology in Society*, *28*(1–2), 63–80.

Cohen, J. (1960). A Coefficient of Agreement for Nominal Scales. *Educational and Psychological Measurement*, *20*(1), 37–46. https://doi.org/10.1177/001316446002000104

Congalton, R. (2016). *Evaluación de la exactitud de los principios y prácticas de los datos de detección remota*. *01*, 1–23.

Congalton, R. G. (1991). A review of assessing the accuracy of classifications of remotely sensed data. *Remote Sensing of Environment*, *37*(1), 35–46. https://doi.org/10.1016/0034-4257(91)90048-B

Cronshey. (1986). Urban Hydrology for Small. *Soil Conservation*, *Technical Release 55 (TR-55)*, 164. http://scholar.google.com/scholar?hl=en&btnG=Search&q=intitle:Urban+Hydrology+for+Small+watersheds#1

Dadi, D., Azadi, H., Senbeta, F., Abebe, K., Taheri, F., & Stellmacher, T. (2016). Urban sprawl and its impacts on land use change in Central Ethiopia. *Urban Forestry and Urban Greening*, *16*, 132–141. https://doi.org/10.1016/j.ufug.2016.02.005

DeMers, M. N. (2009). *GIS for Dummies*. John Wiley & Sons.

Devia, G. K., Ganasri, B. P., & Dwarakish, G. S. (2015). A Review on Hydrological Models. *Aquatic Procedia*, *4*, 1001–1007. https://doi.org/https://doi.org/10.1016/j.aqpro.2015.02.126

Dhawale, A. W. (2013). Runoff Estimation for Darewadi Watershed using RS and GIS. *International Journal Of Recent Technology and Engineering (IJRTE)*, *1*(6), 46–50. https://doaj.org/article/31fcc428fe87488bae0f3726b9ad39f1

Didore, V., Nalawade, D., & Vaidya, R. (2021). Remote Sensing Data Classification Technique: A Review. *International Journal of Advanced Research in Science, Communication and Technology*, 67–75. https://doi.org/10.48175/IJARSCT-2084

Dinka, M. O. (2012). Analysing decadal land use/cover dynamics of the Lake Basaka catchment (Main Ethiopian Rift) using LANDSAT imagery and GIS. *Lakes & Reservoirs: Research & Management*, *17*(1), 11–24.

Dunjó, G., Pardini, G., & Gispert, M. (2003). Land use change effects on abandoned terraced soils in a Mediterranean catchment, NE Spain. *Catena*, *52*(1), 23–37. https://doi.org/10.1016/S0341-8162(02)00148-0

Eastman, J. L. (2012). The country and the city: Mobility dynamics in mining regions. *Extractive Industries and Society*, *5*(2), 307–316. https://doi.org/10.1016/j.exis.2018.02.009

Ebrahim, A. (2014). Investigation in to some of the Engineering properties of soils in Debre Markos Town. *Control*, *10*(2), 01–71.

Edokpa, D., Milledge, D., Allott, T., Holden, J., Shuttleworth, E., Kay, M., Johnston, A., Millin-Chalabi, G., Scott-Campbell, M., Chandler, D., Freestone, J., & Evans, M. (2022). Rainfall intensity and catchment size control storm runoff in a gullied blanket peatland. *Journal of Hydrology*, *609*, 127688. https://doi.org/https://doi.org/10.1016/j.

jhydrol.2022.127688

Efrem, C., & Tesfaunegn, A. (2017). *Urban and Peri-Urban Development Dynamics in Ethiopia Study for Swiss Agency for Development and Cooperation*. May.

El-Tantawi, A. M., Bao, A., Chang, C., & Liu, Y. (2019). Monitoring and predicting land use/cover changes in the Aksu-Tarim River Basin, Xinjiang-China (1990–2030). *Environmental Monitoring and Assessment*, *191*(8). https://doi.org/10.1007/s10661-019-7478-0

Ellis, E., & Pontius, R. (2007). "Land use and Land Cover" In: Encyclopedia of Earth. *Encyclopedia of Earth*, 1–4.

Erena, S. H., & Worku, H. (2019). Dynamics of land use land cover and resulting surface runoff management for environmental flood hazard mitigation: The case of Dire Daw city, Ethiopia. *Journal of Hydrology: Regional Studies*, *22*(January). https://doi.org/10.1016/j.ejrh.2019.100598

Eshanthini, P., & Samuel, S. J. (2018). Rainfall runoff estimation using SCS Model and ARCGIS for Micro watershed in Cuddalore district. *Water and Energy International*, *61*(3), 59–63.

Esubalew. (2006). *a Ho Use Hold Level Analysis*. *August*.

FAO. (2022). The State of the World's Land and Water Resources for Food and Agriculture 2021 – Systems at breaking point. In *The State of the World's Land and Water Resources for Food and Agriculture 2021 – Systems at breaking point*. https://doi.org/10.4060/cb9910en

Fernández-Raga, M., Palencia, C., Keesstra, S., Jordán, A., Fraile, R., Angulo-Martínez, M., & Cerdà, A. (2017). Splash erosion: A review with unanswered questions. *Earth-Science Reviews*, *171*, 463–477. https://doi.org/https://doi.org/10.1016/j.earscirev.2017.06.009

Firew Bekele. (2010). Impact of Horizontal Urban Expansion on Peri-Urban Agricultural Community Livelihood ; Tabor Sub- urb case , Hawass ... The Impact of Horizontal Urban Expansion on Sub- Urban Agricultural Community Livelihood : *Litrachare*, *The Impact of Horizontal Urban Expansion on Sub-Urban Agricultural Community Livelihood: The Case of Tabor Sub-City*, *Hawassa city,1-*, 1–76.

Foody, G. M. (2002). Status of land cover classification accuracy assessment. *Remote*

Sensing of Environment, *80*(1), 185–201. https://doi.org/https://doi.org/10.1016/S0034-4257(01)00295-4

Foody, G. M., & Mathur, A. (2004). A relative evaluation of multiclass image classification by support vector machines. *IEEE Transactions on Geoscience and Remote Sensing*, *42*(6), 1335–1343.

Gajbhiye, S. (2015). Estimation of surface runoff using remote sensing and geographical information system. *International Journal of U-and e-Service, Science and Technology*, *8*(4), 113–122.

Garedew, E., Sandewall, M., Söderberg, U., & Campbell, B. M. (2009). Land-use and land-cover dynamics in the central rift valley of Ethiopia. *Environmental Management*, *44*, 683–694.

Garg, V., Aggarwal, S. P., Nikam, B. R., & Thakur, P. K. (2013). Hypothetical scenario–based impact assessment of climate change on runoff potential of a basin. *ISH Journal of Hydraulic Engineering*, *19*(3), 244–249.

Gashu, K., & Gebre-Egziabher, T. (2019). Comparison of urban sustainability using indicators approach in the cities of bahir dar and hawassa (Ethiopia). *Geography, Environment, Sustainability*, *12*(1), 119–136. https://doi.org/10.24057/2071-9388-2018-39

Geist, H. J., & Lambin, E. F. (2002). Proximate causes and underlying driving forces of tropical deforestation: Tropical forests are disappearing as the result of many pressures, both local and regional, acting in various combinations in different geographical locations. *BioScience*, *52*(2), 143–150.

Getachew, H. E., & Melesse, A. M. (2012). The impact of land use change on the hydrology of the Angereb Watershed, Ethiopia. *International Journal of Water Sciences*, *1*(6).

Gitau, M. W., Chen, J., & Ma, Z. (2016). Water quality indices as tools for decision making and management. *Water Resources Management*, *30*, 2591–2610.

Guo, Y. (2001). Rational Hydrograph Method for Small Urban Watersheds. *Journal of Hydrologic Engineering*, *6*(4), 352–356. https://doi.org/10.1061/(ASCE)1084-0699(2001)6:4(352)

Haase, D., Güneralp, B., Dahiya, B., Bai, X., & Elmqvist, T. (2018a). Global urbanization:

Perspectives and trends. In *Urban Planet: Knowledge towards Sustainable Cities* (Issue April). https://doi.org/10.1017/9781316647554.003

Haase, D., Güneralp, B., Dahiya, B., Bai, X., & Elmqvist, T. (2018b). Global urbanization: Perspectives and trends. *Urban Planet: Knowledge towards Sustainable Cities*, *April*, 19–44.

Hu, S., Fan, Y., & Zhang, T. (2020). Assessing the effect of land use change on surface runoff in a rapidly urbanized city: a case study of the central area of Beijing. *Land*, *9*(1), 17.

Iacono, M., Levinson, D., El-Geneidy, A., & Rania, W. (2012). Markov Chain Model of Land Use Change in the Twin Cities. *TeMA : Journal of Land Use, Mobility and Environment*, *8*. https://doi.org/10.6092/1970-9870/2985

Iwasokun, G. (2014). Image Enhancement Methods: A Review. *British Journal of Mathematics & Computer Science*, *4*, 2251–2277. https://doi.org/10.9734/BJMCS/2014/10332

James W, Elston D, T. J. et al. (20 C.E.). 済無No Title No Title No Title. In *Andrew's Disease of the Skin Clinical Dermatology*.

Jelili, Musibau, O. (2012). Urbanization and future of cities in Africa : The emerging facts and challenges to planners. *Global Journal of Human Social Science*, *12*(7), 7–12. https://www.researchgate.net/publication/346224528

Jiang, Y., Liu, C., Li, X., Liu, L., & Wang, H. (2015). Rainfall-runoff modeling, parameter estimation and sensitivity analysis in a semiarid catchment. *Environmental Modelling & Software*, *67*, 72–88. https://doi.org/https://doi.org/10.1016/j.envsoft.2015.01.008

Kaiser, M. S. (2020). *Land Degradation: Causes, Impacts, and Interlinks with the Sustainable Development Goals BT - Responsible Consumption and Production* (W. Leal Filho, A. M. Azul, L. Brandli, P. G. Özuyar, & T. Wall (Eds.); pp. 1–13). Springer International Publishing. https://doi.org/10.1007/978-3-319-71062-4_48-1

Kindu, M., Angelova, D., Schneider, T., Döllerer, M., Teketay, D., & Knoke, T. (2020). Monitoring of urban growth patterns in rapidly growing Bahir Dar city of northwest Ethiopia with 30 year landsat imagery record. *ISPRS International Journal of Geo-Information*, *9*(9), 1–19. https://doi.org/10.3390/ijgi9090548

Kindu, M., Schneider, T., Teketay, D., & Knoke, T. (2015). Drivers of land use land cover changes in Munessa-Shashemene landscape of the south-central highlands of Ethiopia. *Environmental Monitoring and Assessment*, *187*(7). https://doi.org/10.1007/s10661-015-4671-7

Kohram, M., & Sap, M. N. M. (2008). Composite kernels for support vector classification of hyper-spectral data. *Mexican International Conference on Artificial Intelligence*, 360–370.

Kumar, A., Kanga, S., Taloor, A. K., Singh, S. K., & Đurin, B. (2021). Surface runoff estimation of Sind river basin using integrated SCS-CN and GIS techniques. *HydroResearch*, *4*, 61–74. https://doi.org/https://doi.org/10.1016/j.hydres.2021.08.001

Kumar, P., Tiwart, K. N., & Pal, D. K. (1991). Establishing SCS runoff curve number from IRS digital data base. *Journal of the Indian Society of Remote Sensing*, *19*, 245–252.

Kutter, A., & Neely, C. (1999). The future of our land: facing the challenge. *FAO and UNEP, Rome*.

Lambin, E. F., Geist, H. J., & Lepers, E. (2003). Dynamics of land-use and land-cover change in tropical regions. *Annual Review of Environment and Resources*, *28*, 205–241. https://doi.org/10.1146/annurev.energy.28.050302.105459

Lambin, E. F., Turner, B. L., Geist, H. J., Agbola, S. B., Angelsen, A., Bruce, J. W., Coomes, O. T., Dirzo, R., Fischer, G., Folke, C., George, P. S., Homewood, K., Imbernon, J., Leemans, R., Li, X., Moran, E. F., Mortimore, M., Ramakrishnan, P. S., Richards, J. F., … Xu, J. (2001). The causes of land-use and land-cover change: Moving beyond the myths. *Global Environmental Change*, *11*(4), 261–269. https://doi.org/10.1016/S0959-3780(01)00007-3

Landis, J. R., & Koch, G. G. (1977). Landis amd Koch1977_agreement of categorical data. *Biometrics*, *33*(1), 159–174.

Lee, K., Ling, L., & Yusop, Z. (2023). The Revised Curve Number Rainfall–Runoff Methodology for an Improved Runoff Prediction. *Water*, *15*, 491. https://doi.org/10.3390/w15030491

Legesse, D., Vallet-Coulomb, C., & Gasse, F. (2003). Hydrological response of a catchment to climate and land use changes in Tropical Africa: Case study south central Ethiopia. *Journal of Hydrology*, *275*(1–2), 67–85. https://doi.org/10.1016/S0022-1694(03)00019-2

Leta, M. K., Demissie, T. A., & Tränckner, J. (2021). Hydrological responses of watershed to historical and future land use land cover change dynamics of nashe watershed, ethiopia. *Water (Switzerland)*, *13*(17). https://doi.org/10.3390/w13172372

Levinson, D., & Chen, W. (2005). Paving new ground: a Markov chain model of the change in transportation networks and land use. In *Access to destinations* (pp. 243–266). Emerald Group Publishing Limited.

Li, C., Liu, M., Hu, Y., Shi, T., Zong, M., & Walter, M. T. (2018). *Assessing the Impact of Urbanization on Direct Runoff Using Improved Composite CN Method in a Large Urban Area*. https://doi.org/10.3390/ijerph15040775

Li, X., Gao, J., Guo, Z., Yin, Y., Zhang, X., Sun, P., & Gao, Z. (2020). A Study of Rainfall-Runoff Movement Process on High and Steep Slopes Affected by Double Turbulence Sources. *Scientific Reports*, *10*(1), 9001. https://doi.org/10.1038/s41598-020-66060-3

Liao, R., Yang, P., Wu, W., Luo, D., & Yang, D. (2018). A DNA tracer system for hydrological environment investigations. *Environmental Science & Technology*, *52*(4), 1695–1703.

Liu, K., Li, X., & Wang, S. (2021). Characterizing the spatiotemporal response of runoff to impervious surface dynamics across three highly urbanized cities in southern China from 2000 to 2017. *International Journal of Applied Earth Observation and Geoinformation*, *100*, 102331. https://doi.org/https://doi.org/10.1016/j.jag.2021.102331

Lockaby, G., Nagy, C., Vose, J. M., Ford, C. R., Sun, G., McNulty, S., Caldwell, P., Cohen, E., & Moore Myers, J. A. (2011). Water and forests. *The Southern Forest Futures Project: Technical Report, USDA Forest Service, Southern Research Station, Asheville, NC., General Technical Report*.

Lu, D., Mausel, P., Brondizio, E., & Moran, E. (2004). Change detection techniques. *International Journal of Remote Sensing*, *25*(12), 2365–2401.

Lu, D., & Weng, Q. (2007). A survey of image classification methods and techniques for improving classification performance. *International Journal of Remote Sensing*, *28*(5), 823–870. https://doi.org/10.1080/01431160600746456

Lucas-Borja, M. E., Carrà, B. G., Nunes, J. P., Bernard-Jannin, L., Zema, D. A., &

Zimbone, S. M. (2020). Impacts of land-use and climate changes on surface runoff in a tropical forest watershed (Brazil). *Hydrological Sciences Journal*, *65*(11), 1956–1973. https://doi.org/10.1080/02626667.2020.1787417

Mariye, M., Mariyo, M., Changming, Y., Teffera, Z. L., & Weldegebrial, B. (2020). Effects of land use and land cover change on soil erosion potential in Berhe district: a case study of Legedadi watershed, Ethiopia. *International Journal of River Basin Management*, *20*(1), 79–91. https://doi.org/10.1080/15715124.2020.1767636

Maru Abebaw and Juliet Akola. (2016). Environmental Perspective of Urban Agriculture in Debre Markos Town, Amhara Regional State, Ethiopia. *British Journal of Environmental Sciences*, *4*(2), 24–36. www.eajournals.org

Mather, A. S., & Needle, C. L. (2000). The relationships of population and forest trends. *Geographical Journal*, *166*(1), 2–13.

McGrane, S. J. (2016). Impacts of urbanisation on hydrological and water quality dynamics, and urban water management: a review. *Hydrological Sciences Journal*, *61*(13), 2295–2311. https://doi.org/10.1080/02626667.2015.1128084

Mei, C., Liu, J., Wang, H., Shao, W., Xia, L., Xiang, C., & Zhou, J. (2018). Modelling the ability of source control measures to reduce inundation risk in a community-scale urban drainage system. *Proceedings of the International Association of Hydrological Sciences*, *379*, 223–229. https://doi.org/10.5194/piahs-379-223-2018

Mekuriaw, T., & Gokcekus, H. (2019). The impact of urban expansion on physical environment in Debre Markos town, Ethiopia. *Civil and Environmental Research*, *11*, 16–26.

Memarian, H., Balasundram, S. K., Talib, J. Bin, Teh, C., Sung, B., Sood, A. M., & Abbaspour, K. (2012). Validation of CA-Markov for Simulation of Land Use and Cover Change in the Langat Basin , Malaysia. *Journal of Geographic Information System*, *4*(December), 542–554.

Meyfroidt, P., Lambin, E. F., Erb, K.-H., & Hertel, T. W. (2013). Globalization of land use: distant drivers of land change and geographic displacement of land use. *Current Opinion in Environmental Sustainability*, *5*(5), 438–444.

Miller, J. D., Kim, H., Kjeldsen, T. R., Packman, J., & Grebby, S. (2014). Publication date : University of Bath Assessing the impact of urbanization on storm runoff in a peri-urban catchment using historical change in impervious cover. *JOURNAL OF HYDROLOGY*, *515*, 59–70. https://doi.org/10.1016/j.jhydrol.2014.04.011

Mishra, S. K., & Singh, V. P. (2003). *SCS-CN Method BT - Soil Conservation Service Curve Number (SCS-CN) Methodology* (S. K. Mishra & V. P. Singh (Eds.); pp. 84–146). Springer Netherlands. https://doi.org/10.1007/978-94-017-0147-1_2

Mmbaga, N. E., Munishi, L. K., & Treydte, A. C. (2017). How dynamics and drivers of land use land cover change impact elephant conservation and agricultural livelihood development in Rombo, Tanzania. *Journal of Land Use Science*, *12*(2–3), 168–181. https://doi.org/10.1080/1747423X.2017.1313324

Moniruzzaman, M., Thakur, P. K., Kumar, P., Ashraful Alam, M., Garg, V., Rousta, I., & Olafsson, H. (2020). Decadal urban land use land cover changes and its impact on surface runoff potential for the Dhaka City and surroundings using remote sensing. *Remote Sensing*, *13*(1), 83.

MOUDH. (2015). *Environmental and Social Management Framework,Urban Productivesafetynetproject*. *August*, 1–172.

Mountrakis, G., Im, J., & Ogole, C. (2011). Support vector machines in remote sensing: A review. *ISPRS Journal of Photogrammetry and Remote Sensing*, *66*(3), 247–259.

Moussoulis, E., Mallinis, G., Koutsias, N., & Zacharias, I. (2015). Modelling surface runoff to evaluate the effects of wildfires in multiple semi-arid, shrubland-dominated catchments. *Hydrological Processes*, *29*(20), 4427–4441. https://doi.org/https://doi.org/10.1002/hyp.10509

Msofe, N. K., Sheng, L., & Lyimo, J. (2019). Land use change trends and their driving forces in the Kilombero Valley Floodplain, Southeastern Tanzania. *Sustainability (Switzerland)*, *11*(2), 1–25. https://doi.org/10.3390/su11020505

Nations, U. (2007). World Urbanization Prospects The 2007 Revision Highlights. *New York*, *ESA/P/WP/2*(4), 883.

O’Driscoll, M., Clinton, S., Jefferson, A., Manda, A., & McMillan, S. (2010). Urbanization effects on watershed hydrology and in-stream processes in the southern United States. *Water*, *2*(3), 605–648.

Ozdemir, H., & Elbaşi, E. (2015). Benchmarking land use change impacts on direct runoff in ungauged urban watersheds. *Physics and Chemistry of the Earth*, *79–82*, 100–107.

https://doi.org/10.1016/j.pce.2014.08.001

Parker, D. C. (2005). Integration of geographic information systems and agent-based models of land use: prospects and challenges. *GIS, Spatial Analysis, and Modeling*, 403–422.

Parra, V., Fuentes-Aguilera, P., & Muñoz, E. (2018). Identifying advantages and drawbacks of two hydrological models based on a sensitivity analysis: a study in two Chilean watersheds. *Hydrological Sciences Journal*, *63*(12), 1831–1843. https://doi.org/10.1080/02626667.2018.1538593

Parveen, S., Bashir, J., & Praveen, B. (2018). A LITERATURE REVIEW ON LAND USE LAND COVER CHANGES. *International Journal of Advanced Research*, *6*, 1–6. https://doi.org/10.21474/IJAR01/7327

Passerat, J., Ouattara, N. K., Mouchel, J.-M., Rocher, V., & Servais, P. (2011). Impact of an intense combined sewer overflow event on the microbiological water quality of the Seine River. *Water Research*, *45*(2), 893–903.

Paul, M. J., & Meyer, J. L. (2001). Streams in the urban landscape. *Annual Review of Ecology and Systematics*, *32*(1), 333–365.

Pawan. (2016). Urbanization and Its Causes and Effects: A Review. *International Journal of Research and Scientific Innovation*, *III*(Ix), 110–112. https://doi.org/10.1038/sdata.2016.34.ISSN

Pedroza-Parga, E., Velasquez-Valle, M., Pedroza-Sandoval, A., sanchez cohen, I., & Yáñez-Chávez, L. (2022). The impact of vegetation cover on soil erosion and soil deposition due to runoff. *Ingenieria Agricola y Biosistemas*, *14*, 17–31. https://doi.org/10.5154/r.inagbi.2021.12.135

Phillips, C., Hales, T., Smith, H., & Basher, L. (2021). Shallow landslides and vegetation at the catchment scale: A perspective. *Ecological Engineering*, *173*, 106436. https://doi.org/https://doi.org/10.1016/j.ecoleng.2021.106436

Phiri, D., & Morgenroth, J. (2017). Developments in Landsat land cover classification methods: A review. *Remote Sensing*, *9*(9), 967.

Pieper, G., & Hakalin, M. (2018). *Development of an Open Source Land Records System for Urban Centers in Development of an Open Source Land Records System for Urban Centres in Ethiopia*. March.

Ponce, V. M., & Hawkins, R. H. (1996). Runoff Curve Number: Has It Reached Maturity? *Journal of Hydrologic Engineering, 1*(1), 11–19. https://doi.org/10.1061/(asce)1084-0699(1996)1:1(11)

Psomiadis, E., Soulis, K. X., & Efthimiou, N. (2020). Using SCS-CN and earth observation for the comparative assessment of the hydrological effect of gradual and abrupt spatiotemporal land cover changes. *Water*, *12*(5), 1386.

Rahman, A., & Netzband, M. (2009). An assessment of urban environmental issues using remote sensing and GIS techniques an integrated approach: A case study: Delhi, India Atiqur. *PRIPODE Workshop on Urban Population, Development, and Environment Dynamics in Developing Countries*, *June*, 1–25.

Rahman, M. T. U., Tabassum, F., Rasheduzzaman, M., Saba, H., Sarkar, L., Ferdous, J., Uddin, S. Z., & Zahedul Islam, A. Z. M. (2017). Temporal dynamics of land use land cover change and its prediction using CA-ANN model for southwestern coastal Bangladesh. *Environmental Monitoring and Assessment*, *189*(11). https://doi.org/10.1007/s10661-017-6272-0

Rawat, J. S., & Kumar, M. (2015). Monitoring land use/cover change using remote sensing and GIS techniques: A case study of Hawalbagh block, district Almora, Uttarakhand, India. *The Egyptian Journal of Remote Sensing and Space Science*, *18*(1), 77–84.

Redman, C. L., & Jones, N. S. (2005). The environmental, social, and health dimensions of urban expansion. *Population and Environment*, *26*, 505–520.

Reis, J. P., Silva, E. A., & Pinho, P. (2016). Spatial metrics to study urban patterns in growing and shrinking cities. *Urban Geography*, *37*(2), 246–271. https://doi.org/10.1080/02723638.2015.1096118

Rieniets, T. (2009). Shrinking cities: Causes and effects of urban population losses in the twentieth century. *Nature and Culture*, *4*(3), 231–254.

Rui, Y., & Ban, Y. (2016). *Urban Growth Modeling with Road Network Expansion and Land Use Urban Growth Modeling with Road Network Expansion and Land Use Development*. *February*. https://doi.org/10.1007/978-3-642-19214-2

Rumynin, V. G. (2015). *Surface Runoff Generation, Vertical Infiltration and Subsurface Lateral Flow BT - Overland Flow Dynamics and Solute Transport* (V. G. Rumynin (Ed.); pp. 3–50). Springer International Publishing. https://doi.org/10.1007/978-3-

319-21801-4_1

Sankarrao, L., Ghose, D. K., & Rathinsamy, M. (2021). Predicting land-use change: Intercomparison of different hybrid machine learning models. *Environmental Modelling & Software*, *145*, 105207. https://doi.org/https://doi.org/10.1016/j.envsoft.2021.105207

Saputra, M. H., & Lee, H. S. (2019). Prediction of land use and land cover changes for north sumatra, indonesia, using an artificial-neural-network-based cellular automaton. *Sustainability*, *11*(11), 3024.

Sarukkalige, P. (2011). © 2014 IEEE . Personal use of this material is permitted . Permission from IEEE must be obtained for all other uses , in any current or future media , including reprinting / republishing this material for advertising or promotional purposes , creating new. *2010 International Conference on Business and Economics Research*, *1*, 110–114.

Seif, A., & Mokarram, M. (2012). Change detection of gil playa in the northeast of Fars province. *Iran Am. J. Sci. Res*, *86*, 122–130.

Seltman, H. J. (2018). Experimental design and analysis. *Book Is on the World Wide Web*.

SERTEL, E., & AKAY, S. S. (2015). High resolution mapping of urban areas using SPOT-5 images and ancillary data. *International Journal of Environment and Geoinformatics*, *2*(2), 63–76. https://doi.org/10.30897/ijegeo.303545

Shrestha, P. M. (2018). Application of SCS-CN model in Runoff Estimation. *International Journal for Research in Applied Science and Engineering Technology*, *6*(3), 2363–2369. https://doi.org/10.22214/ijraset.2018.3544

SILVEIRA, L., CHARBONNIER, F., & GENTA, J. (2000). The Antecedent Soil Moisture Condition of the Curve Number Procedure. *Hydrological Sciences Journal*, *45*, 3–12. https://doi.org/10.1080/02626660009492302

Singh, A. (1989). Review article digital change detection techniques using remotely-sensed data. *International Journal of Remote Sensing*, *10*(6), 989–1003.

Sohl, T. L., Sleeter, B. M., Sayler, K. L., Bouchard, M. A., Reker, R. R., Bennett, S. L., Sleeter, R. R., Kanengieter, R. L., & Zhu, Z. (2012). Spatially explicit land-use and land-cover scenarios for the Great Plains of the United States. *Agriculture, Ecosystems & Environment*, *153*, 1–15.

Sonka, M., Hlavac, V., & Boyle, R. (1993). *Image pre-processing BT - Image Processing, Analysis and Machine Vision* (M. Sonka, V. Hlavac, & R. Boyle (Eds.); pp. 56–111). Springer US. https://doi.org/10.1007/978-1-4899-3216-7_4

Soomro, A., Memon, A., Zaidi, A., Ashraf, A., & Lund, J. (2019). Sensitivity of Direct Runoff to Curve Number Using the SCS- CN Method. *Civil Engineering Journal*, *5*. https://doi.org/10.28991/cej-2019-03091445

Stefanov, W. L., Ramsey, M. S., & Christensen, P. R. (2001). Monitoring urban land cover change: An expert system approach to land cover classification of semiarid to arid urban centers. *Remote Sensing of Environment*, *77*(2), 173–185.

Story, M., & Congalton, R. G. (1986). Remote Sensing Brief Accuracy Assessment: A User's Perspective. *Photogrammetric Engineering and Remote Sensing*, *52*(3), 397–399. https://www.asprs.org/wp-content/uploads/pers/1986journal/mar/1986_mar_397-399.pdf

Subedi, P., Subedi, K., & Thapa, B. (2013). Application of a Hybrid Cellular Automaton �C Markov (CA-Markov) Model in Land-Use Change Prediction: A Case Study of Saddle Creek Drainage Basin, Florida. *Applied Ecology and Environmental Sciences*, *1*(6), 126–132. https://doi.org/10.12691/aees-1-6-5

Tejaswini, N. B., Shetty, A., & Hegde, V. S. (2011). Land use scenario analysis and prediction of runoff using SCS-CN method: A case study from the Gudgudi tank, Haveri district, Karnataka, India. *International Journal of Earth Sciences and Engineering*, *4*(5), 845–853.

Terfa, B. K., Chen, N., Liu, D., Zhang, X., & Niyogi, D. (2019). Urban expansion in Ethiopia from 1987 to 2017: Characteristics, spatial patterns, and driving forces. *Sustainability (Switzerland)*, *11*(10). https://doi.org/10.3390/su11102973

Thomas, A., Kanawade, V. P., Chakravarty, K., & Srivastava, A. K. (2021). Characterization of raindrop size distributions and its response to cloud microphysical properties. *Atmospheric Research*, *249*, 105292. https://doi.org/https://doi.org/10.1016/j.atmosres.2020.105292

Thomas, N. W., Ayalew, T. B., Arenas, A. A., Schilling, K. E., Weber, L. J., & Krajewski, W. F. (2021). Characterizing the effects of dry antecedent soil moisture conditions, channel transmission losses, and variable precipitation on peak flow scaling.

Advances in Water Resources, *158*, 104061. https://doi.org/https://doi.org/10.1016/j.advwatres.2021.104061

Tian, Y., Yue, T., Zhu, L., & Clinton, N. (2005). Modeling population density using land cover data. *Ecological Modelling*, *189*(1), 72–88. https://doi.org/https://doi.org/10.1016/j.ecolmodel.2005.03.012

Tigezaw, L. (2014). The Influence of Urban Expansion on Physical Environment : the. *Masters Thesis*.

Tole, L. (2004). A quantitative investigation of the population-land inequality-land clearance nexus. *Population and Environment*, *26*, 75–106.

Turner, B., Meyer, W. B., & Skole, D. L. (1994). Global land- use land-cover change: towards an integrated study. *Ambio. Stockholm*, *23*(1), 91–95.

Turok, I., & Mykhnenko, V. (2007). The trajectories of European cities, 1960–2005. *Cities*, *24*(3), 165–182.

Uk, I. (2017). A Review on Image Enhancement Techniques. *International Journal of Engineering and Applied Computer Science (IJEACS)*, *02*, 232–235. https://doi.org/10.24032/ijeacs/0207/05

United Nations. (2018). The World's Cities in 2018. *World Urbanization Prospects: The 2018 Revision*, 34. https://www.un.org/en/development/desa/population/publications/pdf/urbanization/the_worlds_cities_in_2018_data_booklet.pdf

Verburg, P. H., Schot, P. P., Dijst, M. J., & Veldkamp, A. (2004). Land use change modelling: current practice and research priorities. *GeoJournal*, *61*, 309–324.

Verburg, P. H., Soepboer, W., Veldkamp, A., Limpiada, R., Espaldon, V., & Mastura, S. S. A. (2002). Modeling the spatial dynamics of regional land use: The CLUE-S model. *Environmental Management*, *30*(3), 391–405. https://doi.org/10.1007/s00267-002-2630-x

Vietz, G. J., Walsh, C. J., & Fletcher, T. D. (2016). Urban hydrogeomorphology and the urban stream syndrome: Treating the symptoms and causes of geomorphic change. *Progress in Physical Geography*, *40*(3), 480–492.

Vinithra, R., & Yeshodha, L. (2013). Rainfall- Runoff Modelling Using SCS-CN Method:

A Case Study of Krishnagiri District, Tamilnadu. *International Journal of Science and Research (IJSR)*, *5*(3), 2080–2084. https://doi.org/10.21275/v5i3.nov162365

Vojtek, M., & Vojteková, J. (2019). Land use change and its impact on surface runoff from small basins: A case of Radiša basin. *Folia Geographica*, *61*(2), 104–125.

Walsh, C. J., Booth, D. B., Burns, M. J., Fletcher, T. D., Hale, R. L., Hoang, L. N., Livingston, G., Rippy, M. A., Roy, A. H., & Scoggins, M. (2016). Principles for urban stormwater management to protect stream ecosystems. *Freshwater Science*, *35*(1), 398–411.

Wang, X., Liu, T., & Yang, W. (2012). Elaboration d'une modèle robuste d'estimation du ruissellement fusionnant la méthoderationnelle et une méthode du SCS-CN modifiée. *Hydrological Sciences Journal*, *57*(6), 1118–1140. https://doi.org/10.1080/02626667.2012.701305

Wang, X., Zheng, D., & Shen, Y. (2008). Land use change and its driving forces on the Tibetan Plateau during 1990–2000. *Catena*, *72*(1), 56–66.

Weng, Q. (2001). Modeling urban growth effects on surface runoff with the integration of remote sensing and GIS. *Environmental Management*, *28*(6), 737–748. https://doi.org/10.1007/s002670010258

Woldeamlak, B. (2002). Land cover dynamics since the 1950s in Chemoga watershed, Blue Nile basin, Ethiopia. *Mountain Research and Development*, *22*(3), 263–269.

Wu, P. C., Lay, J. G., Guo, H. R., Lin, C. Y., Lung, S. C., & Su, H. J. (2009). Higher temperature and urbanization affect the spatial patterns of dengue fever transmission in subtropical Taiwan. *Science of The Total Environment*, *407*(7), 2224–2233. https://doi.org/10.1016/J.SCITOTENV.2008.11.034

XIAO, B., WANG, Q.-H., FAN, J., HAN, F.-P., & DAI, Q.-H. (2011). Application of the SCS-CN Model to Runoff Estimation in a Small Watershed with High Spatial Heterogeneity. *Pedosphere*, *21*(6), 738–749. https://doi.org/https://doi.org/10.1016/S1002-0160(11)60177-X

Yang, L., Feng, Q., Yin, Z., Wen, X., Si, J., Li, C., & Deo, R. C. (2017). Identifying separate impacts of climate and land use/cover change on hydrological processes in upper stream of Heihe River, Northwest China. *Hydrological Processes*, *31*(5), 1100–1112. https://doi.org/10.1002/hyp.11098

Yigrem, Y. (2008). *Rainfall-Runoff Modelling for Sustainable Water Resources Management: The Case of Gumara Watershed, Ethiopia*.

Younis, S. M. Z., & Ammar, A. (2018). Quantification of impact of changes in land use-land cover on hydrology in the upper Indus Basin, Pakistan. *The Egyptian Journal of Remote Sensing and Space Science*, *21*(3), 255–263. https://doi.org/https://doi.org/10.1016/j.ejrs.2017.11.001

Zare, M., Samani, A. A. N., & Mohammady, M. (2016). The impact of land use change on runoff generation in an urbanizing watershed in the north of Iran. *Environmental Earth Sciences*, *75*, 1–20.

ZÁRUBA, Q., & MENCL, V. B. T.-D. in G. E. (Eds.). (1982). Chapter 3 - The Classification of Slope Movements. In *Landslides and their Control* (Vol. 31, pp. 49–53). Elsevier. https://doi.org/https://doi.org/10.1016/B978-0-444-99700-5.50008-4

Zeng, Z., Tang, G., Hong, Y., Zeng, C., & Yang, Y. (2017). Development of an NRCS curve number global dataset using the latest geospatial remote sensing data for worldwide hydrologic applications. *Remote Sensing Letters*, *8*, 528–536. https://doi.org/10.1080/2150704X.2017.1297544

Ziena, L. (2017). *Mapping Land Use And Land Cover Change And Their Effects On Urban _ Pre Urban Agriculture In Debre Advisor : Mapping Land Use / Land Cover Changes And Its Effects On Urban _ Peri-Urban Agriculture In Debre By Ziena Lingereh Ayele*. 2–71.

Zoran, M., & Anderson, E. (2006). The use of multi-temporal and multispectral satellite data for change detection analysis of the Romanian Black Sea coastal zone. *Journal of Optoelectronics and Advanced Materials*, *8*(1), 252.

APPENDICES

Appendix A. 24-houre precipitation (from Debre Markos station)

	A	B	C	D	E	F	G	H	I	J	K	L	M	N	O	P	Q	R	S	T	U	V	W	X	Y	Z	AA	AB	AC	AD	AE	AF	AG	AH	AI
1	Station Name		Debre Markos																																
2	Instrument type		GODEBR12																																
3	Data type		Precipitation																																
4	Record time		9:00																																
5	Station Elevation		2446 meter																																
6	Daily Rainfall																																		
7	long	Lat	Year	Mth	1	2	3	4	5	6	7	8	9	10	11	12	13	14	15	16	17	18	19	20	21	22	23	24	25	26	27	28	29	30	31
8	37.74	10.33	1995	01	0	0	0	0	0	0	0	0	0	0	0	0	0	0	0	0	0	0	0	0	0	0	0	0	0	0	0	0	0	0	0
9	37.74	10.33	1995	02	0	0	0	0	0	0	0	0	0	0	0	0	0	0	0	0	0	0	0	0	0	0	0	0	1	0	0	0			
10	37.74	10.33	1995	03	0	0	0	0	0	0	0	0	0	0	0	0	0	0	0	0	0	0	0	0	6.2	13.5	0.5	0	0	0	0	0	0	0.1	0
11	37.74	10.33	1995	04	0	2.8	0	0	0	0	0	0	3	0	0	0.6	0.2	0.9	3.8	1	2.3	1.2	0.4	2.6	28.8	0.3	12.5	20.6	1	0	0	0	7.5	0.9	
12	37.74	10.33	1995	05	0	0	0	4	0.4	10.4	0	0	0.7	0.5	2	3.7	6.2	5.7	0.6	0	21.4	11.2	4.1	16.2	0	0	0	0	0	0	3.1	19.6	10.4	26.4	0
13	37.74	10.33	1995	06	0	0	0	0	0	0	0	0	0	0	0.2	0.6	0	0	0	0	8	32.1	16.4	29.2	0	0	0	0	0	0	7.4	1.5	0	0	0.1
14	37.74	10.33	1995	07	0	0	0	0	0	0	0.3	0	0	0	0	0	0	0.8	0.3	0	0	7.3	0.8	0	3	0	0	12.7	0	0.8	0.7	0	0.9	0	0
15	37.74	10.33	1995	08	0	0	0	0	0	0	0	0	0	0	0	0	0	0	0	0	0	0	0	0	0	0	0	0	4.6	0	0	0	0		
16	37.74	10.33	1995	09	0	0	0	15.1	7.4	0.1	1.5	15	0	0	0	0	0	0.4	10.9	5.7	0	5.2	0	21.9	0	2.5	0.5	3.2	0	3	12	3.6	0	0	
17	37.74	10.33	1995	10	0	0	0	0	0	0	0	26.5	3.6	33.9	15	6.4	0	0	26.6	6.3	1.9	8.6	5.9	2	1.5	0	0.1	0	15.8	0	0	0.1	44.8	16.6	12.4
18	37.74	10.33	1995	11	0	6.7	5.5	2.5	44	37.6	0	4.6	41.3	6.1	7.5	1.2	0.5	13	0	0.7	28.7	8.1	3.3	17.1	8.1	6.2	5.5	3.6	10.8	16.6	9.2	0.2	0.2	2.9	
19	37.74	10.33	1995	12	0	0	0	0	0	0	0	0.2	0	0	0	0	0	0	22.2	0.2	3.8	1.4	0	0	0	3.9	0	2.7	0.8	0	0	0	0	0	
20	37.74	10.33	2000	01	0	0	0	0	0	0	0	0	0	0	0	0.3	0.4	1.3	4.3	0	0	0	4	0	0	0	0	0	1.3	0	0	2.2	0	0	0

	A	B	C	D	E	F	G	H	I	J	K	L	M	N	O	P	Q	R	S	T	U	V	W	X	Y	Z	AA	AB	AC	AD	AE	AF	AG	AH	AI
21	37.74	10.33	2000	02	0	1.3	0	0	25.7	9.5	22.9	1	5.2	0	0	0	0	0	0	0	0	0	0	11	0.2	0	7	0	5.2	0	0	0	9.5	21.6	
22	37.74	10.33	2000	03	0	0.3	13.9	1	2.5	7.8	0.2	0.3	5.8	1.6	10.7	11	2	7.9	1.1	0	0	3.7	16.8	8.1	15.5	18	14.5	5.3	7	5.8	23.5	2.3	7.4	1	
23	37.74	10.33	2000	04	0	0.7	12.2	12.3	3.2	0.8	31.8	7.5	15.6	2.5	0	0.9	0	0	0		0	0	0	0	0	0	0	0	0	0	0	0	0	0	0
24	37.74	10.33	2000	05	0	0	4.7	0	0	0	0	0	1.5	0	0	0	0	0	5.3	0	0	0	0	0	8.1	0	9.9	8.2	0	0	0		0	0	
25	37.74	10.33	2000	06	0	0	0	0	0	0	0	0	0	0	0	0	0	0	0	0	0	1.1	0	0	0	0	0	1.2	0	0	0	0	0	0	0
26	37.74	10.33	2000	07	0	0	0	0	0	0	0	0	0	0	0	0	0	0	0	0	0	0	0	0	0	0	0	0.1	0.5	0	0	0			
27	37.74	10.33	2000	08	0	0	0	0	0	0	0	0	0	0.2	1.6	7.6	2.9	0	1.4	17.9	19.2	2.9	14.2	19.7	23	0	0	0	0	0	0	0	0	0	0
28	37.74	10.33	2000	09	0	0	0	0	0	0	0		0	0	1.4	0	0.2	2.9	0	0	0	6.4	3	0	0	16.8	10.9	0	0	0.5	0.8	0	0	0	
29	37.74	10.33	2000	10	0	0.5	8.2	2.2	4.2	20	0	0	0	0	0	0	0	0	0	0	0	0	0	0	6.3	1.6	0	0.7	0	0	0	0	0	0	0
30	37.74	10.33	2000	11	0	0.1	0.6	13	0	0	0.3	0	0	7.3	4.5	0	0	6.8	2.9	1.6	1	16.1	2.3	4.2	9.9	4.1	16	6	11.1	9.8	7.5	16.8	8.5	0	
31	37.74	10.33	2000	12	0	0	0	2.2	6.4	29.4	2.4	25	11.2	6.6	2.5	3.3	0	0	0	0	0	0	0	1.1	0	0	0	0	0	0	0	0	0	0.1	0
32	37.74	10.33	2005	01	0	0	0	0	0	0	0	0	0	0	0	5.1	0	0	0	0	0	0	0	0	0	0	0	0	0	0	0	0	25.8	0	
33	37.74	10.33	2005	02	0	0	0	0	2.1	1.3	3.7	0	0	0	0	0	0	0	0	0	0	0	0	0	0	0	0	0	0	0	0	0	0	0	0
34	37.74	10.33	2005	03	0	0	0	0	0	0	0	1.6	0	0	0	2	0	0	0	0	0	0	0	0	0	0	0	0	0	0	0	0			
35	37.74	10.33	2005	04	0	0	0	0.9	0	0	3.8	0	0	0	0	0	0	0	0	0	0	0	0	0	0	0	0	0	0	0	0	0			
36	37.74	10.33	2005	05	0	0	0	0	3.1	1.8	0	2.4	0.4	3.3	4.7	0.5	0	0	0	0	0.2	0	0	0	0	0	0	0	0	0	0	0	0	0	0
37	37.74	10.33	2005	06	0	0	0	0	0	0	0	0	0	0	0	0	0	0	0	0	0	3.6	0	0	5.3	2.1	0	0	0	0	0	0.8	0	0	
38	37.74	10.33	2005	07	0	0	0.6	13.5	0.3	0	0	0.5	0.1	4.7	8.4	1.8	29.5	8.4	5.9	2.1	0	2.5	6.7	0	1.7	0.8	2	1.5	11.3	6.5	0	0	0.2	0	16
39	37.74	10.33	2005	08	0	0	0	0	0	0	0	0	1.6	0	0	0.1	2	0	14.7	2.4	0	13.4	0	0	0	0	0	0	0	0	0	0	0	0	
40	37.74	10.33	2005	09	0	0	0	0	0	0	0	0	0	0	0	0	0	0	0	0	0	0	0	0	0	0	0	0	0	0	0	0	0	0	0

	A	B	C	D	E	F	G	H	I	J	K	L	M	N	O	P	Q	R	S	T	U	V	W	X	Y	Z	AA	AB	AC	AD	AE	AF	AG	AH	AI
41	37.74	10.33	2005	10	0	0	0	0	0	0	0	0	0	0	0	0	0	0	0	1.2	0.4	0	0	0	0	0	0	0	0	0	0	0	7.5	0	0
42	37.74	10.33	2005	11	0	0	0	0	0	0	0	0	0	0	0	0	0	0	0	0	0	3.8	0	1.3	0.7	0	0	0	2.8	0	0	0			
43	37.74	10.33	2005	12	0	0	0	1	6.4	0.7	0	0	0	0	5.3	0	0	17.6	0	0	0	0.2	0	0.3	6	5.4	0	0	0	0	0	0	0	0	0
44	37.74	10.33	2010	01	0	0	0	0	0	0	0	0	0	0	2.6	7.8	0	0	0	5.2	4.8	5.4	0	0	1.3	0	19	17.4	13.7	3	2.4	0.3	0.7	1.7	
45	37.74	10.33	2010	02	0	0	0	3.4	0	12.6	0	4.7	1.5	15.6	6.5	5.4	23.3	0	1.3	11.3	0	15.6	22.2	17.3	8.5	34.7	6.1	10.7	1.2	7.4	15.3	12.5	10.1	21.6	
46	37.74	10.33	2010	03	0.1	0	0	0	0	0	0	0.4	0	0	0	1.3	0	0	0	0	0	0	0	0.2	3	0.4	0.7	18	0	0.4	0	2.2	17.4	1.6	1.1
47	37.74	10.33	2010	04	0.2	0.6	1.1	2.1	2.4	13.3	0	0	0.9	0	5.1	3	0	7.6	7.5	6.2	1.2	29.4	1.3	4.9	6.6	8.4	31.5	8.5	0.6	23.8	22.1	9.9	8.1	5.7	
48	37.74	10.33	2010	05	0.3	0.6	1.5	8.3	17.7	1.4	5.2	3.3	8.7	3.8	3.5	7.2	16.3	2	9.8	2.7	3.3	3.5	3	5.5	5.9	1	13	21.5	17.2	28.3	14	16.6	15.2	0.3	5.5
49	37.74	10.33	2010	06	0.3	0.2	8.6	6.1	1.5	4.1	0.1	0.9	0.3	4.2	13.7	3.4	1.6	4.8	0.6	14.8	10	9	5.8	11.4	5.6	0	4.2	8.3	0.4	17	11.6	6.7	17	2.7	
50	37.74	10.33	2010	07	0.3	0	0	0	0	0	0	0	0	0	2.8	7.6	0	0	0	0	0	0	0	0	0	0	0	0	0	0	0	0	0	0	0
51	37.74	10.33	2010	08	0.3	33.1	0.9	26.4	11.3	2.9	12	10.9	0	1.5	1.1	0	13.5	6	7.9	19.5	10	6.2	1.1	6.8	7.2	10.5	1.2	8.4	1.6	11.1	2.4	24.6	3.6	5.6	3
52	37.74	10.33	2010	09	0.3	0.4	12.7	13.2	8.1	9	30.2	14.5	0	1	13.1	9.5	10.5	6.6	0	21	11.2	14	2.1	12.2	12.3	0	3.5	5.4	12.3	5.2	25.8	9.5	10	8.6	3.4
53	37.74	10.33	2010	10	0.4	22.2	13	5.7	11	0	0	4.9	30.5	25.4	0	15.4	10.7	4.1	7.3	1.3	0.7	15.9	0	0	0.8	1	12.5	3.8	3	0	0	0	0	5.2	
54	37.74	10.33	2010	11	0.5	0	9	24.5	14.4	4.1	23.2	2	6.3	0	2.1	0	0	0	1.2	0	0	0	0	0	0	3.6	0	0.8	0	0	0	0	5.6	0	
55	37.74	10.33	2010	12	0.6	1.4	0	0	1.8	0	0	0	0	0	0	0	0	3.2	0	7.4	0	0	0	0	0	0	0	0	0	0	0	0	0	0	0
56	37.74	10.33	2015	01	4	6.1	7	2.5	0.6	8.6	14.4	16.8	14	4	0	5.8	16	4.4	0	4.2	7.6	0	9	14.3	16.1	1.2	20.7	4.8	2.8	0.8	9.2	19.1	1.1	29.6	
57	37.74	10.33	2015	02	4.3	20.7	28	9	9.1	4.1	4	0.3	16.5	3	11.5	7.5	2	6.5	0.4	14.4	13.2	5	13.5	6.2	21.6	11	0.2	0.4	11.1	19	8.1	22.6	6.7	8.4	0
58	37.74	10.33	2015	03	4.6	0	1.1	1.6	3.2	8	0	0	4.5	6.3	2.2	1.6	0	0	2.3	0	0	0	0	0	0	9.2	1.1	0	0	1.6	1.6	5.3	1.1	1	18.3
59	37.74	10.33	2015	04	5	5.7	3.1	0	2.6	11.1	1.6	1.1	0	0	0.7	1.2	0.6	19.5	3	4.4	1.9	8.6	3.4	28.9	10.8	10.8	5.9	2	5.4	7.9	0.2	0.9	1.3	3.4	
60	37.74	10.33	2015	05	5	16	2.9	1.6	11.3	4	16.5	25.8	0.1	2.8	0.3	12	8.5	8.3	0.2	2.5	20.6	4.4	14.6	3.4	4.2	12.5	24.5	21.6	1.6	3.5	12.8	23.7	2	5.7	3.8
61	37.74	10.33	2015	06	5	5	15	5.8	0.1	5	19.5	55	0	0	9.8	8.5	0.1	13.9	11.3	0.8	42.1	10.4	21.9	12.8	0.1	0	2.8	0	23.8	4.5	3.8	15.1	0.4	28.4	18.7
62	37.74	10.33	2015	07	5.2	2.2	5	5.5	11	18.7	3.5	17.2	1.4	0.2	18	2	3	4.8	14.2	58.3	14.5	0	8.5	4.6	15.8	10	6.4	5	7.1	5.9	1	10.3	8.6	6.2	12.5
63	37.74	10.33	2015	08	5.2	5.3	5.5	0	0	0	12.5	0	21.3	5.7	5.4	13.3	5.5	0.2	2.1	8.8	8.3					0	1.7	9.4	3.3	47.3	35.8	10.2	17.7	25	
64	37.74	10.33	2015	09	5.6	0	0.7	0	0	0	0	0	0	0	0	0	0	0	0	0	0	0	0	0	0	0	0	0	0	12.6	0	0	1.2	0	0.2
65	37.74	10.33	2015	10	5.8	24	0.3	3	5.9	8	3.6	1.6	8.2	8.4	18.9	22.3	34.3	0.9	1.8	2.8	20.1	6.4	2.1	6.7	16.4	0	4.1	4.6	3.3	2.4	16.5	13.7	7.7	1.7	
66	37.74	10.33	2015	11	6	1.7	0	0	0	0	0	0	0	0	0	0	0	0	0	4.3	0	0	0	0	0.4	0	0	0	0	0	0	0	0	0	
67	37.74	10.33	2015	12	6.7	4.2	2.2	4.8	0.2	21.9	2.9	7.1	0.4	10.5	13.8	1.7	23.1	11.8	3.9	26.9	0	11.6	12.5	15.7	9.2	5.4	19.4	0	5.4	12	5.7	2.4	27.8	5.6	12
68	37.74	10.33	2022	01	22.8	8.6	0.7	1.7	2.8	15	7.9	8.3	20.4	9.9	4.7	4.8	8.2	23.9	0.4	1.9	10.8	0	0	5.1	16.2	0	8.9	3.6	16.7	5.7	26.7	10.6	13.4	11	
69	37.74	10.33	2022	02	25.1	43.5	0.2	0	0	6.7	2	21.3	8.9	2.6	13.8	12.5	7.3	3.2	28.5	0	9	6.7	23.2	4	8.4	28.9	7	14.5	6	2	0.8	0.5	30.6	12.6	30.7
70	37.74	10.33	2022	03	26	25.9	3	13	15.1	10.5	11.5	0	2.9	15.5	3.8	6.3	27.7	27.6	27.6	7.9	3.3	4.8	4.3	0	4.3	8.8	10.2	8.7	0	10.4	0	20.3	2.1	0	
71	37.74	10.33	2022	04	26.1	1.2	0.4	0.2	9.4	13.1	3.8	12.7	0	0	2.2	16.9	0.4	12.8	1.4	1	16	6.7	0	6.2	4	12.5	1.2	0.7	18.9	0	17	0	0	10.3	
72	37.74	10.33	2022	05	28.1	12.9	21.3	6.7	19.2	14.2	2.9	1	9	13.7	7.9	21.7	8.7	9	6.7	1.3	15.8	5.4	1.8	18.2	4.9	1.8	0.6	38.7	2.5	8.5	2	6.9	4.3	13.8	4.5
73	37.74	10.33	2022	06	34	3	22.2	4.2	3.6	6.8	9.6	12.7	16	15.6	5.6	7.4	6.2	18.5	8.2	44.5	16.8	9.5	19.7	52.6	5	13.5	3.4	2.7	8.5	8.5	21.5	5.1	7.6	40.5	19.3
74	37.74	10.33	2022	07				0	0	0	10	6.9	11.7	18.6	15.2	16	0.1	0	0	0	0	3.7	20.8	0	0	0	0	0	0	0	0	0	0	0	0

Appendix B.

Confusion Matrix: D:\Thesis_Data_2023\Data_analysis\1995\SVM_Classified1995

Overall Accuracy = (1079/1110) 97.2072%
Kappa Coefficient = 0.9618

Class	Ground Truth (Pixels) Vegetation_valid	Meadow_valid	Bare_Land_val	Agri_land_val	Urban_valid
Unclassified	0	0	0	0	0
Vegetation	132	0	0	0	1
Meadow	0	235	12	0	0
Bare_Land	0	11	91	0	0
Farm_Land	0	0	2	462	5
Urban	0	0	0	0	159
Total	132	246	105	462	165

Class	Prod. Acc. (Percent)	User Acc. (Percent)	Prod. Acc. (Pixels)	User Acc. (Pixels)
Vegetation	100.00	99.25	132/132	132/133
Meadow	95.53	95.14	235/246	235/247
Bare_Land	86.67	89.22	91/105	91/102
Farm_Land	100.00	98.51	462/462	462/469
Urban	96.36	100.00	159/165	159/159

i. Confusion matrix of LULC classification for the year 1995

Confusion Matrix: D:\Thesis_Data_2023\Data_analysis\2000\SVM_Classified2000

Overall Accuracy = (1072/1110) 96.5766%
Kappa Coefficient = 0.9530

Class	Ground Truth (Pixels) Vegetation_valid	Meadow_valid	Bare_Land_val	Agri_land_val	Urban_valid
Unclassified	0	0	0	0	0
Vegetation	131	0	0	0	1
Meadow	1	225	9	0	0
Bare_Land	0	7	91	1	0
Agricultural_	0	14	5	461	0
Urban	0	0	0	0	164
Total	132	246	105	462	165

Class	Prod. Acc. (Percent)	User Acc. (Percent)	Prod. Acc. (Pixels)	User Acc. (Pixels)
Vegetation	99.24	99.24	131/132	131/132
Meadow	91.46	95.74	225/246	225/235
Bare_Land	86.67	91.92	91/105	91/99
Agricultural_	99.78	96.04	461/462	461/480
Urban	99.39	100.00	164/165	164/164

ii. Confusion matrix of LULC classification for the year 2000

Confusion Matrix: D:\Thesis_Data_2023\Data_analysis\2005\SVM_Classified2005

Overall Accuracy = (1074/1110) 96.7568%
Kappa Coefficient = 0.9554

Ground Truth (Pixels)

Class	Vegetation_valid	Meadow_valid	Bare_Land_val	Agri_land_val	Urban_valid
Unclassified	0	0	0	0	0
Vegetation	132	0	0	0	0
Meadow	0	228	12	0	0
Bare_Land	0	4	90	0	0
Farm_Land	0	14	3	462	3
Urban	0	0	0	0	162
Total	132	246	105	462	165

Class	Prod. Acc. (Percent)	User Acc. (Percent)	Prod. Acc. (Pixels)	User Acc. (Pixels)
Vegetation	100.00	100.00	132/132	132/132
Meadow	92.68	95.00	228/246	228/240
Bare_Land	85.71	95.74	90/105	90/94
Farm_Land	100.00	95.85	462/462	462/482
Urban	98.18	100.00	162/165	162/162

iii. Confusion matrix of LULC classification for the year 2005

Confusion Matrix: D:\Thesis_Data_2023\Data_analysis\2010\SVM_Classified2010

Overall Accuracy = (1070/1110) 96.3964%
Kappa Coefficient = 0.9503

Ground Truth (Pixels)

Class	Vegetation_valid	Meadow_valid	Bare_Land_val	Agri_land_val	Urban_valid
Unclassified	0	0	0	0	0
Vegetation	132	2	0	0	0
Meadow	0	232	10	0	0
Bare_Land	0	0	83	0	0
Agricultural_	0	12	12	462	4
Urban	0	0	0	0	161
Total	132	246	105	462	165

Class	Prod. Acc. (Percent)	User Acc. (Percent)	Prod. Acc. (Pixels)	User Acc. (Pixels)
Vegetation	100.00	98.51	132/132	132/134
Meadow	94.31	95.87	232/246	232/242
Bare_Land	79.05	100.00	83/105	83/83
Agricultural_	100.00	94.29	462/462	462/490
Urban	97.58	100.00	161/165	161/161

iv. Confusion matrix of LULC classification for the year 2010

Confusion Matrix: D:\Thesis_Data_2023\Data_analysis\2015\SVM_Classified2015

Overall Accuracy = (710/786) 90.3308%
Kappa Coefficient = 0.8766

	Ground Truth (Pixels)				
Class	Vegetation_valid	Meadow_valid	Bare_Land_val	Urban_valid	Agri_valid
Unclassified	0	0	0	0	0
Vegetation	106	0	0	0	0
Meadow	0	199	13	0	0
Bare_Land	0	36	78	1	0
Urban	0	6	5	163	0
Farm_Land	0	5	9	1	164
Total	106	246	105	165	164

Class	Prod. Acc. (Percent)	User Acc. (Percent)	Prod. Acc. (Pixels)	User Acc. (Pixels)
Vegetation	100.00	100.00	106/106	106/106
Meadow	80.89	93.87	199/246	199/212
Bare_Land	74.29	67.83	78/105	78/115
Urban	98.79	93.68	163/165	163/174
Farm_Land	100.00	91.62	164/164	164/179

v. Confusion matrix of LULC classification for the year 2015

Confusion Matrix: D:\Thesis_Data_2023\Data_analysis\2022\SVM_Class2022

Overall Accuracy = (775/850) 91.1765%
Kappa Coefficient = 0.8861

	Ground Truth (Pixels)				
Class	Vegetation_valid	Meadow_valid	Bare_Land_val	Urban_valid	Agri_valid
Unclassified	0	0	0	0	0
Vegetation	103	0	1	0	0
Meadow	3	209	34	0	0
Bare_Land	0	31	70	0	0
Built_up	0	1	0	165	0
Farm_Land	0	5	0	0	228
Total	106	246	105	165	228

Class	Prod. Acc. (Percent)	User Acc. (Percent)	Prod. Acc. (Pixels)	User Acc. (Pixels)
Vegetation	97.17	99.04	103/106	103/104
Meadow	84.96	84.96	209/246	209/246
Bare_Land	66.67	69.31	70/105	70/101
Built_up	100.00	99.40	165/165	165/166
Farm_Land	100.00	97.85	228/228	228/233

vi. Confusion matrix of LULC classification for the year 2022